2016

Effects of concussive impact injury assessed in a new murine neurotrauma model

BOSTON UNIVERSITY

COLLEGE OF ENGINEERING

Dissertation

EFFECTS OF CONCUSSIVE IMPACT INJURY ASSESSED IN A NEW MURINE NEUROTRAUMA MODEL

by

CHAD ALAN TAGGE

B.A., University of Utah, 2009

Submitted in partial fulfillment of the

requirements for the degree of

Doctor of Philosophy

2016

Approved by

First Reader

Lee E. Goldstein, M.D., Ph.D.
Associate Professor of Psychiatry
Associate Professor of Biomedical Engineering
Associate Professor of Neurology
Associate Professor of Ophthalmology
Associate Professor of Pathology & Laboratory Medicine

Second Reader

Mark W. Grinstaff, Ph.D.
Distinguished Professor of Translational Research
Professor of Chemistry
Professor of Biomedical Engineering
Professor of Materials Science and Engineering

Third Reader

H. Steven Colburn, Ph.D.
Professor of Biomedical Engineering

Fourth Reader

John A. White, Ph.D.
Professor and Chair of Biomedical Engineering

Fifth Reader

Ann C. McKee, M.D.
Professor of Neurology and Pathology
Director, Neuropathology Core

ACKNOWLEDGMENTS

I would like to express my special appreciation and gratitude to my advisor Dr. Lee Goldstein. My first semester in the Ph.D. program, I took a class in Pathophysiology for engineers taught by Dr. Goldstein. In all my studies, this class was the most unique and showed me the importance of having clinicians involved in biomedical research. One class period, Dr. Goldstein proposed a problem to us engineers on how to design an injury device for traumatic brain injury. It was this assignment that inspired me to seek a rotation in his lab and started this project. His mentorship and advice has been instrumental in receiving an F31 NHI Fellowship and the success of this dissertation and my development as a biomedical engineer and scientist.

I would also like to thank my fellow PhD colleague, Andrew Fisher. It has been a team effort. As we have worked on projects, I have come to appreciate his company, numerous skills, and expertise. This project would not have been as enjoyable nor as successful without his involvement. I would like to thank Olga Minaeva, Juliet Moncaster, and Noel Casey. Each of them have provided mentorship, advice, helpful critique of my work, and have helped me mature as a student and scientist. I would like to thank Amanda Gaudreau-Balladrama. Her expertise as an electrical and computer scientist was instrumental in helping us process the data. I would like to thank Mark Wojnarowicz for teaching me all the laboratory animal techniques and his support in the numerous projects. I also want to thank Srikant Sarangi for his guidance in blazing the trail of graduating.

This dissertation has been a collaborative effort. I would like to thank the

collaborators Thor Stein, Pat Stanton, Richard Ransohoff, Bruce Lamb, and Willy Moss for their expertise and support in this work. I would also like to thank Haiyan Lu and Ronel Veksler for their contributions in key experiments. This work could not have been accomplished on my own. I want to acknowledge all of our collaborators' support, time, and energy in helping me, my lab, and this dissertation.

I would like to thank my committee members. I would like to thank Ann Mckee for her immense support, time, and energy. Her clinical research has transformed the field and has played a key role in the impact of the work. I would like to thank Mark Grinstaff, my advisor on the T32 Training Grant. I want to thank him for the funding that came from this, which allowed me to pursue this project. I would like to thank Steve Colburn and John White for their time in editing the dissertation and their encouragement.

When I moved to Boston, I had multiple goals. One was to receive a PhD. The second was to find a wife. I am so grateful that I was able to accomplish both of these goals. I am so grateful for the love, support, and encouragement of my beautiful wife, Molly Tagge. I would not have been able to complete my PhD without her. Two years after our wedding, we added a beautiful baby girl to our family, Olive Tagge. She brightened my day and melted away all the stress of lab. Two years after, we welcomed a beautiful baby boy, Dexter, to our lives. I am so grateful for his additional. I could not imagine my life without them.

I would also like to thank my parents, Thayne and Cari Tagge. They set me on the path to pursue science and I am forever grateful. They supported my interests and stoked my desire to constantly better myself. I would not be where I am today without them.

I want to thank the department and all the professors for the high quality education I received, financial support, and for accepting me into this program.

Finally, I want to thank God who gave me strength during difficult times and who answered my and my family's prayers. His inspiration guided me in many of my experiments. I have seen His hand guide my work.

EFFECTS OF CONCUSSIVE IMPACT INJURY ASSESSED

IN A NEW MURINE NEUROTRAUMA MODEL

CHAD ALAN TAGGE

Boston University, College of Engineering, 2016

Major Professor: Lee E. Goldstein, M.D., Ph.D., Associate Professor of Psychiatry, Associate Professor of Biomedical Engineering, Associate Professor of Neurology, Associate Professor of Ophthalmology, Associate Professor of Pathology & Laboratory Medicine

ABSTRACT

Postmortem brains from young athletes with a history of repetitive concussive head injury and military service personnel with history of blast neurotrauma revealed evidence of parenchymal contusion, myelinated axonopathy, microvasculopathy, neuroinflammation, neurodegeneration, and phosphorylated tauopathy consistent with chronic traumatic encephalopathy (CTE) (L. E. Goldstein et al., 2012). The mechanisms by which head trauma induces acute concussion and chronic sequelae are unknown. To elucidate the mechanistic connection between traumatic brain injury (TBI), acute concussion and chronic sequelae, including CTE, require the use of animal models. This doctoral dissertation investigated the hypothesis that closed-head impact injury in mice triggers acute neurological signs associated with sport-related concussion as well as brain pathologies and functional sequelae associated with CTE.

To test this hypothesis, we developed a mouse model of impact neurotrauma that utilizes a momentum transfer device to induce non-skull deforming head acceleration, triggering transient neurological signs consistent with acute concussion and traumatic brain injury (TBI) in unanesthetized C57BL/6 mice. The Boston University Concussion

Scale (BUCS) was developed to assess neurological signs that are consistent with acute concussion in humans. Mice exhibited contralateral circling and limb weakness, locomotor abnormalities, and impaired gait and balance that recapitulate acute concussion in humans. Concussed mice recovered neurological function within three hours, but demonstrated persistent myelinated axonopathy, microvasculopathy, neuroinflammation, and phosphorylated tauopathy consistent with early CTE. Concussive impact injury also induced blood-brain barrier disruption, neuroinflammation (including infiltration peripheral monocytes and activation microglia), impaired hippocampal axonal conduction, and defective long-term potentiation (LTP) of synaptic transmission in medial prefrontal cortex. Kinematic analysis during impact injury revealed head acceleration of sufficient intensity to induce acute concussion, traumatic brain injury (TBI), early CTE-linked pathology, and related chronic sequelae.

Surprisingly, the presence or degree of concussion measured by BUCS did not correlate with brain injury. Moreover, concussion was observed following impact injury but not blast exposure under conditions that induce comparable head kinematics. Empirical pressure measurements and dynamic modeling revealed greater pressure on the head and compression wave loading in the brain during impact compared to blast neurotrauma. These findings suggest acute concussion is triggered by focal loading of energy that transit the brain before onset of macroscopic head motion. By contrast, the forces associated with rapid head motion is sufficient to induce CTE-linked pathology. Our results indicate that while acute concussion and chronic sequelae may be triggered by the same insult, the pathophysiological responses underpinning these effects

are engaged through distinct mechanisms and time domains. Our results indicate that concussion is neither necessary nor sufficient to induce acute brain injury or chronic sequelae, including CTE.

TABLE OF CONTENTS

LIST OF TABLES

LIST OF FIGURES

Chapter 1: The Brain and Traumatic Brain Injury

The brain is made up of different cellular components including an estimated 100 billion neurons with a rich variety of morphologies and glia cells sub-classified into astrocytes, oligodendroglia, ependymal cells and microglia (Azevedo et al., 2009). This resulting brain tissue was described by Ommaya as a 'soft yielding structure, not as stiff as gel nor as plastic as a paste' (Ommaya, Faas, & Yarnell, 1968). and is easily mechanically deformed. The brain is protected by the skull and is encased by three layers of meninges: the dura mater, a thick and tough layer; the arachnoid mater, a delicate layer attached to the dura; and the pia mater, which envelops the surface cortical folds. Cerebral spinal fluid (CSF) surrounds the brain and circulates within the ventricles and subarachnoid space. The blood-brain barrier (BBB) separates the brain parenchyma from the bloodstream, regulates the passage of molecules, and maintains immune privilege of the CNS (Pachter, de Vries, & Fabry, 2003). All of these tissues, compartments, and barrier are subject to pathological disruption as a consequence of traumatic brain injury (TBI).

The Centers for Disease Control and Prevention (CDC) defines a TBI as a bump, blow, or jolt to the head or a penetrating head injury that disrupts normal function of the brain, and according to the CDC over 1.7 million Americans sustain a traumatic brain injury each year (TBI) (Faul, Xu, Wald, & Coronado, 2010). Globally, the World Health Organization (WHO) estimates 10 million TBI cases annually (Hyder, Wunderlich, Puvanachandra, Gururaj, & Kobusingye, 2007). Often cited limitations in many TBI epidemiological studies include injury heterogeneity within populations, missing medical

coding, lack of standardized reporting across countries, and lack of standardized definitions for TBI and TBI subcategories (Hicks et al., 2013; Hyder et al., 2007; Menon et al., 2010). Moreover, most epidemiological studies only included patients who sought medical care and do not completely capture the full magnitude of TBI nationally and globally (Faul et al., 2010).

1.1 Classification of Traumatic Brain Injury

Injury heterogeneity makes TBI classification challenging and leads to misunderstanding in clinical and scientific discourse (Hawryluk & Manley, 2015). Classification of TBI has traditionally relied on a three classification systems based on symptom severity, anatomic pathology, and injury mechanism (Hawryluk & Manley, 2015; Maas, Stocchetti, & Bullock, 2008; Saatman et al., 2008).

1.1.1 Classifying TBI by Injury Severity

Severity of injury is one common method of classifying TBI. The Glasgow Coma Scale (GCS) is commonly administered in emergency departments around the world and serves as a bedside clinical tool for rapid clinical assessment of TBI severity (Graham Teasdale et al., 2014). Proposed by Teasdale and Jennett (1974), the GCS consists of three scaled test categories: eye opening, verbal response, and motor response. (G. Teasdale & Jennett, 1974). The composite score ranges from 3 to 15 points and distinguishes between mild (15–13), moderate (12–9), and severe (8–3) brain injury (Marshall et al., 1983; Rimel, 1981; Rimel, Giordani, Barth, & Jane, 1982; G. Teasdale & Jennett, 1974) The GCS can refer to either the Glasgow Coma Scale, which is applicable

for individual patient management, or the Glasgow Coma Score (summed score) for patient groups or populations for use in clinical trials (Saatman et al., 2008; Graham Teasdale et al., 2014). While the GCS is able to separate groups by TBI severity (i.e., mild, moderate, severe), numerous confounds limit the utility of this instrument. Limitations include presence of CNS-altering medications (e.g., anesthetics, sedatives, analgesics, etc.), limited applicability in infants and children, and confounds associated with neurological comorbidities (Saatman et al., 2008). Moreover, the GCS is limited in discriminating the full spectrum of mild-TBI (Saatman et al., 2008). Furthermore, many common head injuries associated with sports and accidents are below the level of detection of the GCS (Johnston, McCrory, Mohtadi, & Meeuwisse, 2001; McCrory, Meeuwisse, Echemendia, et al., 2013).

1.1.2 Classifying TBI by Anatomical Pathology

Pathoanatomic classification of TBI relates injury abnormalities or lesions with location (Saatman et al., 2008). Pathoanatomic classification commonly uses computed tomography (CT) to determine the type and degree of head injury and include: skull fracture, epidural hemorrhage, subdural hemorrhage, subarachnoid hemorrhage, brain contusion, intraparenchymal hemorrhage, intraventricular hemorrhage and axonal injury (Saatman et al., 2008). Depending on the lesion location, TBI injuries in this scheme are classified as focal or diffuse. Focal injuries include localized cerebral contusion, cerebral laceration, epidural hemorrhage, subdural hemorrhage, intracerebral hemorrhage, and intraventricular hemorrhage. Diffuse injuries include diffuse axonal injury, ischemic brain injury, vascular injury, and global brain swelling (Granacher Jr, 2007). Computer

tomography has advanced pathoanatomic classification of severe brain injuries leading to correlations between abnormalities and outcome (Maas, Hukkelhoven, Marshall, & Steyerberg, 2005; Marshall et al., 1992), and have allowed for better patient management (Zhu, Wang, & Liu, 2009).

Current neuroimaging techniques rely on the use computer tomography (CT) and magnetic resonance imaging (MRI). After head injury, neuroimaging is commonly used to identify macroscopic abnormalities in the brain and to determine the severity of brain injury. CT is typically used for initial screening following clinical examination, while MRI is used as a more sensitive technique to detect and distinguish brain pathologies in patients requiring additional investigation (Lee et al., 2008). Assessment of structural damage (e.g., contusions, hematomas) by neuroimaging has become an integral part of TBI classification (Maas et al., 2008). However, neuroimaging with conventional CT and MRI usually reveal no abnormalities in patients with milder forms of TBI (Shenton et al., 2012).

1.1.3 Classifying TBI by Physical Mechanism

Another TBI classification system focuses on the mechanism of injury, namely, blunt, penetrating, or blast TBI. Blast injury has been recognized as a distinct physical mechanism of brain injury for well over a century (Fulton, 1942; Mott, 1916) and is an area of active research in Dr. Goldstein's laboratory (L. E. Goldstein et al., 2012). Penetrating injuries are generally classified as severe and require acute medical care and are commonly associated with significant acute and chronic morbidity and mortally medical complications (Black et al., 2002). Blunt injuries, also referred to as closed-head

injuries (CHI), are caused by mechanical forces acting on the brain through either static or dynamic loading (Gennarelli & Meaney, 1996; Kumar & Loane, 2012). Static loading entails forces applied to a constraint head typically resulting in a skull-crush injury (Kumar & Loane, 2012). Static head injuries are uncommon (Ommaya & Gennarelli, 1974). Dynamic-loading head injuries are common and can be divided into two distinct sub-types based on input forces: (1) impact loading (i.e., direct-contact loading) results from a direct-head impact; (2) impulsive (i.e., inertial) loading occurs when the head is set into motion or arrested without direct contact loading (Cernak, 2005).

Direct-contact and inertial loading have been postulated as being the primary physical mechanism responsible for brain injury. Contact injures are caused by direct head impact (impact loading), and depending on the applied mechanical force (velocity, acceleration, duration, magnitude), a range of focal injuries can occur (i.e., fractures, contusion, hematomas) (Cernak, 2005). Furthermore, direct impact can induce shock waves which can lead to intracerebral hemorrhages (McAllister, 2011). Importantly, contact injuries induce head motion (i.e., translation and rotation) that is independently associated with brain injury. This mechanism will be a major focus of this dissertation as discussed in detail below.

Inertial injury is defined as an acceleration and/or deceleration injury that typically includes both translational and angular acceleration components (McAllister, 2011). Investigation into automobile accidents and concussion has advanced the research in understanding and differentiating the effects of translational and angular acceleration (Gennarelli, Ommaya, & Thibault, 1971; Gennarelli, Thibault, & Ommaya, 1972;

Gurdjian & Webster, 1947; Gurdjian, Webster, & Lissner, 1955; Ommaya, Hirsch, & Martinez, 1967; Ono, Kikuchi, Nakamura, Kobayashi, & Nakamura, 1980). A study which controlled translation of the head showed that head translation resulted in focal effects (i.e., cerebral contusions, intracerebral hematomas) while translation and rotation induced diffuse injuries (Gennarelli et al., 1971; Gennarelli et al., 1972). Studies investigating angular acceleration have shown that shear and tensile strain are generated by rotation-only motion (Holbourn, 1943). Strich detailed histological findings of diffuse degeneration of white matter tracks from patients who survived closed-head injuries but died after prolonged coma or other severe episodes of loss of consciousness (Strich, 1956). The term for this type of traumatic brain injury is called diffuse axonal injury (DAI) (Adams, Graham, & Gennarelli, 1983; Gennarelli et al., 1982), defined by Gennarelli *et al.* as involving "a prolonged traumatic coma that is not associated with mass lesions orischemic damage, and forms a continuous spectrum of increasing severity associated with increased numbers of damaged axons." (Gennarelli et al., 1982). Multiple studies using non-human primates and physical models have demonstrated that angular acceleration is a primary pathogenic mechanism underpinning diffuse axonal injuries and acute subdural hematomas (Gennarelli et al., 1982; Gennarelli, Thibault, & Graham, 1998). These studies hypothesized DAI are induced by shear strain generated by angular acceleration (Gennarelli & Thibault, 1982; Gennarelli et al., 1982; Thibault & Gennarelli, 1985). Moreover, computer simulation have reported correlation between shear stress and rotational acceleration (L. Zhang, Yang, & King, 2001).

However, other studies have shown direct-contact impacts result in a combination

of linear and angular acceleration injuries (Rowson & Duma, 2013; L. Zhang, Yang, & King, 2004). Most TBI injuries result from combination of both contact and inertial forces (L. Zhang et al., 2004). These forces, when applied to the head, result in the heterogeneity of focal and diffuse injuries commonly observed following acute closed-head injuries (L. Zhang et al., 2004). Mechanistically, focal injuries are attributed to contact forces while diffuse injuries are attributed to inertial forces; however, these forces are commonly not separable making it difficult to attribute a force to a specific of brain injury (McKee & Daneshvar, 2015).

Another common mechanistic classification separates mechanical damage from non-mechanical damage. Primary injury describes the immediate sequelae resulting from the forces (contact/inertial) applied to the brain (McAllister, 2011). Secondary injury describes the delayed events initiated by the primary injury.

In conclusion, approaches to classify TBI have relied on severity classification with the GCS, and structural damage assessed by CT and MRI neuroimaging techniques, and mechanism classification. These classification schemes distinguish moderate and severe TBI, brain injuries which require emergency medical treatment. Moderate and severe TBI are often associated with life-long neurological impairments with chronic physical, cognitive, speech and language, sensory, social-emotional signs and symptoms.

1.2 Definition of Mild TBI (mTBI), Concussion

There is confusion as to how serious a minor blow or jolt to the head is and what differentiates a mild TBI from a concussion. The terms TBI and concussion are

frequently used interchangeably in clinical literature. There is no single, universally-accepted definition for either term. Indeed, both concussion and TBI have been subject to regular revision with respect to definition and interpretation. An overview of this history and current formulations is presented below.

AMERICAN CONGRESS OF REHABILITATION MEDICINE (1993) (Kay, Harrington, & Adams, 1993).
Traumatically induced physiological disruption of brain function WITH AT LEAST ONE OF THESE SIGNS:

- Any period of loss of consciousness ≤30 min
- Loss of memory for events before or after the accident (post-traumatic amnesia <24 h)
- ΔMS at time of injury (e.g., feeling dazed, disorientated, confused)
- Focal neurological deficit(s) that may or may not be transient
- GCS score 13–15 at or after 30 min post injury

WORLD HEALTH ORGANIZATION (2004) (Carroll et al., 2004)
Acute brain injury from mechanical energy to head from external physical force MARKED BY SIGNS:

- Confusion or disorientation
- Loss of consciousness ≤30 min
- Post-traumatic amnesia ≤24 h
- And/or other transient neurological abnormalities and/or focal sign(s)
- GCS score 13–15 after 30 min post-injury or later on presentation

VA-DOD CLINICAL PRACTICE GUIDELINES FOR TBI (2009). (VA/DoD, 2009)
Note: This has been updated with new revised definitions.

- Normal structural imaging
- LOC = 0–30 minutes
- ΔMS = momentary to 24 hours
- PTA (Post-Traumatic Amnesia) = 0–1 day
- GCS = 13–15 at or after 24 hours post-injury

As no established biomarker exists for either mTBI or concussion, diagnosis for both mTBI and concussion is based on injury characteristics and clinical criteria.

Guidelines for diagnosing mTBI have been established by the American College of Rehabilitation Medicine (Kay et al., 1993), Centers for Disease Control and Prevention (CDC, 2003), World Health Organization (WHO)(Carroll et al., 2004), and Department of Veterans Affairs (VA/DoD, 2009). The American Congress of Rehabilitative Medicine (ACRM) has established a definition which describes mTBI as a disruption of normal brain function caused by mechanical force to the head and is defined as loss of consciousness of less than 30 minutes, posttraumatic amnesia lasting less than 24 hours, and a Glasgow Coma Score (GCS) from 13 to 15. (Kay et al., 1993). Using the ACRM and WHO guidelines for mTBI, Ruff *et al*., detailed recommendations on evaluating loss of concussion (LOC), amnesia, confusion and disorientation, neurological signs and associated symptoms, and GCS scores (Ruff et al., 2009). Accurate diagnosis of mTBI is challenging due to the common delay in patient evaluation (Ruff et al., 2009). and a slew of confounding factors (Katz, Cohen, & Alexander, 2015; Menon et al., 2010; Ruff et al., 2009). Identifying suspected injury and early diagnosis play a critical role in management, recovery, and patient outcomes (Kushner, 1998).

The definition of concussion continues to be refined (Gronwall & Wrightso.P, 1974; McCrory, Johnston, Mohtadi, & Meeuwisse, 2001). The International Consensus Conferences on Concussion in Sport has continually refined its consensus statement and currently defines concussion as "a complex pathophysiological process affecting the brain, induced by traumatic biomechanical forces" (Aubry et al., 2002; McCrory et al., 2005; McCrory, Meeuwisse, Aubry, et al., 2013; McCrory et al., 2009). This working consensus statement further defines that concussion appears to be caused by an impulsive

force (i.e., inertial) transmitted to the head, usually through a direct blow; may or may not involve loss of consciousness; typically regarded to cause rapid onset but transient neurological impairments and in 80–90% of concussions fully recover occurs within 7 to 10 days (McCrory et al., 2005; McCrory et al., 2009). Furthermore, the working consensus statement mentions standard neuroimaging techniques are limited due to the absence of objective abnormalities for most cases (McCrory et al., 2005; McCrory, Meeuwisse, Aubry, et al., 2013; McCrory et al., 2009; Shenton et al., 2012). With regards to the GCS, McCroy *et al.* states many sport-related concussions fall below the threshold of overt clinical injury (Johnston et al., 2001; McCrory, Meeuwisse, Echemendia, et al., 2013), thus leading several authorities in the field to a controversial presumption that concussion represents a "minimal" injury subcategory of mTBI (McCrory, Meeuwisse, Echemendia, et al., 2013).

Evaluation of sport-related concussion previously relied on grading the severity of concussion (American Academy of Neurology, 1997). However, recent guidelines have abandoned the grading systems and transitioned to multimodal evaluation assessments that use the GCS, symptom questionnaire, balance assessment, and cognitive function tests (Christopher C Giza et al., 2013). One such assessment tool currently on its third revision is the Sideline Concussion Assessment Tool (SCAT3) proposed by the 4th International Conference on Concussion in Sports (McCrory, Meeuwisse, Aubry, et al., 2013). Several other neuropsychological tests are used to identify cognitive dysfunction and track recovery after sport-related concussion (Collie, Darby, & Maruff, 2001; Collie et al., 2003; Collins et al., 2003; Lovell & Collins, 1998). Recent studies found that 24%

of high-school athletes suffering from concussion report symptom resolution within 24 hours and 78% report complete symptom recovery within 7 days (Meehan, d'Hemecourt, Collins, & Comstock, 2011). However, the pathobiological and clinical relationship between acute concussive signs and symptoms, post-injury recovery, and long-term sequelae after brain injury remain largely unknown.

Furthermore, epidemiological studies have found over 1.7 million Americans sustain a traumatic brain injury (TBI) each year (Faul et al., 2010) and of those an estimated 75% are classified as mild TBI (Report to Congress on Mild Traumatic Brain Injury in the United States, CDC). These estimates only included patients who sought medical care and thus this figure likely underrepresents the true number of injuries. One study has estimated that 75% of individuals who sustain a concussive head injury do not seek medical attention (Willer & Leddy, 2006). The number of sport-related concussions has been estimated to be between 1.6 and 3.8 million each year (Langlois, Rutland-Brown, & Wald, 2006).

1.3 Acute Effects of Mild TBI and Concussion

Inertial forces acting on the brain can induce concussive injury (Meaney et al., 1995). These inertial forces can cause structural deformation that damages neurons, glial cells, and microvasculature. Giza *et al.* reviewed and described the neurometabolic cascade immediately following primary brain injury (C. C. Giza & Hovda, 2001, 2014). This cascade involves a rapid release of glutamate and potassium into the extracellular space and a corresponding influx of calcium. The resulting disruption of normal ionic

homeostasis leads to pathogenic activation of membrane pumps and altered glucose metabolism (C. C. Giza & Hovda, 2001, 2014). Investigation of acute pathology following TBI studies has revealed axonal injury disruption, activated perivascular microglia and reactive astrocytes, micro-hemorrhage, and cytoskeletal disorganization that persist long after the inciting insult (L. E. Goldstein et al., 2012; McKee, Daneshvar, Alvarez, & Stein, 2014).

1.4 Chronic Traumatic Encephalopathy (CTE)

Chronic traumatic encephalopathy (CTE) is a tau protein-linked neurodegenerative disease associated with exposure to repetitive mTBI, concussive or subconcussive head injuries (L. E. Goldstein et al., 2012; McKee et al., 2009; McKee et al., 2014; McKee et al., 2010; McKee et al., 2013; Omalu et al., 2006; Omalu et al., 2005). Clinical symptoms of CTE include affective lability, irritability, distractibility, executive dysfunction, memory loss, and in advanced cases, cognitive deficits and dementia (Stern et al., 2013). Neuropathological findings of CTE in the brain include widespread cortical foci of perivascular phosphorylated tau pathology, disseminated microgliosis and astrocytosis, myelinated axonopathy, and progressive neurodegeneration (McKee et al., 2014). Recently, the first National Institute of Health (NIH) consensus conference for CTE defined the neuropathological criteria for the pathological diagnosis of CTE as abnormal extensive tau-immunoreactive neurofibrillary tangles (NFT) and astrocytic tangles distributed irregularly in the cerebral cortex, with focal hot spots at the depths of sulci and around small cerebral vessels (McKee et al., 2015).

McKee *et al.* has defined 4 pathological stages of CTE pathology: **Stage I**, the mildest stage, is characterized by focal perivascular tau NFT and neurites in discrete cortical foci, often involving sulcal depths of the frontal lobe. In **Stage II** disease, multifocal perivascular tau abnormalities are more numerous, larger, and confluent with superficial NFTs in the adjacent cortex. There is also involvement of deep cholinergic nuclei, including nucleus basalis, septal nuclei, and nuclei of the diagonal band. In **Stage III**, NFTs are widespread in frontal, temporal, and insular cortex with extension into the medial temporal lobe, diencephalon, mammillary bodies, substantia nigra, and, less severely, the striatum and subcortical white matter. In the most advanced stage, **Stage IV**, there is prominent neuronal loss and gliosis of the neocortex, medial temporal lobe, and deep nuclei (with increasing ratio of glial to neuronal tangles), hippocampal sclerosis, and axonal loss (McKee et al., 2013).

The clinical progression of CTE, provisionally termed traumatic encephalopathy syndrome (TES), often begins with an asymptomatic presentation or may include post-concussive symptoms (i.e., depression, headache, attention and concentration deficit). Symptoms in more advanced disease become increasingly more debilitating and commonly include loss of control, hopelessness, impaired attention, and gait disturbances (Montenigro et al., 2014). Ultimately, the syndrome includes executive dysfunction, memory loss, and frank dementia (McKee et al., 2010; McKee et al., 2013; Montenigro et al., 2014; Stern et al., 2013). CTE is often difficult to distinguish from other age-related neurodegenerative diseases and neuropsychiatric disorders. The non-specific nature of the clinical syndrome and the possible progressive nature of CTE underscore the urgent need

to develop new biomarkers and advance neuroimaging techniques to facilitate accurate and early diagnosis as well as post-injury monitoring.

The long-term consequence of mTBI and the relationship of concussive head injury to the latter development of CTE-linked neuropathology remain largely unknown. Preclinical animal models that recapitulate CTE-linked pathology in humans may provide a key pathway for development of new biomarkers, advancing neuroimaging techniques, and increasing understanding of the acute and chronic effects of neurotrauma.

1.5 Animal models for the study of TBI

This section is adapted from Goldstein L.E., Fisher A.M., Tagge C.A., *et al.*, 2012

1.5.1 Blast-Related Traumatic Brain Injury (TBI) and Chronic Traumatic Encephalopathy (CTE)

Individuals exposed to explosive blast are at risk for TBI that is often reported as mild and results in neuropsychiatric symptoms, and long-term cognitive disability (Hoge et al., 2008; Vasterling, Verfaellie, & Sullivan, 2009). We examined a case series of postmortem brains from U.S. military veterans exposed to blast and/or concussive injury (L. E. Goldstein et al., 2012). We found evidence of CTE, a tau protein–linked neurodegenerative disease, characterized by perivascular foci of tau-immunoreactive neurofibrillary tangles (NFTs), axon degeneration, activated focal microglia and astrocytosis (L. E. Goldstein et al., 2012; McKee et al., 2014; McKee et al., 2013). These pathological findings were indistinguishable to the CTE neuropathology observed in young amateur American football players.

We hypothesized that common biomechanical and pathophysiological determinants may trigger development of CTE neuropathology and sequelae in both sport-related concussion and blast injury. To test our hypothesis, we combined clinicopathological correlation analysis and controlled animal modeling studies. We developed a blast neurotrauma mouse model that recapitulated CTE-linked neuropathology in wild-type C57BL/6 male mice 2 weeks after exposure to a single blast. Blast-exposed mice demonstrated phosphorylated tauopathy, myelinated axonopathy, microvasculopathy, chronic neuroinflammation, and neurodegeneration in the absence of macroscopic tissue damage or hemorrhage. Blast exposure induced persistent hippocampal-dependent learning and memory deficits that persisted for at least 1 month and correlated with impaired axonal conduction and defective activity-dependent long-term potentiation of synaptic transmission. Intracerebral pressure recordings demonstrated that shockwaves traversed the mouse brain with minimal change and without thoracic contributions. Kinematic analysis revealed blast-induced head oscillation at accelerations sufficient to cause brain injury. Head immobilization during blast exposure prevented blast-induced learning and memory deficits. The contribution of blast wind to injurious head acceleration may be a primary injury mechanism leading to blast-related TBI and CTE. These results identify common pathogenic determinants leading to CTE in blast-exposed military veterans and head-injured athletes and additionally provide mechanistic evidence linking blast exposure to persistent impairments in neurophysiological function, learning, and memory (L. E. Goldstein et al., 2012).

Our findings revealed blast neurotrauma induces lateral-head acceleration sufficient to cause brain injury. We hypothesize that impact neurotrauma can induce lateral-head acceleration sufficient to cause brain injury. We reviewed the available literature to determine which injury models could induce lateral-head acceleration in mice.

1.6 Evolution of Neurotrauma Models

Animal models allow for the investigation into specific pathophysiological responses following TBI in a controlled setting. While the pathophysiological heterogeneity following TBI has been described in patients (Saatman et al., 2008), there also exists a heterogeneity of animal neurotrauma models which vary widely by injury mechanism (Cernak, 2005; Xiong, Mahmood, & Chopp, 2013). A review of neurotrauma animal models presented insights into model design and motivation. The following section will describe the motivation for the model, animal species used, mechanism of inducing brain injury, injury parameters, head kinematics, and limitations.

1.6.1 Direct-Head Impact Models of TBI

The model developed by Denny-Brown and Russell at Boston City Hospital, then the flagship hospital of Harvard Medical School, was designed to understand the loss of cerebral function following a blow to the head and to define concussion (Denny-Brown & Russell, 1941). A pendulum was devised as the method of impact. Animals (cats, dogs and monkeys) were situated where the pendulum would hit the head and allow for a rapid change in velocity. The pendulum was stopped 2 mm after the hit while the

unconstrained head was able to freely move after impact. Assessment of concussion was judged by the loss of the corneal and pinna reflexes. The resulting injury was classified as "acceleration concussion" and provided the basic understanding of the role of inertial forces in induction of concussion. Limitation of the model includes use of anesthesia, concussion assessment that relied on loss of corneal and pinna reflexes, and use of non-rodent animal subjects.

Following upon the work by Denny-Brown, Nilsson *et al*. designed a neurotrauma model for the rat. Motivation for the development of this model was based on the observation that clinical concussive injuries involve acceleration with a freely moving head. The neurotrauma model was designed to standardize impact accelerations and investigate impact velocity and physiological results. Impact injury consisted of a 600 g piston accelerated by compressed nitrogen allowing for an impact velocity range of 6 m/s to 11 m/s. The rat was lightly anesthetized and placed on the back on a foam bed. The piston hit the rat through a hole in the bottom. (see Figure 1.1). The piston transferred its momentum, accelerating the head upwards. The piston was stopped 10 mm above the initial impact level. A high-speed camera (5000 – 7000 frames per second) was used to observe the resulting head kinematics. After injury, rats were either paralyzed or non-paralyzed. For the non-paralyzed group concussion was defined by loss of corneal reflexes and of motor reaction to pain stimulation. Mortality was reported following the injury at impact velocities greater than 8 m/s. At lower impact velocities, some rats showed no response to pain and other rats exhibited tonic-clonic episodes in the hindlegs lasting less than one minute. Gross pathology showed that concussion could occur

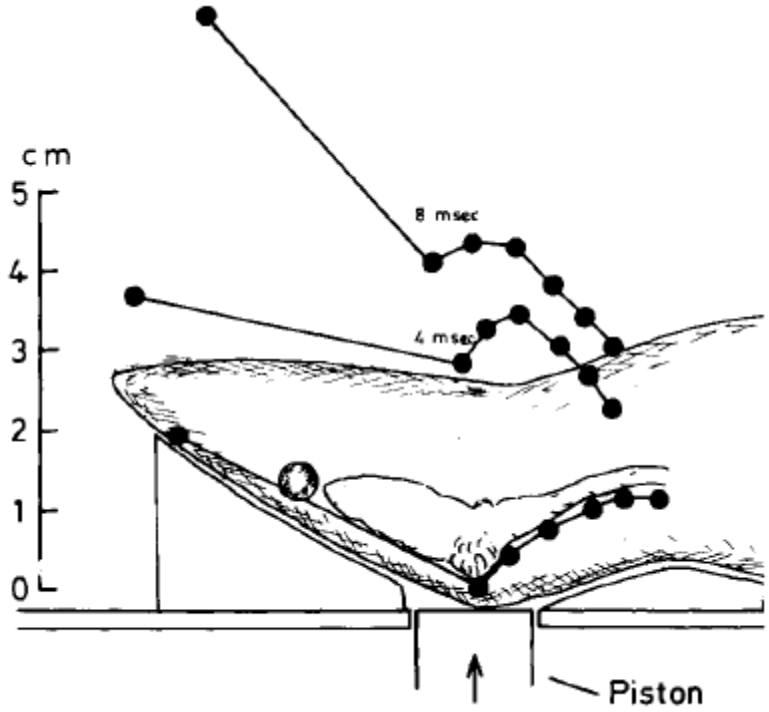

Figure 1.1: Diagram of Nilsson et al. concussion neurotrauma model.
The model uses a piston to accelerate the head vertically. Kinematics of head motion were obtained at 4 msec intervals. Reprinted from (Nilsson, Pontén, & Voigt, 1977)

without visible lesions but at 7 m/s impact velocity about 50% of the subjects showed some degree of subarachnoid hemorrhage at the location of impact. The authors postulate that concussion occurs because of an immediate change of neuronal function elicited by mechanical stress (Nilsson et al., 1977). Limitations with this model was the use of anesthesia and confounding effects of assessing loss of reflexes, high rate of subarachnoid hemorrhage suggesting skull crush, and horizontal rotation of the head.

Other neurotrauma models were developed to investigate concussion injury. One model used a slow motion film strips to analyze the kinematics of boxers and created a grading system of concussion in humans (Parkinson, West, & Pathiraja, 1978). Non-

anesthetized rats were then impacted with lead-tipped darts to match the grading system and observed signs of concussed boxers (Parkinson et al., 1978).

Another model was designed to reproduce reversible loss of consciousness in a rat (Bakay et al., 1977). The device was designed from a pendulum which would be raised to a specific angle. The pendulum was set to hit the occipital protuberance. During the hit the head would move under the impacting pendulum so as to replicate a human receiving a blow to the head (Figure 1.2). Light anesthesia was used to place the animal in location but once the animal started to show signs of waking up the pendulum was released. After the hit the pendulum was stopped similar to the other pendulum model (Denny-Brown & Russell, 1941). Unconsciousness was defined by the researchers as a loss of corneal and light reflexes and unresponsiveness to pain stimulation which typically lasted for 3 to 10 minutes after impact. Ultrastructure analysis using electron microscopy showed signs of mitochondrial swelling in the neurons and changes in the myelin sheaths in the white matter. Ultrastructural changes were observed 30 minutes after concussion with peak damage observed at 1 hour, and were not evident within 24 hours. Mitochondrial damage resolved within 24 hours. Although these pathological changes did not explain concussion, the model demonstrated that microscopic injury does occur and can resolve after a single brain insult (Bakay et al., 1977). Limitations include skull crush seen in some rats with hemorrhagic contusions and use of anesthesia.

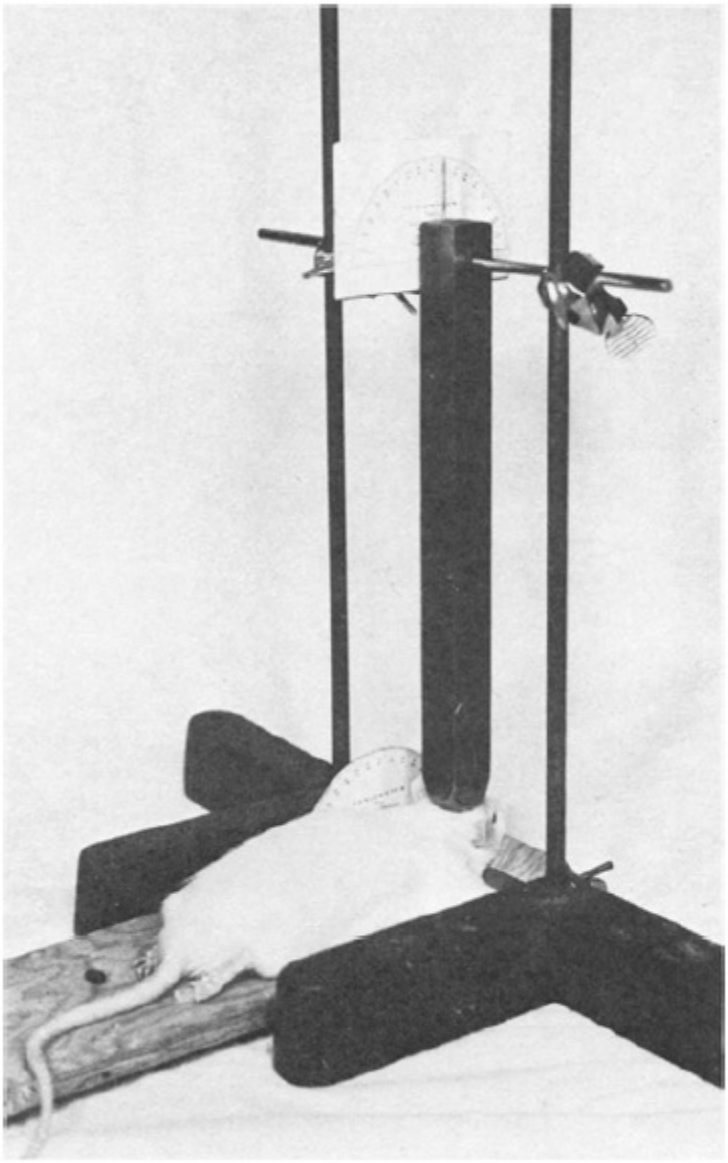

Figure 1.2: Pendulum concussion model.
Animals recovered within 3 to 10 minutes. Electron microscopy showed mitochondrial dysfunction and swollen astrocytes (Bakay, Lee, Lee, & Peng, 1977).

These models were designed to allow for unrestrained head movement and revealed an inherent attribute of clinical traumatic brain injuries which was that unrestrained head motion results in outcome heterogeneity. The lack of kinematic control

along with the inability to investigate pure linear or angular acceleration was an experimental weakness that later investigators attempted to address (Gennarelli et al., 1982). The inability to experimentally control head kinematics led to the development of new neurotrauma models. While these models allowed for greater experimental and user control, these new models shifted away from clinically-relevant concussion injury.

1.6.2 Inertial Loading Neurotrauma Model without Impact (Whiplash Injury)

The next set of models moved away from investigating TBI with rapid and complete recovery (Ommaya & Gennarelli, 1974). The motivation for development of this type of model was to investigate brain injury through non-contact inertial loading. These animal models were designed to rapidly accelerate the head without direct contact. Along with this new model the understanding and direction of concussion/TBI research changed. Instead of focusing primarily on concussion defined in animals by recovery of reflexes, researchers suggested focusing on expanding the definition of concussion to include head injuries in which prolonged unresponsiveness was observed (Ommaya & Gennarelli, 1974). This new experimental model focused on recreating diffuse brain injury that resulted in what was designated “traumatic unconsciousness.” This condition described an experimentally-induced paralytic coma that was reliably induced by exposure to substantial inertial loading on the head as a result of translational and angular acceleration. The resulting forces were hypothesized to induce shear strain in the brain that led to diffuse subdural hematomas and coma (traumatic unconsciousness) in animals (Ommaya & Gennarelli, 1974).

The main design feature was to eliminate direct contact with the head and was

accomplished through the use of an actuator capable of moving the head in the sagittal plane, with a 60-degree arc at different speeds (Figure 1.3). A single acceleration-deceleration pulse would induce shear strains in the brain leading to diffuse axonal injury. One major pathological finding from this type of strain-acceleration model in non-human primates was acute subdural hematomas (ASDH) (Gennarelli & Thibault, 1982; Gennarelli et al., 1982; Gennarelli et al., 1998). These types of injuries are most often seen in patients with severe brain injuries with GCS scores in the 3–5 range (Gennarelli et al., 1982). The resulting pathology in this model is similar to that observed in severe whiplash injury (Bandak, 2005; Ommaya et al., 1968). When deployed in non-human primates, this model successfully reproduced graded coma as observed in human patients with severe TBI. However, this model was designed to investigate moderate and severe TBI. It was limited to non-human primates and is confounded by the use of anesthetics during experimental injury.

A related animal model used an inertial loading system in a pig model (Meaney et al., 1995; Ross, Meaney, Sabol, Smith, & Gennarelli, 1994; Smith et al., 1999; Smith, Chen, Xu, et al., 1997). The motivation for the design of this injury model was to investigate diffuse axonal injury (DAI), which is seen in patients with severe TBI (Adams et al., 1983; Gennarelli et al., 1982). The model utilized a similar design to that deployed in the non-human primate model. In this model, miniature pigs were anesthetized and the head was rapidly rotated left to right in a 60º–105º arc with an actuator. The traumatic insult lasted less than 25 milliseconds. Unresponsiveness measured by lack of spontaneous eye opening, corneal reflexes, and response to pain would persists for 5 to 7

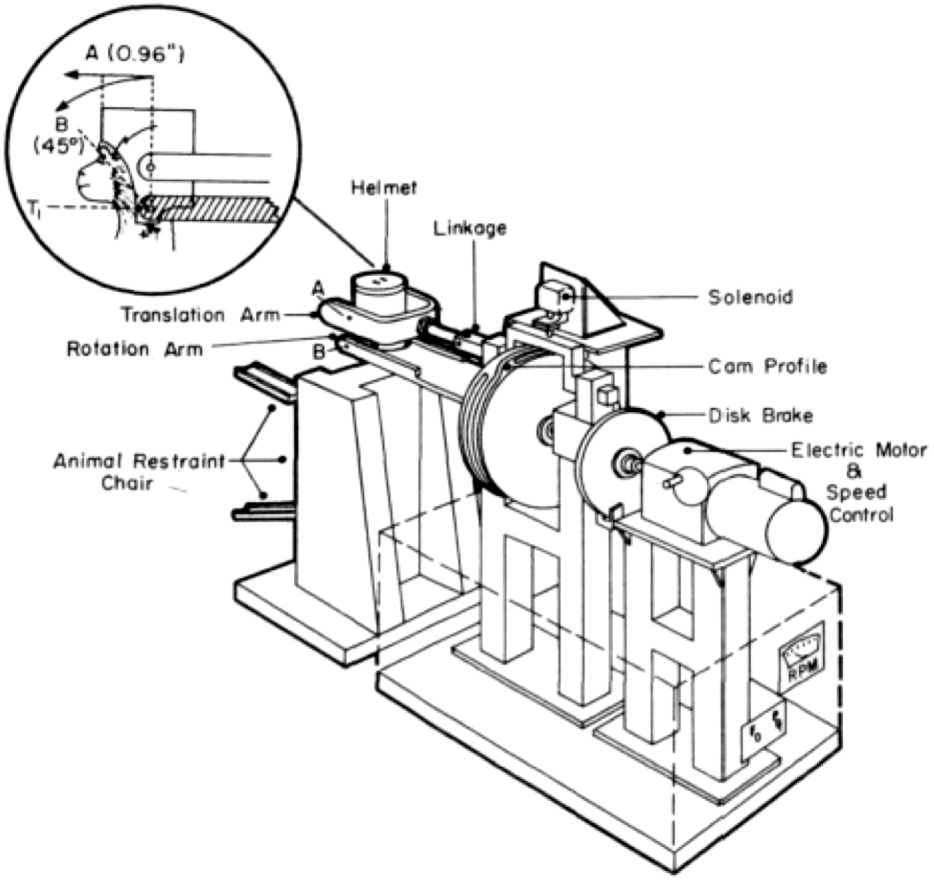

Figure 1.3: Inertial loading neurotrauma model (Head Acceleration Device).
The device allowed for both translational and angular acceleration without impact to the head. Reprinted from (Ommaya & Gennarelli, 1974).

minutes after a single experimental injury and resulted in brain pathology consistent with diffuse axonal injury (DIA) with hallmark axonal retraction bulbs that characteristically immunostain with antibodies directed at the amyloid precursor protein (APP) (Smith et al., 2000). These inertial loading models relied on an unnatural pulse of acceleration-deceleration motion to induce brain injury, consistent with DAI and ASHD (Lighthall, 1988). As with the previous inertial model this model was limited to a specific animal species and is confounded by the use of anesthetic during experimental injury and restricted in modeling only non-contact inertial injuries.

1.6.3 Open-Head Impact Models without Head Motion

The next groups of TBI injury models consists of direct brain deformation without head motion. The motivation for these models was to investigate the pathophysiology of brain injury by recreating aspects of clinically relevant pathology. As TBI requires an application of mechanical forces, injury devices were chosen to provide reliable and repeatable insults. These type of injury models typically used either a pressurized fluid column or a rigid metal piston to directly impact the dura through a craniotomy. Head motion was undesirable and unnecessary to induce injury because the fluid or piston directly transferred energy to the brain tissue.

Fluid Percussion Models

The fluid percussion injury is a common method for the study of TBI. The model

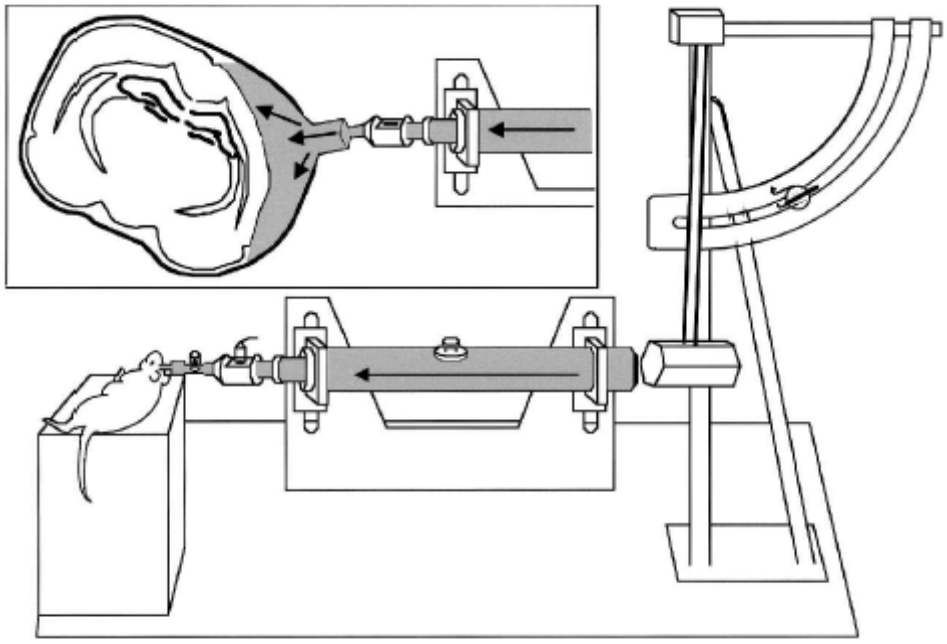

Figure 1.4: Cartoon of the fluid percussion injury model.
This model is used to cause diffuse brain movement in the epidural space with a pulse of fluid. Reprinted from (Prins & Hovda, 2003)

was initially used with rabbits (Lindgren & Rinder, 1965) and cats (Sullivan et al., 1976). The injury was later adapted for rodents (Dixon et al., 1987; McIntosh et al., 1989) (Figure 1.4). The injury requires a craniotomy prior to injury leaving the dura intact. The location of the craniotomy is usually located between bregma and lambda on the sagittal suture (McIntosh, Noble, Andrews, & Faden, 1987) (midline) or 4 mm lateral of the suture (lateral) (McIntosh et al., 1989) The device consists of a cylindrical reservoir filled with an isotonic saline solution. Before injury the animal is anesthetized and a volume of fluid is injected into the epidural space at a specific pressure. Injury severity is based on injected pressure with low-grade injury (1.0 Atm), moderate injury (1.5–2.0 Atm), and high-grade injury (2.5–3.6 Atm) (McIntosh et al., 1989). The fluid percussion model is limited in modeling direct energy transfer injuries and is confounded by the use of anesthetic during experimental injury and the use of a craniotomy to induce injury.

Controlled Cortical Impact

The motivation to develop the controlled cortical impact model (CCI) was to independently control both the velocity of impact and the resulting brain deformation (Lighthall, 1988). The model has been applied to a variety of animal species: ferret, mouse, rat, swine, and primate (see review (Bolouri & Zetterberg, 2015)). The device relies on either a pneumatic piston or solenoid to drive an attached impactor tip to a desired velocity up to 10 m/s (Lighthall, 1988). Before injury the mouse is restrained in a stereotaxic frame where a craniotomy is performed. Injury severity is determined by depth of impact, tip dwell time, tip diameter, and impact velocity. Solenoid-drive CCI remains a popular choice among investigators and is commercially available (Figure 1.5).

The model is limited in modeling direct energy transfer injuries, contusion injuries, and clinical validity. The CCI model is confounded by the use of anesthetic during experimental injury and use of a craniotomy for injury. Moreover, serious concerns remain with the validity of these models when control animals undergo a craniotomy procedure. The craniotomy itself was found to induce morphology, biochemical, and behavioral changes compared to sham (no craniotomy) mice (Cole et al., 2011).

Figure 1.5: Controlled-Cortical Impactor.
Reproducible controlled cortical trauma device sold by Leica Biosystems. Reprinted from Leica Biosystems product website (www.leicabiosystems.com).

1.6.4 Closed-Head Impact (CHI) Models Designed to Eliminate Head Motion

Closed-head impact models were designed to overcome the limitation and confounders associated with craniotomies. This specific class of TBI model is designed to eliminate head motion. The motivation was to investigate closed-head injuries found in motor vehicle accidents and were able to model focal head injury including skull fracture and cortical contusion.

Weight drop model

Weight drop method of injury involves a free falling weight guided by a tube. The weight's mass, size and height can be adapted to change energy transferred to the skull. One model of note was designed and used by Shohami et al. (Shapira et al., 1988; Shohami, Shapira, & Cotev, 1988). Rats or mice are anesthetized and a weight (250 grams) is dropped from a height ranging between 1 – 2 cm onto the exposed skull with the skin retracted (Y. Chen, Constantini, Trembovler, Weinstock, & Shohami, 1996; Flierl et al., 2009; Shapira et al., 1988; Shohami et al., 1988; Stahel et al., 2000). The weight drop device uses a metal rod and a flat silicone tip attached to the impacting end. The animal is placed on a flat surface below the tip. The device can be adapted in injury severity and modified for different animal species by adjusting the rod diameter and increasing the weight of the rod. Unique to these series of research publications was the addition of evaluating the motor and reflex function of the animals after injury at different times and assigning a score, called the Neurological Severity Score (NNS). Further description of the NSS will be discussed later in chapter 3. Survivability after injury is a concern. Immediately following injury, apnea is the leading cause of death. Following 24 hours, mortality is attributed to hypoxia, ischemia, edema and hematoma. Surviving mice show signs of skull fracture and skull depression at site of injury (Y. Chen et al., 1996). To increase survivability supporting oxygen is administered to the animals after injury (Tsenter et al., 2008).

Closed-head CCI model

Motivation for the development of the closed-head CCI model was (1) eliminate

the need for a craniotomy and (2) allow for repetitive TBI. These type of models use the exact same or similar device as the CCI such as a pneumatic or solenoid driven piston (Laurer et al., 2001). Mice are typically used. Before injury either the skin is retracted (Laurer et al., 2001; Uryu et al., 2002) or the skin is pulled tight (Mouzon et al., 2012) so at to maximize energy transfer. Head motion is constrained during impact by a rubber pad placed under the head and head holders are positioned to remove lateral movement. As this model uses the already designed and validated CCI device the repeatability of injury is established. The main advantage is the model allows the examination of multiple reparative hits with the same animal. Following injury, it has been reported that all animals hit showed signs of acute apnea lasting from 3 to 30 seconds. Apnea has been observed to significantly increase after multiple hits on the animal (Mouzon et al., 2012). The closed-head CCI model is limited in modeling only crush injuries and is confounded by the use of anesthetic during experimental injury and resulting trauma from skull crush.

1.6.5 Closed-Head Impact (CHI) Models Designed for Restrained Head Motion

The next set of models is characterized as CHI models with restrained head motion. The motivation was to model traumatic coma and create a diffuse brain injury. The main requirement for these models is to allow restrained head motion with the use of a foam pad.

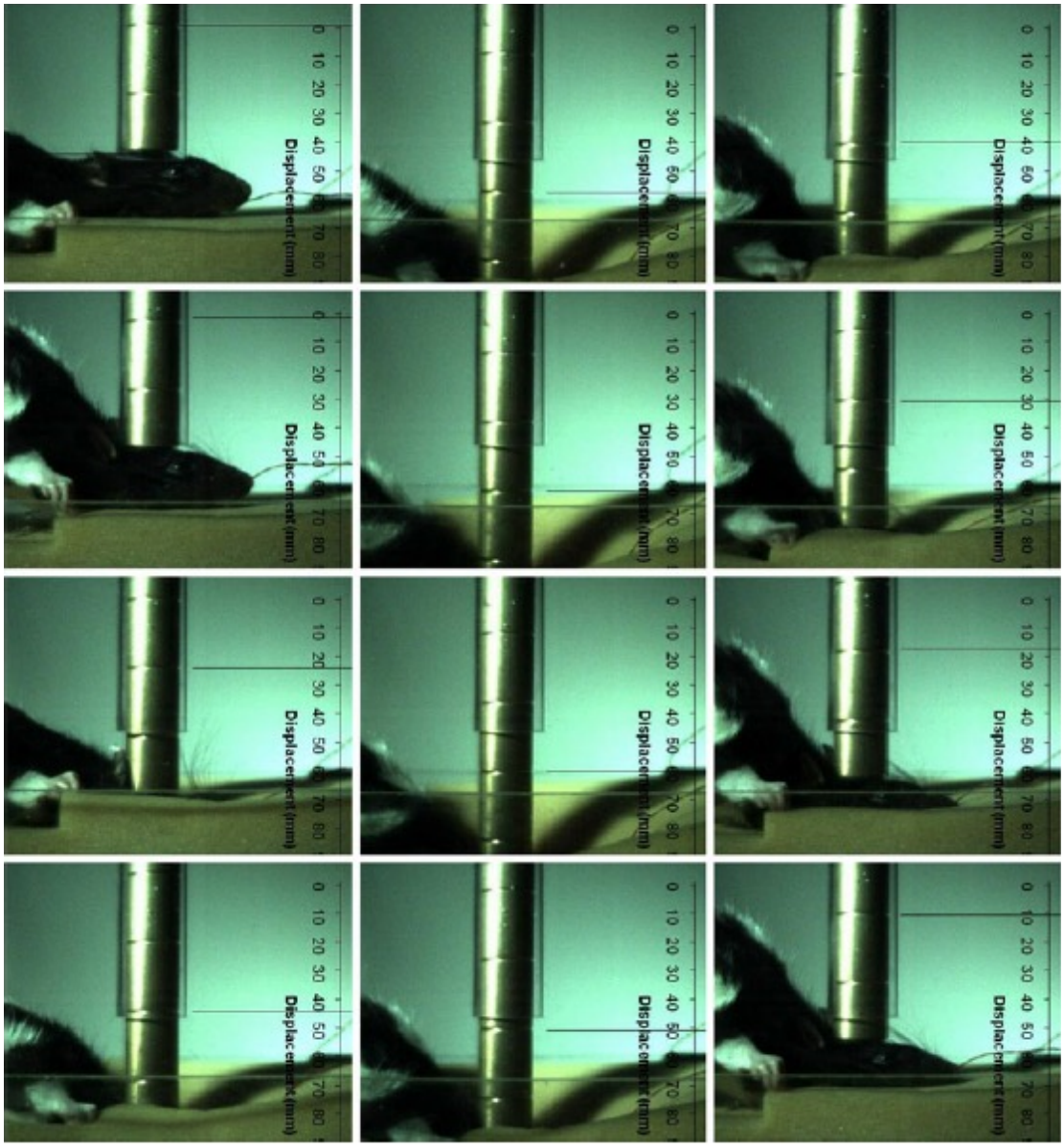

Figure 1.6: Head kinematics for the weight-drop model.
The upper left image shows time of impact and subsequent images were taken at 8 ms intervals. The kinematics show an initial impact followed by a second impact after the head rebounds. Reprinted from (Viano, Hamberger, Bolouri, & Saljo, 2012).

Marmarou's weight-drop model

The Marmarou's weight-drop is the classical closed-head injury model which allows for limited head motion (Marmarou et al., 1994). The device was designed as an

alternative to the fluid percussion model. This closed-head injury model was developed to allow for impact acceleration of the head in rats. Two different trauma levels were decided based on 100% survival rate, which they classified as mild injury and a 50% survival rate, which was classified as severe injury. To accomplish this the design incorporated a stainless-steel disk, which was fixed to the top of the skull to prevent skull fracture and increase survivability. Head motion would be allowed by placing the animal on a foam bed with a known spring constant. This model concept consisting of a weight-drop and a foam pad resulting in vertical acceleration has been adopted for mice (DeFord et al., 2002). Although, the model allowed for head acceleration, the model is confounded by severe skull compression and contusion. Further confounding factors include the need for mechanical ventilation to increase survivability after severe injury (Marmarou et al., 1994), the use of anesthetics, and kinematic analysis during impact revealed a rebound impact of the weight, leading to an additional unintended hit (Viano et al., 2012) (Figure 1.6).

Closed-Head CCI Model with Helmet and Foam Base

This next model was designed by Petraglia et al. and improves upon the closed-head CCI model which was designed to eliminate head motion (Petraglia, Plog, Dayawansa, Chen, et al., 2014; Petraglia, Plog, Dayawansa, Dashnaw, et al., 2014) (Figure 1.7). The main design requirement for the model was not to induce skull fracture. The injury is induced by a CCI device. Modifications to the impactor rod included adding rubber to reduce the likelihood of skull fracture. Further care was made to design a helmet of stainless-steel measuring 3mm thick with a 6 mm diameter. Placement of the

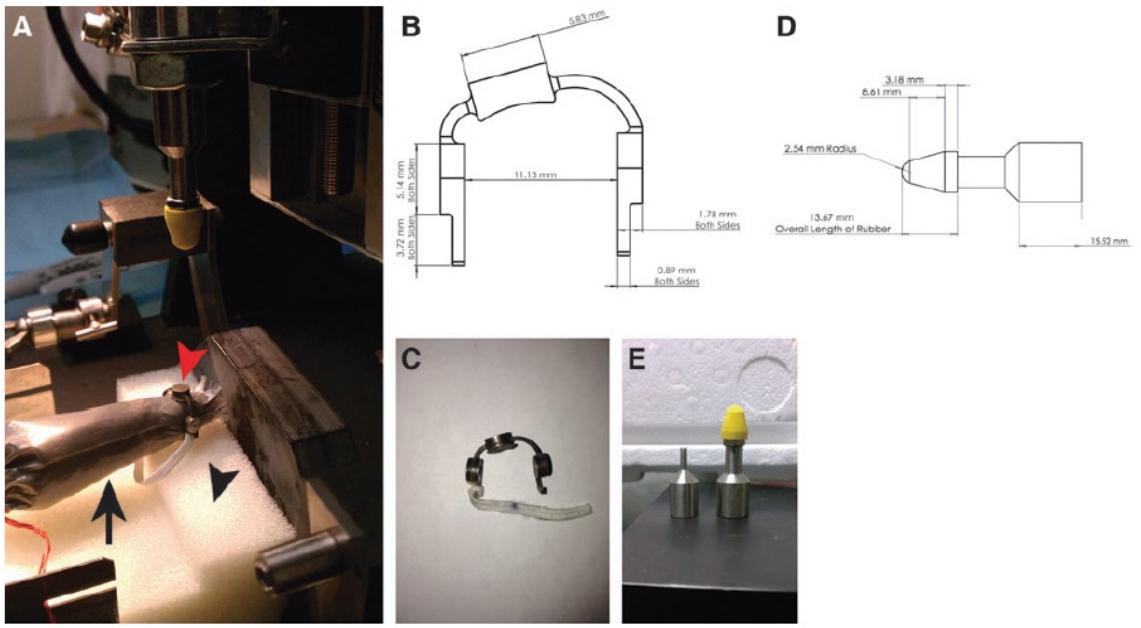

Figure 1.7: Closed-head impact model using a CCI device.
A) Device set-up with non-anesthetized mouse (black arrow) with helmet (red arrow). The impactor tip hits helmet accelerating the head into the white foam bed (black arrowhead). B-C) Drawing and photo of helmet. D-E) Drawing and photo of modified impactor rubber tip. Reprinted from (Petraglia, Plog, Dayawansa, Chen, et al., 2014)

helmet prevented skull fracture and spread the force of impact. Head motion was restrained by placing the mouse on a foam bed. The impacting angle of attack was specifically chosen to limit rotational acceleration but allow linear acceleration of the head into the foam bed. Velocity of the impact was chosen to be 5 m/s with an impact duration of 100 msec. Unique to this model was the use of non-anesthetized animals immobilized by a plastic bag with a hole allowing for head movement and ventilation. This model also performed a neurological assessment using the NSS protocol after final impact injury. The focus of the work was on repeated impacts entailing 6 impacts daily for 7 days (42 total hits). As categorized, this model has many similarities to the Marmarou's weight drop and overcomes many of the weaknesses with the helmet and

padded rod. By doing so, the model is based on a design to limit head motion, allow for linear acceleration only and ignores the angular acceleration component of head injury. (Petraglia, Plog, Dayawansa, Chen, et al., 2014; Petraglia, Plog, Dayawansa, Dashnaw, et al., 2014).

1.6.6 Closed-Head Impact (CHI) Models Designed for Unconstrained Head Motion

The next set of models move away from the classical ideas associated with closed-head injuries (restraint head motion). Motivation for these models focus on reproducing the biomechanics associated with concussions seen in sports. Analysis of head impacts showed that high velocity impacts and rapid rotational acceleration were the major drivers in mild TBI and concussion (Viano et al., 2009; L. Zhang et al., 2004). Using similar devices, these models set to deliver closed-head injuries with rapid rotational or angular head acceleration.

1.6.7 Horizontal-rotation closed-head impact model

Two models have been published to induce horizontal (anterior-posterior plane) rotational head motion. The basic input mechanics are the same as the Marmarou method (Marmarou et al., 1994). Using a hollow tube guide a bolt/mass with a desired weight is dropped at a set height on top the head of a mouse. The anesthetized mouse lays prone on either a delicate task wiper (Kimwipe) or a slit piece of aluminum foil (Figure 1.8). For the Kimwipe model the researcher places the animal's head under the guide tube holding onto the tail (Meehan, Zhang, Mannix, & Whalen, 2012). When hit the mouse breaks the delicate tissue, drops horizontally and a researcher holds the tail, preventing the body

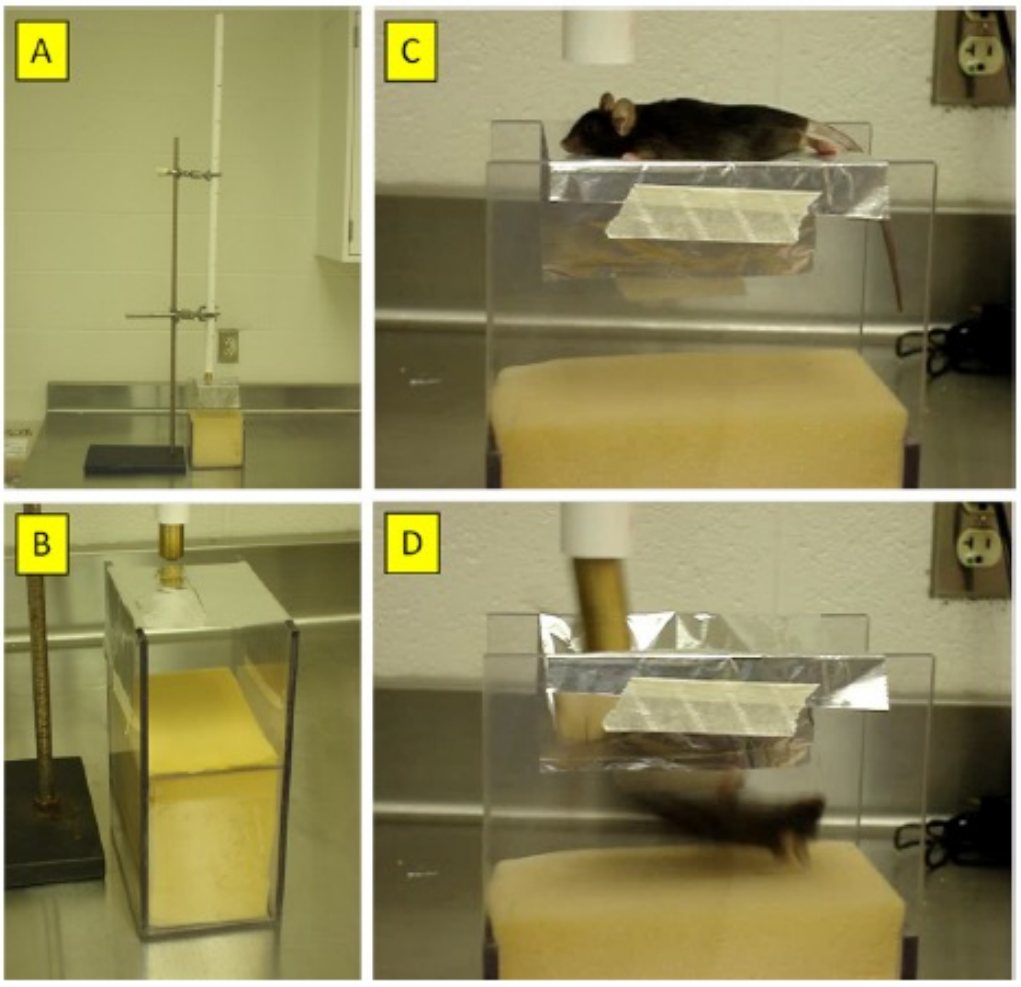

Figure 1.8: Horizontal-rotation CHI model.
A) The model uses a modified weight drop method (Marmarou et al., 1994). B) Photograph of the aluminum foil with slit and foam pad. C) Location of mouse prior to impact injury. D) After impact the whole body of the mouse rotates 180º horizontally. Reprinted from (Kane et al., 2012).

from falling. The aluminum foil model uses an H- shaped framed box in which the foil is placed on top and a sponge is located 10 cm below the foil. The animal rests on the foil and when hit rotates from prone on the foil to supine on the sponge (Kane et al., 2012). What sets these models apart from the other models discussed is that they allow for unconstrained rapid horizontal head rotation, use a reliable gravity driven impact method and can provide repeat hits to the same animal. Yet, the models are limited in horizontal

head motion and are confounded by anesthesia and possible skull crush.

Another approach to inducing horizontal head acceleration has been the development of the CHIRMA (closed-head impact model of engineered rotational acceleration) model (Namjoshi et al., 2014). The model is a re-engineered design similar to the model developed by Nilsson et al. and modified to be done with mice. The model has been extensively calibrated with the use of a 10,000 fps video camera to measure piston velocity. The mouse lays supine and a piston is accelerated with compressed air to directly hit the top of the head. The resulting head motion is in an upwards trajectory resulting in horizontal rotational acceleration. Max angle of head deflection was measured at 149 degrees (2.9 radians). This high angle of deflection is a result of the model design and causes neck flexion (chin to chest). The murine kinematics results were scaled by using an equal stress/ equal velocity approach. The purpose and reasoning behind the choice of input parameters such as piston velocity is not elaborated. The model is limited by flexion head motion and is confounded by anesthesia, and directly impacts the head possibly causing skull crush injury.

Momentum Transfer model

The momentum transfer model inflicts an injury by transferring the momentum of a moving object to the head. To be classified as this model the moving object cannot directly impact the head of the animal and must allow unrestrained head motion after impact. A design of this type of model uses a custom fabricated helmet attached to the head of a rat (Viano et al., 2009) (Figure 1.9). Viano *et al.* developed a momentum transfer model with the purpose to simulate head injuries found in professional football.

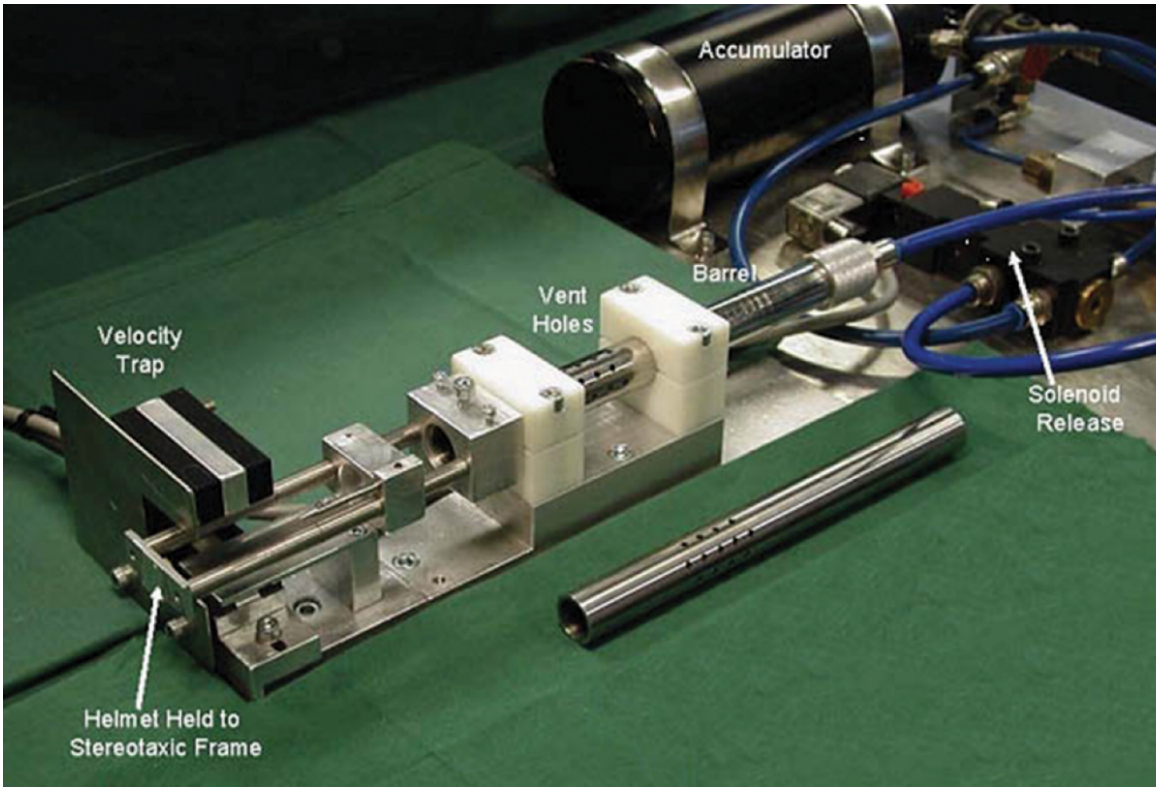

Figure 1.9: Ballistic impact momentum transfer model.
The model uses compressed gas to accelerate a weight down a barrel. The weight leaves the barrel traveling at a constant velocity and measured by the velocity trap. The helmet is attached to the head and the rat is allowed to freely move after impact. Reprinted from (Viano, Hamberger, Bolouri, & Saljo, 2009).

The motivation for the model was to simulate concussion. The model needed to incorporate a high impact velocity in order to induce rapid head acceleration. A unique aspect to the design of the model was using measured football kinematics which result in injury and scale those injuries to a rat. The equal stress / equal velocity approach was used to scale conditions seen in football to a rat. With this approach impact velocity and change in head velocity given to the rat should match what is seen in football. Acceleration and duration of the hit needed to be scaled to the rat. To model different severity of head injuries seen in football concussions three impact velocities of 7.2 m/s,

9.3 m/s, and 11.2 m/s were chosen. The resulting human head accelerations (Pellman, Viano, Tucker, & Casson, 2003) from those impact velocities were scaled to the rat. The model was then developed to reproduce the impact velocities and scaled accelerations calculated.

Viano *et al.* model was designed with two major requirements to meet the objective to simulate football head injuries in a rat. The first was the device needed to have an impact velocity range of 7.2 m/s to 11.2 m/s. The second was to incorporate a helmet, which would allow for short duration and acceleration of the head. The helmet also protected the skull from the high velocity impacts. To achieve these requirements, the ballistic impactor fired a weight and transferred the momentum to the helmet attached to the head. The inspiration for the momentum design was based on testing equipment used for concussion with the Hybrid III crash-test dummies. The ballistic impactor worked by filling an air tank with a set pressure and releasing the pressure with a solenoid value. A barrel connected to the value housed a weigh and when the value opened the gas would accelerate the weight down the barrel. Near the end of the barrel vent holes were placed to vent the gas and allow for constant velocity. The weight left the barrel (ballistic impactor) and a light gate measured the velocity. The helmet was fixed to left-side of the head and an accelerometer was attached to the non-impact side, measuring the head kinematics. 125 mm from the end of the tube magnets were used to help place the helmet in the proper location. The weight would impact the helmet and the rat's head and whole body was free to move (Viano et al., 2009).

Viano *et al.* model is unique because the purpose and objective of the model

dictated the design and injury parameters. It is noteworthy to mention the model is able to match the velocities and scaled accelerations of that seen in concussive football players. At the same time equal stress and equal velocity scaling assumes similar geometries. This caveat brings to questions the validity and interpretations of the results from the model. This model is limited to a specific animal species and the requirement of a helmet. Results are confounded by the use of anesthetic during experimental injury, unrestricted body motion after impact, and added mass to head (Viano et al., 2009).

1.7 Conclusion

Many animal models have been developed to study TBI. These models play a key role in the development and testing of hypotheses. The spectrum of models each have characteristics which allow the researcher to control certain conditions relating impact TBI. The early models were interested in the study of concussion and their models reflected their purpose. The critiques of those early models led researchers to control certain aspects of the impact and the motion of the head. While these models are able to produce TBI injuries and investigate the resulting sequelae, the purpose of the models and the clinical relevance remains ambiguous.

For example, we described two categories of close-head impact models. One model constrains head motion while the other allows for horizontal rotation. Both categories claim to model repeat, mild TBI but it is evident the resulting head motions are completely different by design. Which goes back to the question, what is the purpose of the model? Each closed-head impact model (constrained or unconstrained) induces brain

injury and subsequent TBI pathology. These results are not new and have been previously reported in other completely different TBI models (such as the CCI). The more significant interpretation of experimental results would be comparing how one CHI model differs from the other using similar input injury parameters. A clearer understanding of the similarities and difference between these two CHI models with regards to the input, kinematics and sequelae would provide generality and explanatory power to the close-head impact classification.

1.8 Thesis Overview

Early stage CTE pathology shows early and prominent perivascular tau accumulation with glial and neurofibrillary tangles supporting the likely early pathogenic involvement of microvascular, blood-brain disruption pathology leading to secondary neuroinflammation. Studies indicate an important role for neuroinflammation involvement in the pathogenesis of tau neuropathology (Bhaskar, Hobbs, Yen, & Lee, 2010; Tan et al., 1999). Furthermore, activated microglia, reactive astrocytes, and infiltrating perivascular macrophages produce potent pro-inflammatory mediators that induce aberrant tau phosphorylation, oxidation, and aggregation (Bhaskar et al., 2010; Tan et al., 1999).

Taken together, this putative pathogenic cascade provides a plausible and testable mechanism linking impact neurotrauma to mild TBI and late-emerging CTE. From a mechanistic perspective, we hypothesize that closed-head impact neurotrauma injury causes biomechanical forces in the brain that lead to (i) focal cerebrovascular damage and

blood-brain barrier (BBB) disruption; (ii) loss of neurovascular integrity; (iii) extravasation of red blood cells and plasma proteins into the brain parenchyma; and (iv) perivascular accumulation of hemolytic products.

We postulate that impact-induced head acceleration is the primary mechanism of injury leading to impact-related CTE. We hypothesize that biomechanical forces transmitted to structures in the brain during closed-head impact neurotrauma induce acute concussion and disrupt microvascular integrity, damage neuronal axons, and activate secondary neuroinflammatory responses that progressively lead to development of the clinical signs and symptoms of persistent TBI and late-emerging CTE. Testing these hypotheses requires the use of animal models.

Therefore, we hypothesize that mice exposed to closed-head impact injury will trigger acute neurological signs associated with sport-related concussion as well as brain pathologies and long-term functional sequelae associated with CTE.

To test this hypothesis, we required an animal model and performed a diligent review of the current TBI animal models. In the following chapter we provide the rational for why these models are insufficient in testing our hypothesis. We discuss the design and development of a new impact neurotrauma model, methods used in measuring head kinematics and details comparing the kinematics between the blast and impact neurotrauma models. Chapter 3 presents the Boston University Concussion Scale and report on the acute effects following closed-head impact injury. In Chapter 4, we present results on brain pathologies and long-term functional sequelae after impact neurotrauma. Chapter 5 discusses the comparison between Blast and impact neurotrauma and the

resulting acute effects. We use numerical simulations to investigate the mechanism of concussion. The thesis concluded with a discussion and implications of this work.

Chapter 2: Impact Neurotrauma Model

Design controls provide the framework to prove the developed product meets user need and requirements. For medical device development the product development process follows Design Controls stated in FDA 820.30 and are similar to ISO-13485-7.3. These processes include design and development planning, design input, design output, design review, design verification, design validation, design transfer, design changes, and design history file (FDA 21 CFR 820.30). Chapter 2 describes the rationale for a new impact neurotrauma model and how injury requirements for the impact neurotrauma model guided constructing a prototype. We proceeded to use applicable product development and design controls in order to achieve a suitable model that would enable testing the hypotheses under consideration.

We developed a new murine closed-head impact injury model to elucidate the biomechanical and pathobiological mechanisms that trigger acute and chronic effects of impact neurotrauma. Specifically, we sought to understand what conditions trigger acute neurological effects (e.g., concussion) and relationship to long-term sequelae (e.g., CTE neuropathology) following closed-head impact injury.

2.1 Rationale for a New Impact Neurotrauma Model

2.1.1 Findings from Blast Neurotrauma Model

We developed a new murine blast neurotrauma model system to investigate the mechanisms of tau protein-linked neurodegeneration following blast exposure (L. E. Goldstein et al., 2012). This work was led by Mr. Andrew Fisher, a Ph.D. student in

Biomedical Engineering who is conducting his doctoral research in Dr. Goldstein's laboratory on this topic. The experimental shock tube simulates military exposure to blast resulting from improvised explosive devices (IEDs). Our system utilized a custom-designed 27-foot-long, 10-inch diameter helium-driven stainless steel shock tube developed and installed at the Boston University Neurotrauma Laboratory and was used to deliver reproducible, graded, non-lethal blast shock waves that are comparably military IED blasts (L. E. Goldstein et al., 2012). Mice were exposed to a left-lateral single sublethal blast. Anesthetized mice were secured in the prone position with torso protection to eliminate blast-lung injury (Figure 2.1). This assembly is connected to a metal armature that precisely positions the secured animal subject at a set distance within the open-ended shock tube. Placement of secured mice allowed for full range of motion (i.e., flexion, extension, lateral flexion, rotation) of the head in all three cardinal planes of motions. Multi-axial high-speed videography (100,000 frames per second) and post-acquisition kinematic analysis during blast exposure revealed rapid head acceleration that resulted in persistent focal microvascular disruption, neuroinflammation, cytoskeletal reorganization, and tau pathology in blast-exposed mice compared to sham controls. We also detected persistent changes in phosphorylated tau protein neurochemistry, abnormal neurophysiology (decreased axonal conduction velocity, impaired long-term potentiation of synaptic plasticity in the hippocampus), and corresponding deficits in hippocampal-dependent learning acquisition and memory retrieval in the Barnes maze (L. E. Goldstein et al., 2012). These brain pathologies and functional deficits mirror many of the key changes observed in humans after blast exposure (L. E. Goldstein et al., 2012). Moreover,

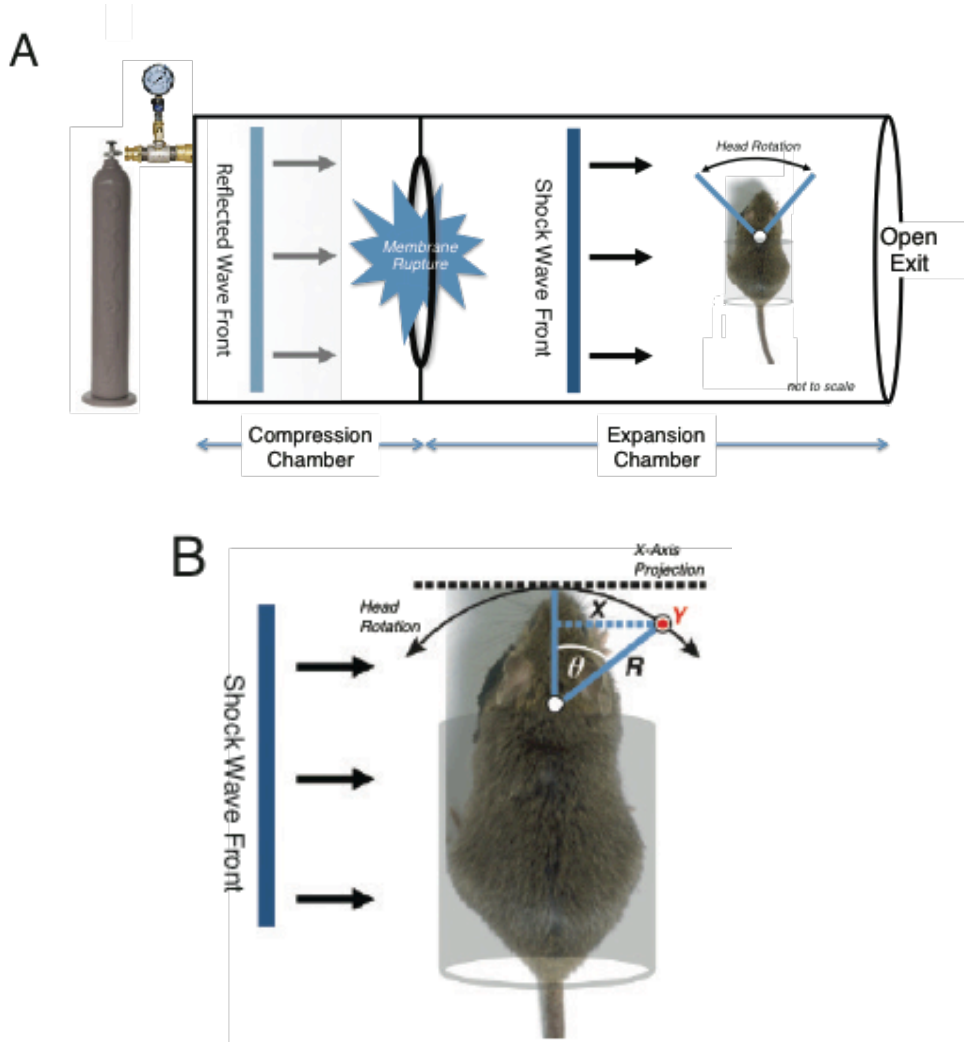

Figure 2.1: Schematic of the murine blast neurotrauma shock tube model system. A) Cartoon of shock with mouse placed inside the open end. B) Head motion during blast neurotrauma (L. E. Goldstein et al., 2012).

these effects were not observed when the head was immobilized during blast exposure. This key finding supports the hypothesis that long-term sequelae following blast exposure results from acceleration of the head induced by inertial forces associated with blast wind ("bobblehead effect"; (L. E. Goldstein et al., 2012)) rather than the direct effect of the blast shock wave traversing the brain as previously thought.

Our blast neurotrauma work reveals two key findings supportive to the investigation into the effects of sport-related concussion; (1) Long-term effects of military-related blast injury are very similar, if not identical, to the long-term effects of sports-related concussive mTBI in human brain; (2) Angular acceleration resulting from blast neurotrauma is sufficient to induce brain injury and CTE-linked neuropathology. We hypothesize that angular acceleration resulting from impact neurotrauma would be sufficient to induce brain injury and CTE-linked neuropathology. This hypothesis guided the development of specific injury requirements and is discussed in the next section.

2.1.2 Critical Review of Prior Models and Injury Requirements for Impact Neurotrauma Model

A number of animal models have been designed to induce an injury comparable to moderate and severe TBI through controlled-cortical impact, fluid percussion and weight drop (Brody et al., 2007; Dixon et al., 1987; Lighthall, 1988; Lighthall, Dixon, & Anderson, 1989; McIntosh et al., 1989; Prins & Hovda, 2003; Shapira et al., 1988; Shohami et al., 1988). Fluid percussion and controlled-cortical impact method of injuries have also been scaled to produce a mTBI (Alder, Fujioka, Lifshitz, Crockett, & Thakker-Varia, 2011; Hamm et al., 1992; Xiong et al., 2013). Investigation into the basic mechanisms and sequelae of human traumatic brain injury (TBI) has led to the development of numerous animal models which rely on different methods of producing brain injury (see chapter 1). Gennarelli stated the “assumptions associated with past animal models has been that the mechanism of inducing head injury is not important” (Gennarelli, 1994). However, the procedure, method and mechanisms of producing the

injury in an animal models has immense implications on the model's ability of recreating a specific type of brain injury, clinical validity and translational capabilities of the model (L. E. Goldstein, McKee, & Stanton, 2014). Firstly, the modeling of the type of brain injury received must represent the human brain injury. Some widely used TBI animal models (i.e., controlled-cortical impact, fluid percussion) rely on a craniotomy procedure before brain injury and categorize sham mice as receiving only a craniotomy. Research into this sham procedure has revealed significant sensory and motor behavioral impairments, significant increase in cytokine concentration and morphology changes due to the craniotomy itself (Cole et al., 2011). However, clinically mild TBI usually does not include an open-head injury and therefore researchers adapted the weight-drop method and controlled-cortical impact model to induce closed-head mTBI injuries (Y. Chen et al., 1996; Flierl et al., 2009; Mouzon et al., 2012; Zohar et al., 2003). Similarly, sport-related concussions are closed-head injuries, which would require also a closed-head model for study.

Secondly, the forces and velocity parameters modeled must reflect the human case. Analyses of acceleration data and video footage from football impacts have revealed the heterogeneous response of head motion resulting from helmet impacts (Broglio et al., 2010; Guskiewicz et al., 2007; Hernandez et al., 2015; Pellman, Viano, Tucker, & Casson, 2003; Pellman, Viano, Tucker, Casson, & Waeckerle, 2003; Viano, Casson, & Pellman, 2007; Viano & Pellman, 2005). Although the multifaceted biomechanical responses have made determining the threshold of concussion injury elusive (Broglio et al., 2010; Guskiewicz et al., 2007), these recorded hits can be

classified as having both contact and inertial forces present (Meaney & Smith, 2011). The helmet has played a key role in dissipating the high velocity energy from direct contact loading and has greatly decreased skull fractures in sports (Gurdjian, Lissner, & Patrick, 1962; Rowson & Duma, 2011). Impulsive head motion absent of head contact with any object has been defined as pure inertial loading (Meaney & Smith, 2011). Inertial loading has been shown to reproduce diffuse axonal injury in animal models (Smith, Chen, Xu, et al., 1997; Smith et al., 2000). These models of inertial brain injury differ from other TBI injury mechanisms due to their specific design to eliminate contact/impact forces. Research has suggested that rotational acceleration induces shear-stress which causes tissue damage (Meaney & Smith, 2011; Ommaya & Gennarelli, 1974; Smith, Chen, Pierce, et al., 1997; Smith et al., 2000). Although, our blast model does not have direct impact from a solid object, the blast winds induced oscillating head acceleration through contact with the left-lateral side of the brain (L. E. Goldstein et al., 2012). Therefore, to model impact-induced concussion seen in sport athletes and compared to our blast-wind impact blast model, the impact neurotrauma model had the injury requirement of inducing motion by direct contact loading.

Additionally, TBI animal model designs have varied on the extent of allowed head motion (see chapter 1). Considerations regarding head motion played a key role in early concussion research when Denny-Brown and Russell reported that impacting an unrestrained head readily induced concussion, while fixing the head proved to be nearly impossible in inducing concussion (Denny-Brown & Russell, 1941; Shaw, 2002). Accelerometers embedded in football helmets have revealed rapid-rotational acceleration

as specific biomechanical characteristic associated with concussive injuries (Guskiewicz et al., 2007; Meaney & Smith, 2011). Studies using 6 degree-of-freedom accelerometers in football athletes have provided evidence to suggest head rotation may be a predictor of brain injury (Hernandez et al., 2015). While some animal models have been designed to limit the amount of angular acceleration (Kane et al., 2012; Meehan et al., 2012; Namjoshi et al., 2014; Petraglia, Plog, Dayawansa, Chen, et al., 2014; Petraglia, Plog, Dayawansa, Dashnaw, et al., 2014), our blast neurotrauma model allowed for head rotation (L. E. Goldstein et al., 2012). The blast wave initially interacts with the left-lateral side of the head inducing rapid-head acceleration from left to right and we hypothesized that this motion led to the development of CTE-linked neuropathology. Moreover, restraining the head resulted in prevention of behavioral deficits. Based on clinical and experimental results, allowance for unrestrained head motion was designated as a model injury requirement. Furthermore, the impact neurotrauma model was designed to complement the blast neurotrauma model, as such, injury requirements included; torso body restraints similar to the blast model and inducing a left-lateral head motion similar to the blast model.

Skull fractures are a particular concern especially with murine impact TBI models due to the thickness of the skull. As research investigations eliminated the craniotomy procedure and moved to a close-head injury, injury models started to include the addition of impactor tips and helmets to prevent skull fracture and allow repetitive injuries (Flierl et al., 2009; Mouzon et al., 2012; Namjoshi et al., 2014; Petraglia, Plog, Dayawansa, Chen, et al., 2014; Petraglia, Plog, Dayawansa, Dashnaw, et al., 2014; Viano et al., 2009).

In our mouse model, use of a pad was incorporated into the injury requirements to prevent skull fractures. In addition, the use of helmet or any other device that attached directly to the head was omitted and stated as an injury requirement in order to match the blast model.

In conclusion, we identified (7) essential injury requirement (Table 2.1). The designs and features of the impact neurotrauma model were incorporated to fulfill these requirements.

Injury Requirements	
R1	Closed-head injury
R2	Unconstrained head motion
R3	Torso body restraint
R4	Left-Lateral impact
R5	Padding on ipsilateral side of impact
R6	No head attachments (i.e., helmet, accelerometers)
R7	Direct contact loading

Table 2.1: Injury requirements

2.2 Feasibility Model: Pilot Concept Model and Design Inputs

A concept model was designed by using a commercial controlled-cortical impact device (MyNeuroLab) (Figure 2.2). Injury was induced by a solenoid-driven actuator with a modified impact probe. A steel metal part acted as a “helmet” by spreading the force of the impactor across the side of the mouse head, which rested on the opposite side. The sled-like system proved to eliminate skull fracture and crush injury by not directly hitting the skull with the impactor tip (Marmarou et al., 1994). By requiring the impactor to hit of the left-lateral side, the model allowed the freedom to control of head

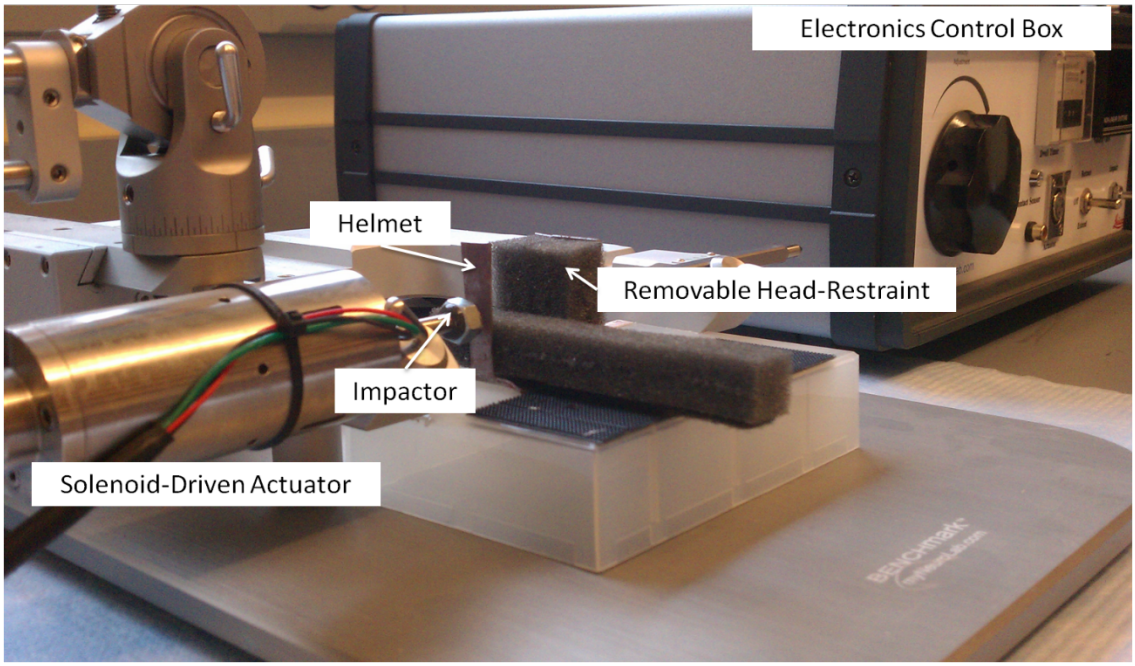

Figure 2.2: Concept model using a CCI commercial device.
A purpose-designed stereotaxic impactor system with custom-built head restraint system permit precisely controlled and highly reproducible impact neurotrauma with isolated rotational motion (without head restraint) or translational motion (with head restraint).

rotation with an adjustable foam pad. Velocity of the actuator was controlled electronically with a control box and could be set to impact velocities between the range of 1.5 m/s to 6 m/s. The crude concept model proved the feasibility of designing an impact neurotrauma model to satisfy the injury requirements (Table 2.1) . Furthermore, completion of a small cohort of animals and use of the device provided insights into specific design inputs, which were incorporated into the final design.

Design inputs for the new impact neurotrauma model included functional, performance, and user requirements chosen to improve upon the prototype and enhance the users' interaction and experimental efficiency of the new device:

(1) The impactor model is required to deliver impact velocities comparable to other published impact TBI models (4–9 m/s) (Viano et al., 2009, 2012) and human impact injury kinematics (Viano et al., 2009). We hypothesized this velocity range would be sufficient to recapitulate acute and chronic neuropathology and functional deficits associated with the corresponding head injuries observed in human subjects (L. E. Goldstein et al., 2012; McKee et al., 2009; McKee & Daneshvar, 2015; McKee et al., 2014; McKee et al., 2010; McKee et al., 2013).

(2) Impact velocity repeatability relative standard deviation is required to be less than 10%.

(3) Linearity of impact velocity range is required to have a coefficient of determination less than 0.95.

(4) Impact materials are required to exceed a workable life of 100 impacts.

(5) To satisfy IACUC protocols, all surfaces are expected to be bleachable and disinfectable and manufactured with appropriate materials.

(6) Impact design is required to meet all animal use and safety guidelines instituted by the University as well as local, state, and federal regulations.

(7) Graphical user interface (GUI) is designed to control input parameters, maintain experimental record (i.e., animal number, hit number, date time, injury group, experiment description), and maintain part records.

(8) Integrated software is designed to warn users with a countdown before impact.

(9) Ergonomic is designed to be at the same height level as a desk or lab bench.

(10) Impact device is required to be movable in a laboratory setting.

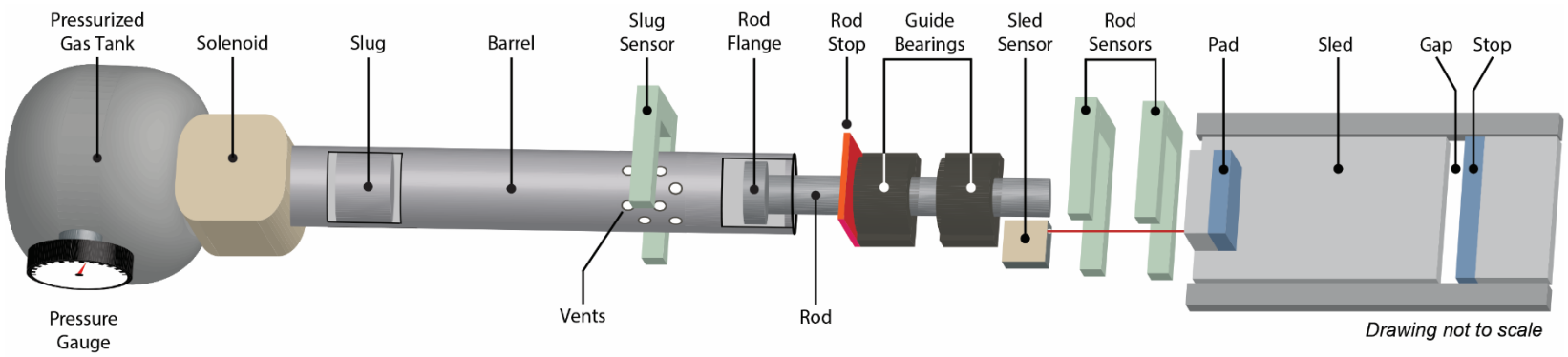

Figure 2.3: Cartoon schematic of the impact neurotrauma device.
Cartoon of the experimental murine impact neurotrauma model device. Compressed nitrogen fills the tank to a user-defined pressure. After tank pressure stabilizes the user activates the impact device software to open the solenoid value releasing the tank pressure. Released pressure accelerates the slug down the barrel until pressure is exhausted through the vent holes. Slug velocity is measured with a light gate prior to transferring its momentum to the rod. Rod traverses on guide bearings and velocity is measured before impacting the sled. Rod stop is a safety feature to prevent the slug from exiting the barrel. Rod transfers momentum to sled which travels 10 mm while the displacement of the sled is measured by a 100 kHz laser sensor. Non-anesthetized mice are restrained using a cone and Velcro. The mouse's head rests on sled with the left-side touching the pad. Sled transfers momentum to the head allowing for impact-induce head motion.

2.2.1 Design Output and Verification

Design outputs included the impactor, mechanical drawings created with Solidworks, part drawings, specifications, instrument use protocols, and instructions (Figure 2.3). The Initial design elements were based on a ballistic air gun system described by Viano *et al.* (Viano et al., 2009). Our new device was designed as a gas-driven captive- momentum-transfer instrument. To operate the device, the user enters a desired fill pressure into the custom-designed control software program collaboratively developed with fellow doctoral research, Mr. Andrew Fisher. Compressed nitrogen is then automatically discharged into a storage tank until the desired pressure (19 psig) is achieved. Tank pressure is continuously monitored to ensure pressure stability (+/- 3 %). The user is then directed by the software prompt to initiate the firing sequence. After a set safety delay, a computer-controlled, electronically-actuated solenoid is automatically opened, thus releasing the compressed nitrogen in the tank acceleration a precision-milled steel slug of known mass and dimensions through the instrument barrel. Vent holes near the end of the barrel release pressure behind the slug, thereby changing slug kinematics from an initially accelerating mass to a mass traveling at constant velocity. At the end of the barrel, the slug contacts a stainless steel rod of known mass and momentum and is transferred from slug to rod with high efficiency. The rod then travels a set distance on high-performance, low-resistance ceramic bearings before transferring momentum again after contact with a movable stainless steel sled. The sled consists of a stainless steel "helmet" analog with a foam pad where the mouse's head is placed next to the pad. Following impact by the rod, the sled directly contacts the mouse's head, resulting in

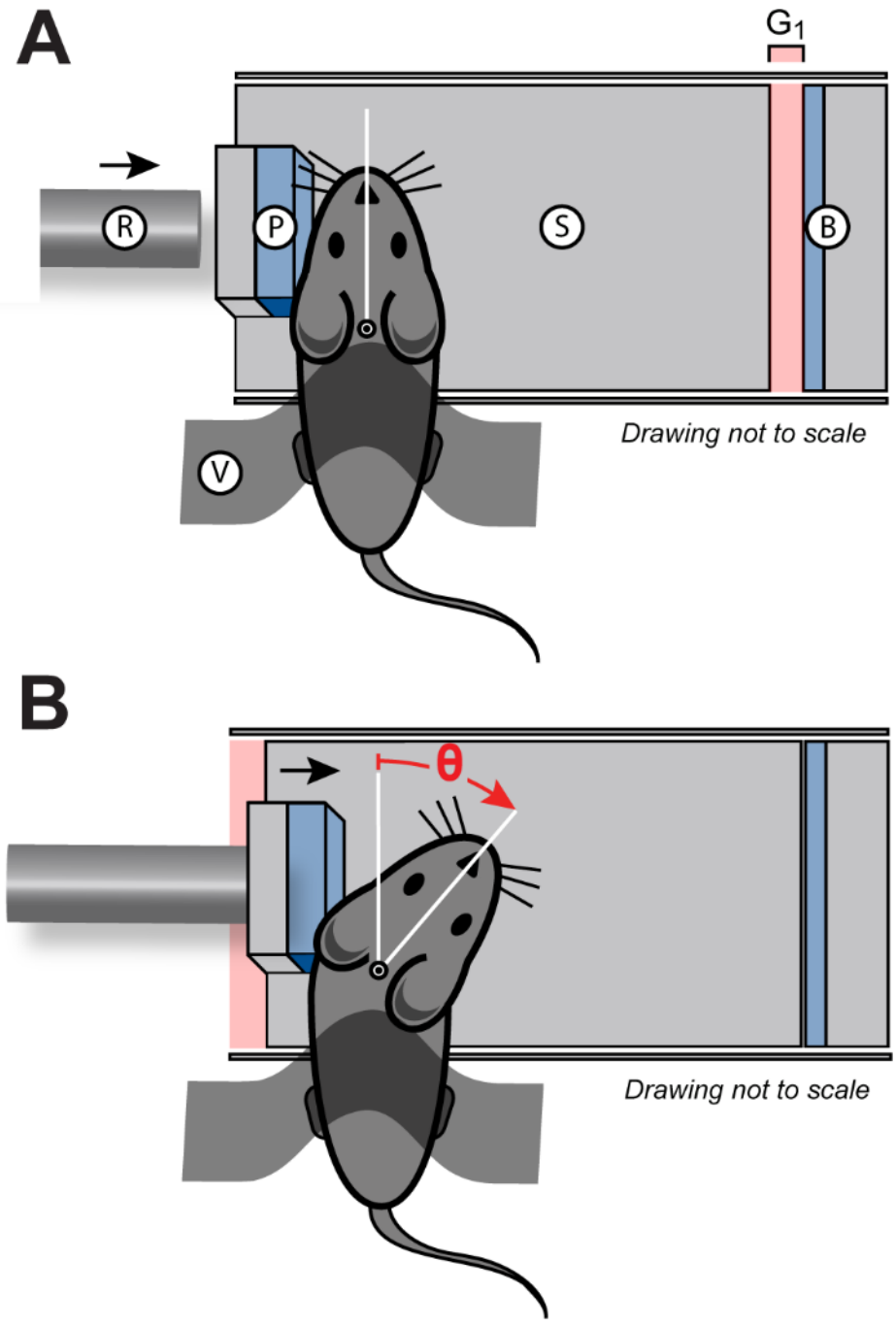

Figure 2.4: Cartoon of the sled and mouse during impact.
Panel A) The mouse rests on top of the sled (S). G_1 is the gap the sled is able to travel. Panel B) The rod (R) traveling at a constant velocity impacts the sled. The sled transfers its momentum to the head. The head is able to move freely and is rapidly accelerated. The kinematics of the hit can be measured. The sled is stopped by the back-stop (B). The body is restraint by a Velcro strap (V).

head acceleration. The head is able to move freely. The sled stops after a specific distance (Figure 2.3 and 2.4). Light gates are positioned between the vent holes and 1 cm before the rod to accurately record velocities of the slug and rod, respectively, for each impact. A precision laser displacement sensor is positioned above the rod and the laser directed to the left side of the sled, opposite of the pad.

Instrument safety was taken very seriously during instrument design and development. Pressure ratings and valves were all chosen to exceed the range of pressures anticipated for experimental operation. The tank is rated at 600 psig and stores pressure prior to impact. The tank is fitted with a 150 psig pressure relief value. The tank is also outfitted with a second ball valve to allow manual pressure release in the event the first ball valve fails. The movement of the slug, rod, and sled were designed to operate within a closed (i.e., "captive") structural system, thus eliminating the possibility of projectile injury to the operator or mouse. The impactor software was coded in Matlab and designed to meet specified user requirements. The software was developed through collaborative sessions with Mr. Fisher in which safety features, including an operator-initiated stop-fill mechanism, pressure stabilization monitor, automatic fill-pressure protection system, and an automatic countdown delay before solenoid activation were incorporated.

A software algorithm controlled the tank filling operation so as to match the user defined fill pressure to the digital pressure sensor attached to the tank. Performance of the filling algorithm was assessed by reliability tests that demonstrated a strong linear relationship between set fill pressure and tank pressure (slope 1.012, $R^2 = 0.99$, $p <$

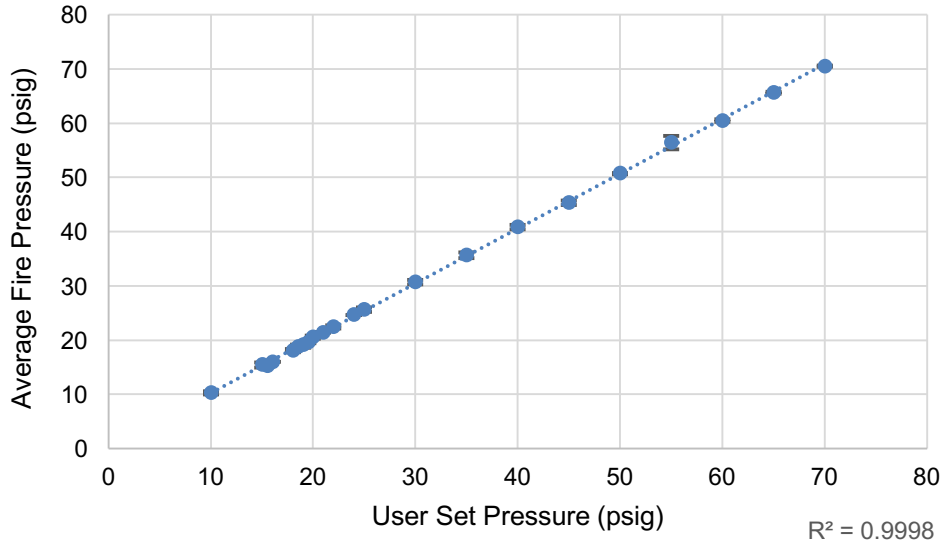

Figure 2.5: Reliability and accuracy of user-defined fire pressure.
The set pressure is set in the software by the user and the fire pressure is the pressure released to drive the slug.

0.0001, 95% CI [1.003, 1.021]) and a deviation from linearity of less than 0.2 % (Figure 2.5). The impactor software was operated through a user interface that allowed the user to enter in the animal number, experimental information and fill pressure. All relevant impact information including experimental information, the animal number, tank pressure, and velocity metrics for the slug, rod, and sled are automatically recorded and saved for future analysis.

Stainless steel slugs were designed and precision milled to specification for length, diameter, and mass. Engineering drawings with specific tolerances were provided to the Boston Universities Scientific Instrument Facility (SIF) for machining. Slug specifications required a mass tolerance of 0.3 grams to ensure reliable operation. Velocity of the slug was measured for each impact by a (LED diode) light gate positioned over a vent hole in the barrel. Length, mass, and slug number were entered into the

control software and the values used to calculate slug velocity for each impact. Velocity range, repeatability, and scalability tests were performed at different operational tank pressures. Linear regression analysis showed a linear fit (R^2 = 0.98) with a maximum 1.3% RSD for quality control instrument tests. The average life of the slug was 391.8 impacts, far exceeding initial design specification (Figure 2.6).

Incorporating a captive rod into the impactor design enabled a key safety feature by preventing the slug from exiting the barrel. The captive rod design solved a rather complex problem. To prevent the slug from becoming a projectile, the rod was designed as momentum transfer intermediate between the slug and sled. Starting position of the rod was designed to start inside the barrel so as to allow momentum transfer from the slug to the rod. After impact rod velocity was measured with light gates. To prevent the slug from exiting the tube, the total distance traveled by the rod was such that the slug was unable to exit. The rod-stop was designed as an added feature to prevent the rod from exiting its bearings. The rod was expected to sustain the greatest mechanical stress during operation and has the lowest service life (157.8 impacts). However, this was incorporated into the design of the impactor. When the rod fails the cap is disconnected from the steel shaft and drops next to the rod-stop. This failure occurs after the slug has stopped thereby always preventing the slug from exiting the barrel. Rod velocity was measured with two light-gates and had a velocity operating range between 6 m/s to 10 m/s with a linear fit of R^2 = 0.98. The maximum % RSD at different fire pressures was 1.6% and exceeds the design requirement (Figure 2.6). After impact with the sled the rod traveled a certain distance and its energy would be absorbed by the rod stopper.

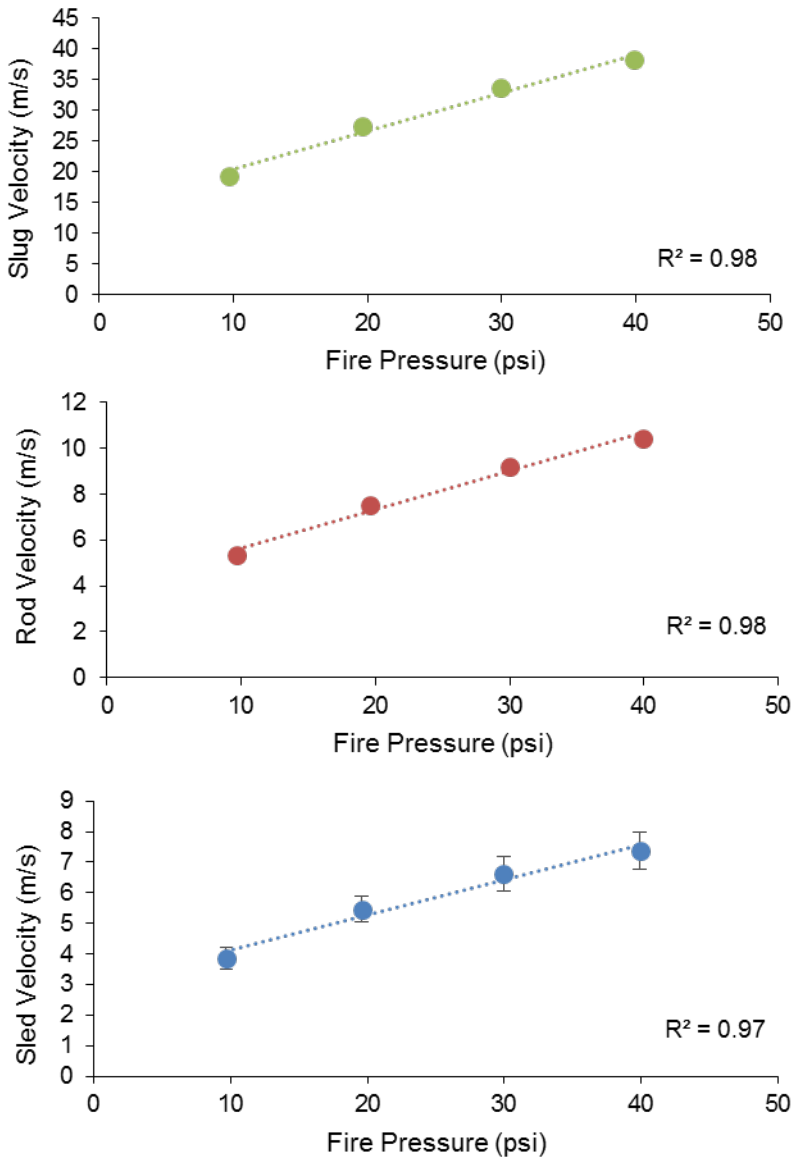

Figure 2.6: Repeatability and scalability of the developed impact neurotrauma device. (Instrument operation only). Repeatability was evaluated by performing five independent tests at each of four different tank fill pressures (9.6 psi, 19.6 psi, 30 psi and 40 psi) that covers the range of pressures anticipated for use in animal experiments. Relative standard deviation (RSD) of slug velocity was 0.5% to 1.3%. Rod velocity had a RSD range from 0.6% to 1.6 % and sled velocity RSD ranged from 7.6% to 9.3%.

The sled was designed to be a momentum transfer intermediate between the impacting rod and the animal's head. Briefly, contact of the impact rod with the sled results in momentum transfer to and linear translation of the sled. This was designed so that the impact rod does not directly contact the head. Engineering drawings were made in Solidworks and machined at the SIF. Sled part materials were chosen to withstand direct impact from the rod and prevent skull flexure and fracture. Sled velocity was determined by a 100 kHz laser displacement sensor and measured continuously during impact. Static measurement tests were performed to generate a calibration curve for the laser displacement sensor, determine reliability, and deviation from linear fit. The sensor deviation from linearity was measured at <4% (Figure 2.7). Results from the repeatability and scalability tests showed the sled velocity has a maximum %RSD of 9.5% and R^2 = 0.97 (Figure 2.6).

The animal platform was machined from aluminum to withstand cleaning solution required by the IACUC. The impactor device was built on a desk-height cart with lockable casters allowing for easy movement.

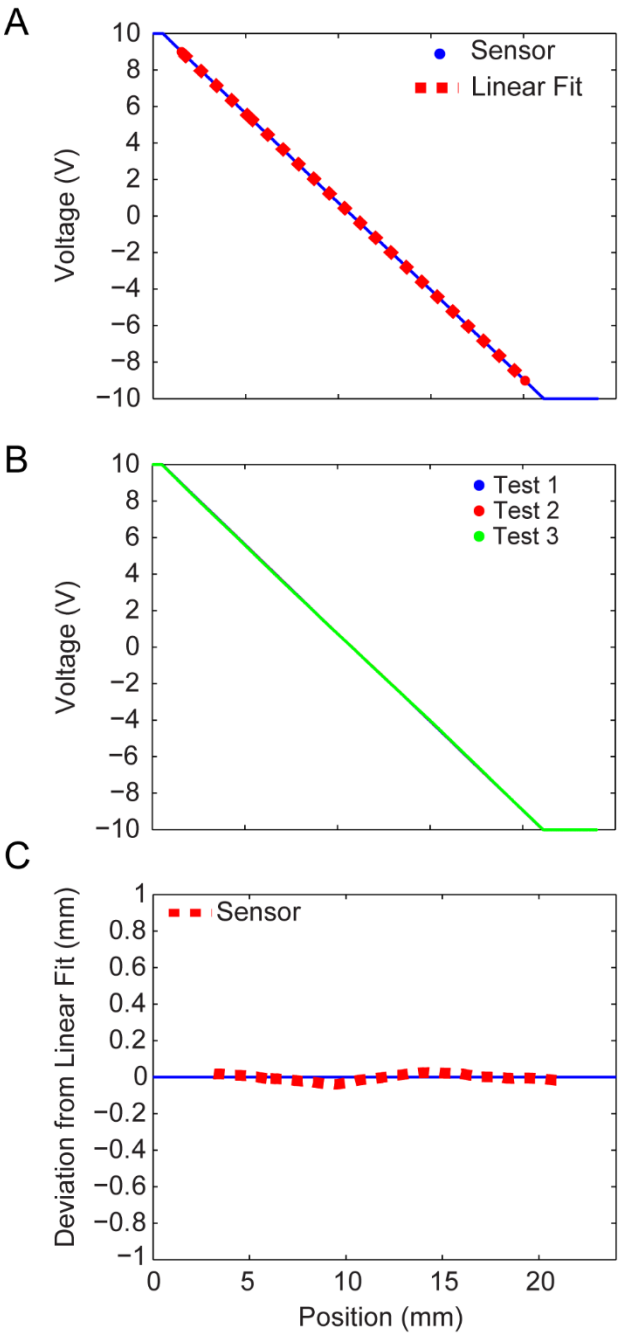

Figure 2.7: Laser displacement sensor calibration, repeatability, and deviation from linearity.

A) The laser displacement sensor was calibrated by static displacement. B) Repeated test with the laser sensor to show repeatability. C) Sensor meets the deviation from linear fit requirement (Deviation < 4%).

2.3 Kinematic Analysis of Impact and Blast Neurotrauma Models

The impact neurotrauma instrument was designed to model clinically-relevant concussive head injury and induce murine neuropathology similar to that observed in the brains of athletes with neuropathologically-confirmed CTE. From a biomechanics perspective, impactor was also designed to recapitulate head kinematics induced by our blast neurotrauma mouse model described (Section 2.1.1). Before validating the neuropathology of our model with animal subjects, we performed range finding experiments to determine operational and input parameters for the impact injury device. We hypothesized that by producing comparable head kinematics in both experimental models (i.e., blast, impact), we would induce similar acute and chronic effects of neurotrauma, including CTE-linked neuropathology. As described in this and subsequent chapters of this thesis, our results were surprising and illuminating.

2.3.1 High-Speed Videographic Kinematic Analysis

Pilot Experiment

In our previous research on blast neurotrauma (L. E. Goldstein et al., 2012), we conducted high-speed videography and analyzed head kinematics in anesthetized C57BL/6 mice (adult males, 10 weeks of age) (L. E. Goldstein et al., 2012). As described above, our new impact neurotrauma instrument was designed, built, and operationalized to produce head kinematics and resulting brain pathology comparable to our blast neurotrauma mouse model (see previous section). A pilot experiment was conducted to: (1) test the feasibility of capturing high-speed videography records for kinematic analysis using the newly-designed impact model, and (2) compare and calibrate instrument

parameters to reliably induce head kinematics comparable to that observed in our blast model. To accomplish these aims, we positioned the high-speed camera above the sled and painted the snout of the mice so as to track head kinematics. Coordination between all members of the laboratory was organized to allow for smooth operation between capturing videos and preparing mice for injury. Sled velocity calibration was calculated and compared to the resulting head kinematics. Processing and storage of the data was divided between lab members to allow for prompt analysis.

Kinematic analysis conducted with high-speed cameras revealed instrument design problems that resulted in inconsistent motion and structural weakness of the sled. Inspection of the sled after a large series of pilot tests indicated a number of sources of instrument variability and vulnerability: rod started to indent the contact location on the aluminum sled, sled bearings shifted during impact, and screws loosened and were bent at the completion of the experiment. Design adjustments were carried out to addresses these issues: both the slug and rod masses were increased requiring lower fire pressures for similar sled velocities. Design changes to the sled involved creating a new chasse and setting protocols on testing sled motion.

Sled Velocity	Anesthetized	Awake
2.0 m/s	4	4
3.5 m/s	4	5
4.5 m/s	5	4
5.5 m/s	6	5
6.0 m/s	6	4

Table 2.2: High-speed videography impact range finding design

2.3.2 High-Speed Videography and Kinematic Analysis: Initial Animal Experiment

Adult male C57BL/6 mice, 10–12 weeks-of-age (Taconic) were subjected to either blast or impact neurotrauma using the instruments developed and deployed at the Boston University Neurotrauma Laboratory. The blast neurotrauma model utilized a custom-designed 27-foot-long 10-inch diameter helium-driven stainless steel shock tube capable of delivering highly-reproducible, graded, non-lethal blast shock waves that closely model acute and chronic effects of blast exposure in humans (see 2.1.1). Mice subject to blast were secured in the prone position in a thoracic-protected restraint system inside the shock tube (L. E. Goldstein et al., 2012). The shock tube delivers a blast shock wave with measured blast overpressure of 72.3 ± 2.8 kPag. Exposure to this blast intensity results in head motion (see 2.1.1).

Closed-head impact injury was induced by a custom-built momentum transfer instrument that reliably delivers a left-lateral head impact injury. All mice were secured in the prone position with a modified DecapiCone (Braintree Scientific) such that the head and cervical spine extended outside the plastic restraint. A Velcro strap was used to secure the torso while allowing full range of lateral flexion of the cervical spine in the horizontal plane of motion. Concussive impact injury in our mouse model was compatible with 100% survival with no evidence of skull fracture (assessed by CT) or crush injury (assessed by neuropathology).

Mice in both groups (i.e., blast, impact) were pretreated with an anesthetic-analgesic cocktail (“anesthetized”; ketamine, 75 mg/kg, i.p.;xylazine, 4.3 mg/kg, i.p.; buprenorphine, 0.2 mg/kg, s.c.; “KXB cocktail”) or analgesic without anesthetic

(“awake”;buprenorphine, 0.2 mg/kg, s..c.) before experimental injury. Anesthetized and non-anesthetized (awake) mice were exposed to either a single blast or a single impact.

Mice subjected to experimental impact injury were grouped by pretreatment (anesthetic-analgesic or analgesic alone) sled velocity (2.0 m/s, 3.5 m/s, 4.5 ms/ 5.5 m/s 6.0 m/s) Table 2.2). Each mouse subject was placed in modified Decapicone such that the head and neck protruded from the cut end of the plastic restraint, thus enabling unconstrained head movement. The animal’s body was placed on the platform and secured with Velcro straps. The left side of the head was positioned such that the left lateral side of the head was in contact with the pad on the sled. Contact of the rod with the sled resulted in momentum transfer to, and linear translation of, the sled, thereby inducing traumatic head motion with no skull flexure or fracture.

After experimental injury, the mice were returned to their cage (analgesic only groups) or placed on a heat pad (anesthetic-analgesic groups). A 15 min interval separated the two impact exposures. After the second impact, the mice were monitored for 3 hours and then returned to the home cage. Blast mice received a single blast exposure as previously reported (L. E. Goldstein et al., 2012). Briefly, anesthetized mice were removed from the restraint and placed on a heating pad until gross motion returned and then were returned to their home cage. Unanesthetized mice were immediately returned to the home cage.

High-speed videography was conducted with two FASTCAM cameras (Photron). The cameras were positioned above and directly facing the mouse. FASTCAM software was used in conjunction with our custom impactor software. Cameras were triggered

when the rod passed the first light gate (impact neurotrauma model) or when a pressure sensor located in the wall of the shock tube in-line with the mouse head detected the leading edge of the supersonic blast shock wave (L. E. Goldstein et al., 2012). The cameras were operated at 10 μs frame capture rate (100,000 frames/second; 100 kHz) and captured 40 msec of motion. The camera set-up consisted of a horizontal camera facing the nose of the mouse and another camera placed vertically. These two planes of motion were recorded and saved for each mouse subject. High tolerance targets were used to determine calibration constants for each camera. High-yield LED illuminators were required for adequate image capture at the chosen frame rate (10 μs per frame; 100,000 frames/second).

Head kinematics were assessed by tracking a white dot of high-contrast paint that was strategically spotted on the mouse snout and served as a marker for videographic tracking of head motion.

2.3.3 Kinematic Analysis of Head Motion during Experimental Neurotrauma

Kinematic analysis of head motion during experimental blast or impact neurotrauma was assessed from individual high-speed videographic records calculated by tracking a white dot on the snout of the mouse. Commercially available tracking software exists; however, a custom-designed tracking software developed in Matlab by Ms. Amanda Guadreau-Balladrama (ECE), a collaborating engineering doctoral students in the Goldstein laboratory, provided flexibility, batch processing, and applied image processing algorithms applicable to enhance snout tracking. The custom-designed tracking software outputted raw pixel location. Applying calibration photos taken after

high-speed cameras were setup, we determined the centroid X and Y coordinates for the snout at each frame of the high-speed videographic record. A second-order, 2 kHz, zero-phase Butterworth filter was applied only to the position curve. First, second, and third derivatives (velocity, acceleration, and jerk) were calculated from position and time vectors using discrete differentiation. The experimental impact injury was designed to induce a left-lateral neck flexion and resulting head movement. This injury is analogous to a left hook to the zygomatic region of the head in boxing or a flying tackle with left-lateral helmet contact in football. Use of the Depicone restraint prevented videographic recording and kinematic analysis of the cervical pivot point. Angular velocity and acceleration head position (X and Y coordinates) were fitted to a circle by the method of Taubin (Taubin, 1991). Circle-fit regression provided a pivot point that was used to

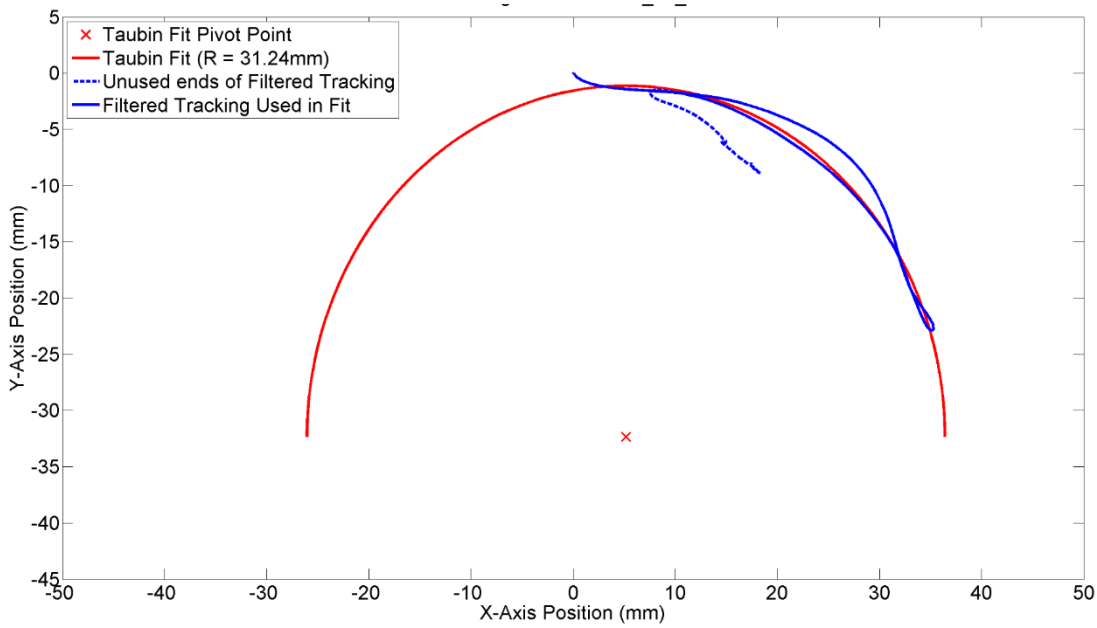

Figure 2.8: Method for determining the pivot point during impact.
The experimental set-up limited the ability to determine the pivot point during impact head motion. Using the Taubin circular fit method, the pivot point could be calculated for each impact.

calculate angular acceleration. To compare head kinematics between the two neurotrauma models, we determined peak X-acceleration, peak X-jerk, radius of swing, and peak angular acceleration as metrics for comparison. Blast kinematic analysis was performed by Mr. Andrew Fisher.

2.3.4 Comparison of Head Kinematics Induced by Experimental Impact and Blast Neurotrauma Mouse Models

High-speed videography was used to access the kinematics of both blast and impact at different injuries intensities. The objective was to find a sled velocity in the new impact neurotrauma mouse model that would result in head kinematics comparable to that previously reported in our blast neurotrauma mouse model (L. E. Goldstein et al., 2012). For the blast model the animals were pretreated with anesthetic-analgesic cocktail or analgesic alone, secured in place in the blast shock tube, and exposed to a blast shock wave (peak pressure 72.3 ± 2.8 kPag) that matched the blast intensity in our previous blast study (L. E. Goldstein et al., 2012). Head kinematics during blast exposure was evaluated in 8 mice. During blast, the head had a swing radius of 28.4 ± 3.1 mm. Peak X-acceleration of the head was measured at 9,020 ± 2,420 m/s^2, peak angular acceleration of the head was 300.1 ± 93.4 $krad/s^2$, and peak X-jerk of the head was 49,300 ± 14,700 km/s^3. Analysis of head kinematics in the impact model indicated a sled speed of 5.0 ± 0.2 m/s in anesthetized mice was capable of inducing comparable head motion as seen in the blast mice (Table 2.3). Mice subjected to closed-head impact injury at this sled velocity had a swing radius of 30.0 ± 2.3 mm. Peak X-acceleration of the head in the

Kinematic Parameters	Impact TBI Model	Blast TBI Model *
Injury Intensity Parameter	5.08 ± 0.2 Sled Speed (m/s)	72.3 ± 2.8 Peak Pressure (kPag)
Peak X-Acceleration (m/s^2)	12,600 ± 3,430	9,020 ± 2,420
Peak X-Jerk (km/s^3)	53,100 ± 25,000	49,300 ± 14,700
Radius of Swing (mm)	30.0 ± 2.3	28.4 ± 3.1
Peak Angular Acceleration ($krad/s^2$)	426.6 ± 114.4	300.1 ± 93.4
Number (N)	18	8

Table 2.3: Kinematic comparison between two TBI models.
No significant difference between the impact and blast kinematics using Holm-Sidak method for multiple Student's t-test comparisons.

impact model was measured at 12,600 ± 3,430 m/s^2, peak angular acceleration of the head was 426.6 ± 114.4 $krad/s^2$, and peak X-jerk of the head was 53,100 ± 25,000 km/s^3. Statistical analysis using the Holm-Sidak method for multiple t-tests indicated an absence of significant difference between blast and impact models with respect to head kinematics. This result represents an engineering achievement that allows direct comparison of these two brain injury mechanisms and evaluation of the fundamental hypothesis under investigation in this dissertation.

2.4 Discussion

The method of inducing impact neurotrauma varies across different models. We

determined specific injury requirements based on clinical pathology, concussion biomechanics, and results from our previous research on acute and chronic effects of blast exposure in our mouse model of blast neurotrauma (L. E. Goldstein et al., 2012). The developed momentum transfer instrument reliably delivers a closed-head impact injury that induces comparable head kinematics to our blast model without evidence of skull flexure, fracture, or crush. Mice were restrained in a similar fashion to the blast model. The decision to develop a new impact injury device proved to be essential to achieve comparable head kinematics in both models. Custom design and development allowed for modifications and adjustments that would be challenging with a commercial TBI model. We were able to determine our injury requirements that allowed for these unique results. Comparable kinematics between two neurotrauma models likes these opens new possibilities to elucidate mechanisms of concussion and will be a major focus in Chapter 5 of this dissertation.

The main innovation and unique aspect of the device that differentiates it from other models is in how the impact injury is induced. The only published rodent model we know of that induces a lateral head injury and could be comparable to the blast head motion was reported by Viano et al. (Viano et al., 2009). To induce lateral motion a projectile is fired and hits a helmet attached to the rat's head resulting in linear and rotational head motion. Yet, the rat's body is not restrained and is allowed to roll after injury. While providing a starting point for our device design, we required that the mouse's torso remain secured while allowing the head to move unrestrained. We also required that we could not use a helmet attached to the head to prevent skull fracture.

These non-trivial tasks were accomplished through the design and development of the sled. The sled consisted of a flat surface with a "helmet" analogue extruding from the top and a pad attached to the "helmet" to prevent skull fracture. During injury the "helmet' section directly contacts the head after the rod hits the sled, accelerating the head and allowing for unconstrained rotational head motion. Although the sled design has enabled the impactor to meet all injury requirements set forth, the variability of the sled velocity differs from the rod and slug. While the current design produced meets functional requirements, slight design changes could be introduced to decrease sled velocity variability.

The purpose of the high-speed analysis experiment was to determine the injury input for the impact neurotrauma model. We designed an experiment to expose mice with the same intensity as reported in our blast work. We performed a range finding study to determine what sled speed would induce similar head kinematics in both experimental models. We found a sled speed of 5 m/s sufficient to induce comparable kinematics. This experiment was thoughtfully designed to provide a clinically-relevant injury analogous to closed-head impact injuries sustained during contact sport play.

2.4.1 Study Limitations

Results of the kinematic comparison experiments described above are subject to several important study limitations that warrant interpretive caution. Primary comparison of head kinematics in both experimental models (i.e., blast, impact) involved anesthetized mice. The rationale for comparison was that our previously reported studies (L. E. Goldstein et al., 2012) were conducted with anesthetic-analgesic pretreatment as a

condition of animal protocol approval at the time of initial experiments. We have since secured IACUC animal subject use approval and henceforth non-anesthetized mice will be used in all other experiments reported in this dissertation.

Mice pretreated with analgesic alone ("awake") may demonstrate different head kinematics than mice pretreated with anesthetic-analgesic cocktail and subjected to the same experimental injury parameters. Moreover, the head kinematics described above are based on tracking a marker strategically painted on the skin of the snout. Motion of the soft tissue (i.e., skin, subcutaneous fat, galea aponeurotica, areolar connective tissue, and periostium) may not accurately track the motion and kinematics of the skull and cranial contents for two reasons: (1) soft tissue overlying the skull can move with some degree of independence relative to cranial motion, and (2) the position of the tracking marker represents a more distal fiducial than the center of mass of the brain with respect to the reference pivot point in the cervical spine. (This second error source can be corrected by introducing a normalization factor based on known anatomical metrics that do not vary significantly between individual mice of the same age and weight.). These considerations notwithstanding, the results presented above show that the impact neurotrauma model recapitulates key features seen in sport-related concussive injury.

2.5 Conclusion

We developed and verified the design of an impact neurotrauma model. We used design and engineering principles to development and verify our device to meet our experimental requirements. High-speed videography and kinematic analysis was used to

compare experimental models and validate operational parameters for instrument use in the experiments to follow. The next step in the design of the model is called validation. The criteria for validation will be recapitulation of acute and chronic effects of closed-head impact injury in humans, including acute concussion and CTE-linked brain pathology.

Chapter 3: Assessment of Concussion and Acute Blood Brain Barrier Disruption in Mice Following Impact Neurotrauma

This chapter introduces the neurological assessments for TBI, signs and symptoms after sport-related concussion and side-line concussion assessments. We discuss the current neurological assessments performed in mice after impact neurotrauma and introduce the Boston University Concussion Scale (BUCS). We induce closed-head impact injury in mice without anesthesia and hypothesize that closed-head impact injury triggers acute neurological signs associated with sport-related concussion as well as brain pathologies such as blood-brain barrier disruption.

3.1 Neurological Assessment in Humans and Mice after Impact Neurotrauma

3.1.1 Neurological Assessment for TBI and Concussion in Humans

The Glasgow Coma Scale (GCS) is commonly administered in emergency departments as a clinical tool to assess the severity of TBI. Proposed by Teasdale and Jennett in 1974, the GCS consists of three test categories scaled by response: eye opening, verbal response, and motor response. (G. Teasdale & Jennett, 1974) The composite score ranges from 3 to 15 points and distinguishes between mild (15–13), moderate (12–9), and severe (8–3) brain injury (Marshall et al., 1983; Rimel, 1981; Rimel et al., 1982; G. Teasdale & Jennett, 1974). The GCS refers to either the Glasgow Coma Scale, which is applicable for individual patient management, or the Glasgow

Coma Score (summed score) for patient groups or populations (Graham Teasdale et al., 2014). Henceforth in this dissertation, the acronym GCS will refer to the Glasgow Coma Scale. The GCS is commonly used for clinical assessment of TBI around the world (Graham Teasdale et al., 2014) and has been incorporated into a variety outcome prediction scores (Boyd, Tolson, & Copes, 1987; Champion et al., 1990; Champion et al., 1989; Knaus, Draper, Wagner, & Zimmerman, 1985). The GCS has shortcomings and limitations, especially with regard to classification of specific clinical subtypes (Starmark, Stalhammar, & Holmgren, 1988) and observer agreement (Gill, Reiley, & Green, 2004; Green, 2011). The GCS is used as a simple bedside test to evaluate level of consciousness. Consequently, patients who are sedated, intoxicated, or exhibit altered mental status for reasons unrelated to the injury undermine clinical interpretation and utility of GCS scoring in such patients (Middleton, 2012; Zuercher, Ummenhofer, Baltussen, & Walder, 2009).

The Glasgow Coma Score is commonly used to categorize patients with head injury into subgroups based on global impairment severity (mild, moderate, severe) 6 hours post-injury. A consequence of this testing (and reporting) delay has resulted in the inability of the GCS to accurately capture the full spectrum of head injuries, especially mild forms of head injury that include most sport-related concussions (Johnston et al., 2001; McCrory, Meeuwisse, Echemendia, et al., 2013). A large number of mild TBIs fall below the detection limit of the GCS. McCrory *et al.* diagrammatically represent the clinical conundrum presented by differential diagnosis of sport-related concussion and mild TBI using the GCS (McCrory, Meeuwisse, Echemendia, et al., 2013), Figure 3.1)

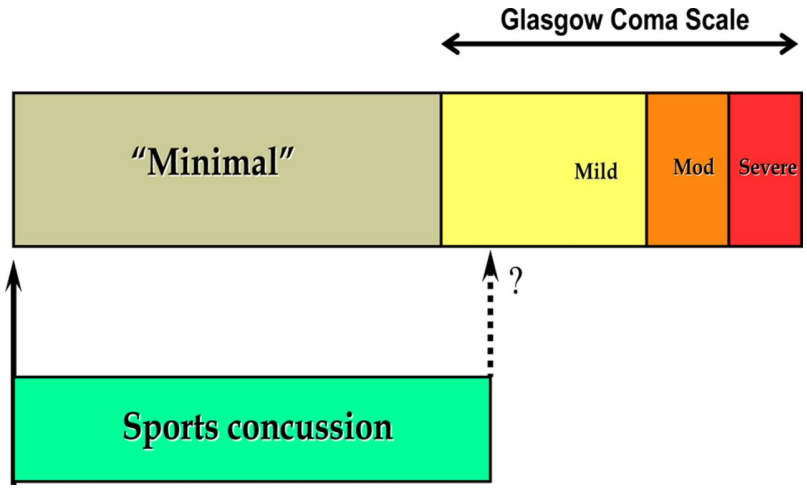

Figure 3.1: Conceptual understanding of sports concussion relating to Glasgow Coma Scale.
Reprinted from (McCrory, Meeuwisse, Echemendia, et al., 2013)

The inability to accurately classify concussion with the GCS led to the development of numerous concussion grading systems (see review by (Johnston et al., 2001)). While each concussion scale differs with respect to specific test elements, the commonly used clinical grading scales focus on three primary domains: level of consciousness (and degree of confusion), post-traumatic amnesia, and duration of post-concussive symptoms (Cantu, 1986; Kelly & Rosenberg, 1997; Nelson, 1984; Roberts, 1992). Several concussion grading systems were developed through empirical experiments conducted in non-human primates (Ommaya, 1985; Ommaya & Gennarelli, 1974) that focus on coma. It should be noted that these animal models were designed to induce moderate-to-severe brain injuries that included diffuse axonal injury (DAI) and neurovegetative alterations that are not commonly observed following mild concussive head injury (Johnston et al., 2001; Slobounov, Cao, Sebastianelli, Slobounov, & Newell, 2008). Initially, all of these grading systems focused on the presence and duration of

unconsciousness and amnesia to define concussion severity. By contrast, modern definitions of concussion do not require loss of consciousness (Guskiewicz et al., 2003; Guskiewicz, Weaver, Padua, & Garrett, 2000) or amnesia (Erlanger et al., 2003; Guskiewicz et al., 2003) for diagnosis. To date, concussion remains a poorly defined clinical syndrome with ever-changing criteria that are based on incomplete knowledge of the underlying pathophysiology. Not surprisingly, the medical community has not reached consensus on or defined validated criteria for concussion grading (Johnston et al., 2001).

The difficulty of diagnosing concussion with both the GCS and the limited validity of concussion grading has steered researchers, clinicians, and sport medicine practitioners to shift focus from classifying the severity concussion to an approach of injury detection using a wide variety of sideline evaluations tools. These evaluation tools purport to recognize concussion, guide recovery management, and direct return-to-play decisions through use of various target symptom checklists, balance and eye tracking tests, and cognitive evaluations. Concussion symptom scales rely on a series of subject-report questions and have been reviewed extensively (Alla, Sullivan, Hale, & McCrory, 2009; Eckner & Kutcher, 2010; McLeod & Leach, 2012). Alla *et al*. reviewed 60 articles published from 1995–2008 and identified six core symptom scales that utilize 10–34 symptom items with a majority grading with a 7-point Liker scale (Alla et al., 2009). Alla *et al.* discussed that inclusion of certain symptoms relied mostly on experience and observation of the developers (Alla et al., 2009). A recent empirically-derived symptom scale called the Concussion Symptom Inventory (CSI) uses normative data from 16,000

athletes and includes 641 post-concussed athletes (Randolph et al., 2009). The studies used to develop the CSI had 5 common post-concussion assessment time points: immediate post injury, post-game (~3 hours), 1 day, 3 days, and 5 days post injury. Analysis of the CSI data resulted in inclusion of 12 core concussion symptoms: headache, nausea, balance problems including "dizziness", fatigue, drowsiness, "fogginess", difficulty concentrating, memory disturbances, photophobia, phonophobia, blurred vision, and feeling slowed down (Eckner & Kutcher, 2010; Randolph et al., 2009).

Balance dysfunction is often noted in the acute period following concussion. An epidemiology study by Guskiewicz *et al.* conducted in high-school and college athletes who sustained a witnessed concussion found that 30% of reported injuries had a positive Romberg test immediately after concussion (Guskiewicz et al., 2000). Additional studies have reported postural instability following acute TBI (Geurts, Ribbers, Knoop, & van Limbeek, 1996; Guskiewicz, Perrin, & Gansneder, 1996; Guskiewicz, Riemann, Perrin, & Nashner, 1997; Guskiewicz, Ross, & Marshall, 2001; McCrea et al., 2003; Peterson, Ferrara, Mrazik, Piland, & Elliott, 2003; Riemann & Guskiewicz, 2000; Rubin, Woolley, Dailey, & Goebel, 1995). McCrea *et al.* reported that college football players who sustained a concussive head injury reported post-injury balance impairments that were more pronounced during the initial 24 hours post-concussion and appeared to resolve slightly earlier than other symptoms, including those affecting cognition (McCrea et al., 2003). A comprehensive review by Guskiewicz details the many different balance assessment tools in current use (Guskiewicz, 2011). The Sensory Organization Test (SOT) is a commonly used balance test tool that uses a force plate and moveable platform

to assess balance based on a derived measure, the Balance Error Scoring System (BESS) (Guskiewicz, 2011). Since most post-injury balance deficits are transient, "best practice" use of this and other balance assessment tools require baseline testing for clinically meaningful score interpretation (Guskiewicz, 2011).

Further advances have led researchers to the development of multifaceted approaches to identify suspected concussion. Commonly used multifaceted sideline tests include the Standardized Assessment of Concussion (SAC) (McCrea et al., 2003; McCrea et al., 1998) and various versions of the Sport Concussion Assessment Tool (SCAT), (McCrory et al., 2005; McCrory, Meeuwisse, Aubry, et al., 2013; McCrory et al., 2009). SCAT3 is administered by a medical professional and includes: Glasgow Coma Score, Maddocks Score; symptom evaluation checklist, simple cognitive test (SAC) (McCrea et al., 1998), BESS testing, neck examination and coordination examination (McCrory, Meeuwisse, Aubry, et al., 2013).

The deployment of neuropsychological tests has allowed researchers to assess and observe the course of cognitive recovery after concussion. In McCrea *et al.,* concussed athletes exhibited a mild decline 2 days after injury on neuropsychological measures of cognitive processing speed, new learning and memory, and mental flexibility (McCrea et al., 2003). With the development of computer guided neuropsychological tests, recent surveys have found 40% of high school athletes injured will use a computer-based neurocognitive assessment. The most common used test includes: Immediate Post-Concussion Assessment and Cognitive Testing (ImPACT), Automated Neuropsychological Assessment Metrics (ANAM), CogSport, HeadMinder, and

Concussion Vital Signs. The ImPACT test introduced in 1990 measures the range of attention span, working memory, sustained and selective attention time, response variability, non-verbal problem solving, and reaction time (www.impacttest.com).

The definition of concussion continues to be revisited and refined, yet historically has been described as a non-pathological injury in which symptoms resolve over time (McCrory, Meeuwisse, Aubry, et al., 2013). As such, different forms of assessing concussion have evolved over time but the purpose for such assessments has remained consistent, namely, the management of sports-related concussion and return-to-play guidelines. However, the field experienced a paradigm shift suggesting the correlative effect of sport-related concussion to long-term pathological sequelae detailed in postmortem case studies regarding chronic traumatic encephalopathy (CTE) (L. E. Goldstein et al., 2012; McKee et al., 2009; McKee et al., 2013; Omalu et al., 2006; Omalu et al., 2005).

Here, we hypothesize that closed-head impact injury triggers acute neurological signs associated with sport-related concussion as well as brain pathologies and long-term functional sequelae associated with CTE. The biomechanical and pathobiological underpinnings of the relationship between acute concussion and chronic sequelae will be a major focus of the work presented in this dissertation. To test our hypothesis, we developed a murine concussion assessment tool called the Boston University Concussion Scale (BUCS) that recapitulates key features of acute effects of closed-head concussive impact injury in humans.

3.1.2 Neurological Assessment After TBI in Mice

One of the standard tasks for assessment of neurobehavioral changes following injury in animal TBI models has been measuring righting reflex suppression duration (Dixon et al., 1987; G. B. Fox, Fan, LeVasseur, & Faden 1998; G. B. Fox, LeVasseur, & Faden, 1999; Fujimoto, Longhi, Saatman, & McIntosh, 2004; Hamm, 2001). The task involves placing an animal immediately after injury on its back and recording the time until the animal returns to normal upright posture ("righting reflex"). Durations of reflex suppression has been a metric to determine severity of injury and a method to compare different TBI injury models (Alder et al., 2011; Eakin et al., 2014; Gennarelli, 1994; Hamm, 2001). For example, in a paper using the fluid percussion model a righting reflex time of 2 – 4 minutes was classified as mild TBI and 6–10 minutes righting time as moderate TBI (Alder et al., 2011). Recently researcher have relied on the righting reflex as justification in comparing severity of injury between two different types of injury models; fluid percussion and weight drop model (Eakin et al., 2014). While Hamm *et al.* stated the suppression of the righting reflex is analogous to the human unresponsiveness after concussion or coma (Hamm, 2001), the validity of the comparison has not been fully investigated. Further, almost all animal models that assess righting reflex administer anesthesia before injury. The confounding effects of the anesthetic agent may compromise interpretation of righting reflex time.

Neurological Severity Scale

The Neurological Severity Scale (NSS) was designed to evaluate the severity of neurological injury following experimental TBI in a mouse model (Beni-Adani et al.,

2001; Y. Chen et al., 1996; Shohami et al., 1988; Shohami, Shapira, Yadid, Reisfeld, & Yedgar, 1989). The original NSS consisted of 25 tests and was scored in a binary faction. Failure on one test would result in a point. Combining all the test scores would reveal the NSS score, a metric that is assumed to reflect the degree of neurological injury. The test could then be repeated at different time intervals after injury, ranging from the first test at 1-hour post-TBI to 1-month post-TBI. The NSS was later modified from 25 tasks to 10 tasks (Beni-Adani et al., 2001; Stahel et al., 2000). The ten tasks were designed to objectively assess motor function, alertness, and physiological behavior (Table 3.1).

Task	Description	Points
Exit Circle	Ability and initiative to exit a circle of 30 cm diameter within 3 min	0/1
Monoparesis/ hemiparesis	Paresis of upper and/or lower limb of the contralateral side	0/1
Straight walk	Alertness, initiative and motor ability to walk straight	0/1
Startle reflex	Innate reflex; the mouse will bounce in response to a loud hand clap	0/1
Seeking behavior	Physiological behavior as a sign of 'interest' in the environment	0/1
Beam balancing	Ability to balance on a beam of 7 mm width for at least 10 s	0/1
Round stick balancing	Ability to balance on a round stick of 5 mm diameter for at least 10 s	0/1
Beam walk: 3 cm	Ability to cross a 30-cm long beam of 3 cm width	0/1
Beam walk: 2 cm	Same task, increased difficulty on a 2-cm wide beam	0/1
Beam walk: 1 cm	Same task, increased difficulty on a 1-cm wide beam	0/1
Maximal Score		**10**

Table 3.1: Neurological Severity Score (NSS) for mice.
Reprinted from (Flierl et al., 2009).

Modified NSS would be taken serially at multiple different time points. A methods paper suggests assessments at t = 1, 4, 24, 72 hours and 7 days after TBI with the option of longer follow-up time points at 3 months (Flierl et al., 2009). Of note, the NSS has been performed in non-anaesthetized mice (Petraglia, Plog, Dayawansa, Chen, et al., 2014; Petraglia, Plog, Dayawansa, Dashnaw, et al., 2014) with a closed-head impact model with helmet on the dorsal surface of the head and the first NSS assessment occurring 1 hour post-injury. Researchers have relied on the NSS to classify severity of injury and determine long-term outcome (Tsenter et al., 2008). While the NSS functions well for gross neurological assessment following impact TBI, no studies have assessed animals immediately following injury, nor have pre-tests or normative data studies been performed.

3.1.3 Development of the Boston University Concussion Scale

We hypothesized that mice subjected to closed-head impact injury would exhibit transient lateralized neurological signs that recapitulate core clinical features of acute sports-related concussion in humans. As we wanted to assess concussion we received approval of our animal use protocol from Boston University's Institutional Animal Care and Use Committee (IACUC) to eliminate the confounding influence of anesthetic pretreatment before experimental injury. The approved IACUC protocol also allowed for the assessment of concussion immediately following injury. To test our hypothesis, we developed the initial pilot version of the Boston University Concussion Scale (BUCS-1) as a 6-point modification of the NSS (Beni-Adani et al., 2001; Stahel et al., 2000; Tsenter et al., 2008) with a point given when a criterion metric was not achieved. The BUCS-1

test required testing the mouse prior to injury as baseline scores are necessary for accurate assessment of injury-induced neurological impairment (Guskiewicz, 2011). BUCS-2 was similar to BUCS-1 with the addition of a righting reflex task and the elimination of the circle exit task. Observations from pilot studies using BUCS-1 and BUCS-2 provided insights into the limitations of the NSS binary point scoring system, especially the difficulty of determining the startle reflex and inconsistency of index metrics for mouse locomotion.

The first major adaption of the BUCS that differentiates this test from the NSS was the elimination of the binary scoring system and the reduction of the number of tasks. In the published research using the NSS, results are reported by summing all points (Beni-Adani et al., 2001; Y. Chen et al., 1996; Flierl et al., 2009; Shapira et al., 1988; Shohami et al., 1988; Shohami et al., 1989; Stahel et al., 2000; Tsenter et al., 2008). Some tests are straight forward in assigning points, such as failure to balance on a 0.5 cm beam. An issue arises when multiple points are assessed in a similar task. For example, in the Flierl *et al*. protocol paper, mice are placed in the center of the circle task and scored if the mouse fails to exit in 3 minutes (Flierl et al., 2009). The seeking behavior places the mouse back into the circle task to assess exploration with no cut-off time. The straight movement task places the mouse again on a flat surface to assessment straight movement with no cut-off time.

From our observations with BUCS-1 and BUCS-2 following closed-head impact injury in our mouse model, mice regularly showed evidence of a dramatic and transient clockwise circling behavior with rotation away from the side of impact injury (i.e., left-

sided lateral impact resulted in transient right-sided hemiparesis (weakness) with clockwise rotation). This dramatic lateralized behavior was not completely captured with a binary scoring system but could be assessed in a graded fashion using a single-exposure open-field test. This distinct lateralizing neurological deficit was also easily captured by two additional tasks, a balance beam test and inverted wire mesh test. By combining individual movement tests into a three domain-focused neurological task, we were able to change from a binary-scoring system to a graded system similar to the Glasgow Coma Scale (G. Teasdale & Jennett, 1974). Subsequent modifications resulted in combining the multiple beam balance tasks into a single beam test. We observed in impacted mice a dependency between balance and locomotion on a 1 cm width beam. We noticed that the degree of the balance deficit diminished in a graded fashion based on total traversal distance in a given time period. By increasing the length of the beam and monitoring distance traveled, a graded scale for the beam test was developed.

The second addition was the inclusion of an inverted wire mesh test as a means to assess upper and lower extremity weakness and grip strength. Wire hang and grip tests are commonly used to measure strength (Hall, 1985; Panter, Braughler, & Hall, 1992). The test consists of a mouse hanging on a metal wire and measuring the latency to fall. After impact we observed lateralized limb weakness and decreased grip strength that was restricted to the contralateral side relative to the injury. Thus, left-sided impact yielded right-sided hemiparesis (weakness), consistent with neurological injury to the cortical motor strip. By placing an injured animal on a wire mesh and inverting the sheet, we observed the mice would move exclusively in a circle opposite to the side of injury

(clock-wise, left sided hit). Front or hind paws on the right side showed loss of function in the ability to grip mesh, requiring the mice to circle with 3 functional paws. More severe injuries resulted in loss of motion altogether and mice would hang with one or both right-sided paws not being used. Decrease in movement and paw functions show weakness following injury. Control animals after inverted explored, circling in both directions. All paws functioned normally and mice rarely stopped moving. No observable signs of weakness in paws were seen in any control mice. Observed contralateral limb and grip weakness also affected movement on all three subtests—open-field exploration (0.5 min), inverted wire mesh (0.5 min), balance beam (0.5 min). The graded observed loss of movement, paw weakness, and balance during all tests allowed for the development of a graded scoring system that was ultimately incorporated into the fully-validated BUCS-3 system. BUCS-3 consists of graded scales for the three-component assays (i.e., open-field test, wire mesh test, a beam walk test). Each test was to be performed before injury (pre-injury baseline), after each injury (acute post-injury), and 3 hours post last injury (recovery). (see Figure 3.2)

BUCS-3R contained revisions included adding a score for traumatic seizures that are clinically observed after serious closed-head impact injuries in humans (McCrory, 1997; McCrory & Berkovic, 1998, 2000; McCrory, Bladin, & Berkovic, 1997). We observed classical Jacksonian March tonic-clonic seizures in a subset of impact-injured mice following acute closed-head impact injury. BUCS-3R clarified grading criteria and was used for all animal experiments included in this dissertation. Detailed description of the tests, criterion, and grading procedure will be presented below.

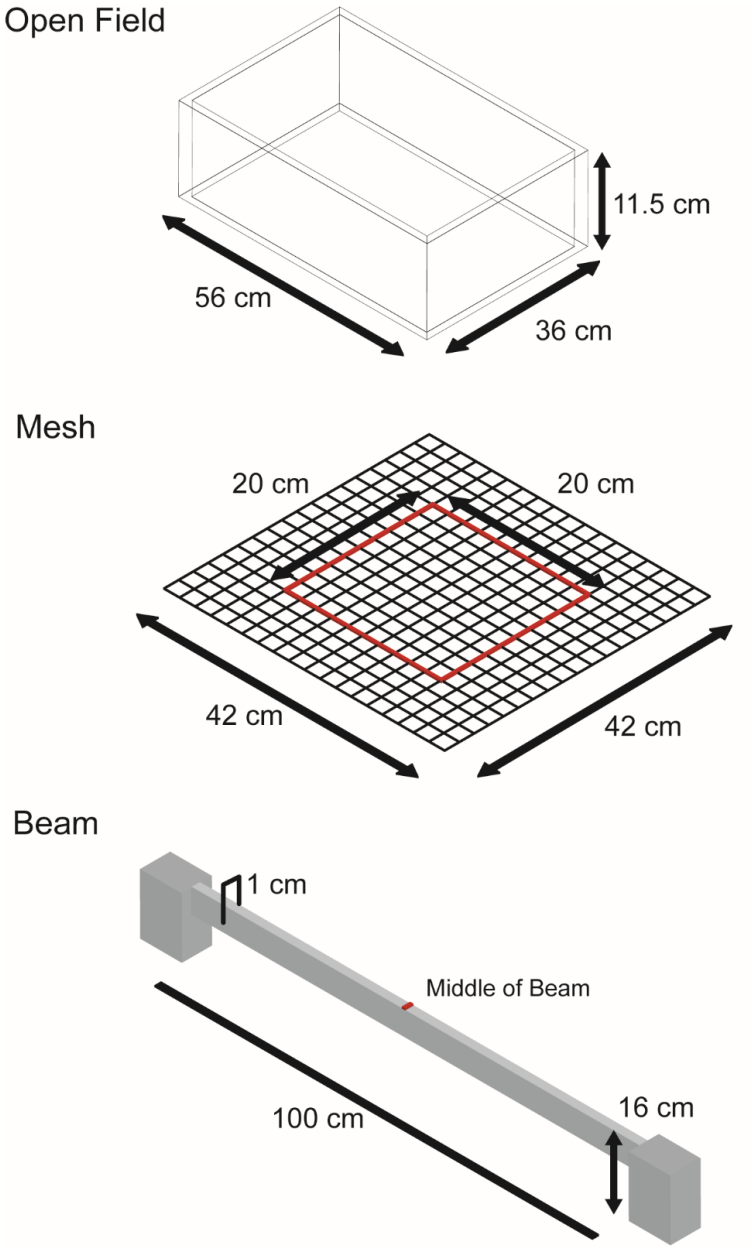

Figure 3.2: Equipment used to assess BUCS.
Open field: Place the mouse in the center of the box and observe the movement. Wire mesh: Place the mouse in the center of mesh and invert resting the mesh on top of the open field box. Observe motion and weakness of paws. Beam walk: Place the mouse on the center of the beam and observe motion and distance travel. 30 seconds is given for each test

3.1.4 BUCS instructions and Scoring

The Boston University Concussion Score (BUCS) is a composite of three different tests: open-field exploration, inverted wire mesh navigation, beam walk. Each test is graded on a 5-point scale according to observable metrics that capture graded neurological impairment. Points are awarded based on meeting an "A" criterion based on locomotion and a "B" criterion modifier (Figure 3.3). BUCS testing occurs before injury (baseline), after injury (acute post-injury), and 3 hours after last TBI (recovery). Prior to the baseline testing and experimental injury, each mouse receives an analgesic injection (buprenorphine, dose, route) without anesthesia according to an approved IACUC protocol (Boston University School of Medicine, Protocol Number - 15088). After analgesic injection, baseline BUCS testing commences by placing the animal subject in the center of the open field box.

The open field test consists of placing the mouse in an open box 38 cm x 56 cm, with walls 11.5 cm tall. The wire mesh test uses a 0.5" stainless-steel wire mesh with a dimension of 42 cm square. On one side of the mesh, a box is drawn centered on the mesh measuring 20 cm square. Beam walk test consists of a 1 cm wide beam 100 cm long, placed 16 cm from the table.

During experiments the baseline and recovery BUCS testing requires the mouse to be removed from its home cage and placed in the center of the open field. Acute post-injury BUCS testing occurred after the mouse underwent a closed-head impact or control injury and the mouse would be removed from the restraint cone, placed in the open field, and monitored for abnormal signs such as post-traumatic apnea. After a 2-minute waiting

period in which the mouse is free to explore the open field, BUCS testing started by placing the mouse in the center of the field. Close observation is mandatory as signs of seizure are often noted during this two-minute interval.

Procedures for BUCS testing and scoring are described in the following steps. (1) Open Field Test: Place the mouse in the center of the open field box. Observe the locomotion and exploratory nature of the mouse for 30 seconds. A normal, healthy mouse will move with linear locomotion and usually will hug the walls (criterion A) and explore more than 2 corners within 30 seconds (criterion B). This mouse has met both criteria and would be awarded 5 points for the open field test. If the mouse exhibits linear locomotion but explores no more than 2 corners this mouse would be awarded 4 points. If the mouse moves in a unidirectional rotation (clockwise or counter-clockwise direction) and explores less than 2 corners, note the direction and give the mouse 3 points. If the mouse is placed in the center of the box and remains still with no locomotion or circular rotation and the ventral abdomen of the mouse is in contact with the floor of the box, give the mouse 2 points. A mouse who remains still during the 30 second test and lays with its lateral abdomen touching the floor, award 1 point. The zero score can be awarded at any time after removing the mouse from the cone. If the mouse exhibits impact seizures, note limbs involved and give the mouse zero points.

(2) Inverted Wire Mesh Test: Immediately following the open field test, place the mouse in the center of the wire mesh and slowly invert the mesh. Place the mesh on top of the open field with the mouse directly above the center of the open field. Observe the locomotion, direction of motion, and distance traveled performed in 30 seconds. Make

notes on the scoring sheet. A normal, healthy mouse will show multidirectional locomotion (A criterion) and exit the 20 cm x 20 cm box with at least one paw (B criterion). If the mouse moves using all four paws, the BUCS would be a 5 for the wire mesh test. The wire mesh allows observation of paw weakness in the animal following injury. During the wire mesh tests observe the number of paws the mouse uses to move around. If the mouse uses 3 paws for movement but then uses 4 paws, criterion is met with the higher score and should be scored as such. If a mouse moves with multidirectional locomotion but does not exit the drawn box on the mesh while using all four paws, the score would be a 4. If the mouse is placed in the center of the mesh, inverted and moves only in a unidirectional rotation, note the rotational direction and award 3 points. If the mouse does not exhibit any movement but is able to hang with four paws, award 2 points. A mouse that shows no movement and hangs with the use of less than four paws, award 2 points. A mouse that is unable to grip the mesh or falls from the mesh is awarded zero points. The test is administered for 30 seconds after the mesh is inverted. If the mouse does not start in the center of the mesh, compensate the exit box accordingly. Multidirectional locomotion included both clockwise and counter-clockwise rotation. Some mice will move in a straight line and straight movement is defined by forward motion for more than half the body length of the subject.

(3) Beam Walk Test: After 30 second on the mesh, the mouse is removed from the mesh and is placed on the center of the beam. For the baseline score, the animal undergoes two practice tests where the mouse is guided to move half of the beam's length. These practice tests only occur for the baseline score. After the practice test for

baseline or immediately after the mesh test for all other time points, the animal is placed on the beam to observe locomotion and balance for 30 seconds. A normal, healthy mouse will traverse the beam and travel a total distance of greater than or equal to half the beam and is awarded 5 points. A mouse that is able to traverse the beam but only able to travel a total distance of less than ½ the beam but greater than or equal to ¼ is awarded 4 points. A mouse that receives a score of 3 points would traverse the beam but only travel a total distance of less than ¼ beam. If the mouse is placed in the center of the beam and does not move but can perch on top of the beam, the mouse is awarded 2 points. If the mouse is able to be placed on the beam, but does not traverse and is unable to perch on top of the beam, award 1 point. A score of zero would be awarded if the mouse is unable to be placed on the beam or falls from the beam.

After the beam walk test the animal is replaced back to its home cage and can receive a TBI injury/control, wait 3 hours for a post-3 hour BUCS or be returned to the animal facility. The BUCS assessment was designed to provide a quick and reliable test battery for assessment of transient post-traumatic neurological impairment. The baseline and post-3 hour BUCS scores are essential to capture the transient nature of the observed neurological impairments. Statistical analyses compare baseline, post-impact and recovery scores. All mice fully recover to baseline neurological function within 3 hours after injury.

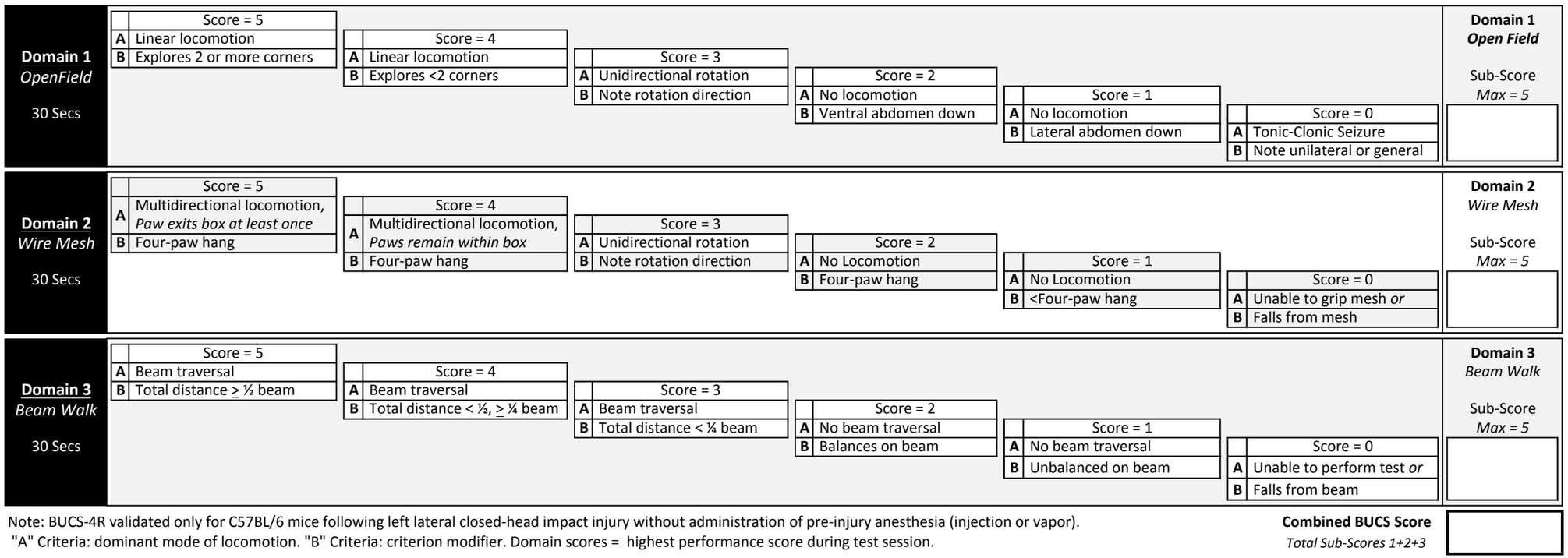

Figure 3.3: BUCS-3R scoring criteria

3.2 Assessment of Concussion using BUCS following impact neurotrauma injury

3.2.1 Methods

Animal Subjects

Adult wild-type C57BL/6 male mice were purchased from Charles River Laboratories and were group-housed 2 per cage at the Laboratory Animal Science Center, Boston University School of Medicine, Boston, MA. All animal experiments utilized 2.5-month-old (10 weeks old) mice (Table 3.2). All mice were assessed with the Boston University Concussion Scale by the same scorer. Mice were provided with standard mouse chow and water *ad libitum*. Ambient temperature was controlled at 20–22 ºC with 12-hour light-dark cycles. Animal housing and utilization were conducted in accordance with guidelines from the Association for Assessment and Accreditation of Laboratory Animal Care (AAALAC) and all applicable institutional, local, state, and federal regulations. All experiments involving animal subjects were reviewed and approved by Institutional Animal Care and Use Committees at Boston University School of Medicine, Boston, MA.

3.2.2 Experimental Closed-Head Impact Injury Parameters and BUCS Assessment

Prior to BUCS assessment animals were weighted and received an intraperitoneal injection of analgesic (buprenorphine, 0.2 mg/kg, i.p.) but without anesthesia before receiving a baseline BUCS score. Assessment of the BUCS score followed outlined protocols (see 3.1.5). Mice were secured in the prone position with a modified

Animal Parameters	Impact				Control			
Strain (C57BL/6)	Mean	SD	CV	N	Mean	SD	CV	N
Weight (g)	25.3	1.8	0.07	203	25.3	2.0	0.08	117
Age (weeks)	10.2	0.7	0.07	203	10.1	0.5	0.05	117

Table 3.2: Summary animal parameters used in all experiments.
No significant difference in weight and age between impact and control groups.

Operational Parameters	Mean	SD	CV	N
Fire Pressure (psig)	19.12	1.26	0.066	406
Slug Velocity (m/s)	25.38	0.72	0.028	381*
Rod Velocity (m/s)	7.20	0.28	0.039	406
Sled Velocity (m/s)	5.08	0.50	0.098	406

Table 3.3: Impact neurotrauma operational parameters with mouse subjects.
Each mouse received two hits. Impactor design utilized a pressure sensor, light gates and a laser displacement to measure fire pressure, slug/ rod velocity and sled velocity. Custom developed software recorded the operational parameters for each hit into a database with animal information. (* Excluded samples due to slug light-gate error)

DecapiCone (Braintree Scientific) such that the head and cervical spine extended outside the plastic restraint. A Velcro strap was used to secure the torso while allowing full range of motion of the cervical spine. If the front paws were able to leave the cone, the mouse was removed and repositioned in the cone. The head was positioned on the sled with the padding on the left-lateral side. Experimental parameters were optimized to model impact injury conditions in humans and head kinematics in our blast neurotrauma mouse model

(L. E. Goldstein et al., 2012). Fire pressure was 19.12 ± 1.26 (psig), slug velocity was 25.38 ± 0.72 (m/s), rod velocity was 7.20 ± 0.28 (m/s), and sled velocity was 5.08 ± 0.05 (m/s) (mean ± SD) (Table 3.3). Concussive impact in our mouse model was compatible with 100% survival and there was no evidence of skull flexure, fracture, or crush injury. Non-anesthetized mice were exposed to two impacts separated by 15:00 ± 3:36 (mean ± SD) minutes between injuries. The rationale for this design was to model the minimal number of injuries consistent with repetitive closed-head impact neurotrauma associated with contact-sport play. Control/sham impacted mice were subjected to all experimental procedures as the impact group but did not receive the impact injury (i.e., analgesic injection and placement in cone restraint). As described in Chapter 2, all impact operational parameters were recorded after each impact. Following injury, mice were removed from the cone and placed in the open field box for two minutes before BUCS assessment. A total of 217 impact and 117 control mice were assessed for concussion at baseline, after 1st injury (Impact 1), after 2nd injury (Impact 2), and 3 hours post 2nd injury (Recovery).

3.2.3 Statistical analysis

Linear mixed-effects regression analyses were used to test for the group differences for BUCS score and to test the association of BUCS score. We allowed for outcome-specific fixed effects and subject-specific random effects. Outcomes of the same mice were correlated using a single between-subject correlation by applying a compound-symmetry model for the covariance matrix. These mixed effect analyses are more realistic models of the outcomes than using independent regression models for each

outcome. Since all information within each subject is utilized, we are able to provide more interpretable and consistent results than simpler statistical models. Moreover, the problem of multiple comparisons is removed when viewed from these models (Gelman, Hill, & Yajima, 2012). These multivariate models provide higher power for detecting small but clinically important differences compared to independent regression models for each outcome (H. Goldstein, 2011). Spearman's rank order correlation was performed used for correlation analysis. Comparison of animal parameters used Student's t-test with post-hoc correction. Levels of significance were indicated as follows: *, $P < 0.05$; **, $P < 0.01$; ***, $P < 0.001$. Statistical significance was set at $P < 0.05$. All values are reported as mean ± S.D. for animal and operational parameters. BUCS scores are reported as mean ± S.E.M.

3.3 Results

Closed-Head Concussive Impact Neurotrauma Mouse Model

We designed a closed-head concussive impact neurotrauma mouse model to induce acute neurological signs and chronic sequelae that recapitulate core clinical features of sports-related concussive head injury in humans. Our mouse model was designed to impact the left-lateral side of the head of an unanesthetized mouse ("awake") and allow for free movement of the head as is the case in sport-related impact TBI in humans (Figure 3.4). Our model was also designed to be comparable to the same head motion reported in our blast model (L. E. Goldstein et al., 2012). Operational parameters for experimental impact neurotrauma were chosen to closely match head kinematics

observed in our blast neurotrauma model (See Chapter 2).

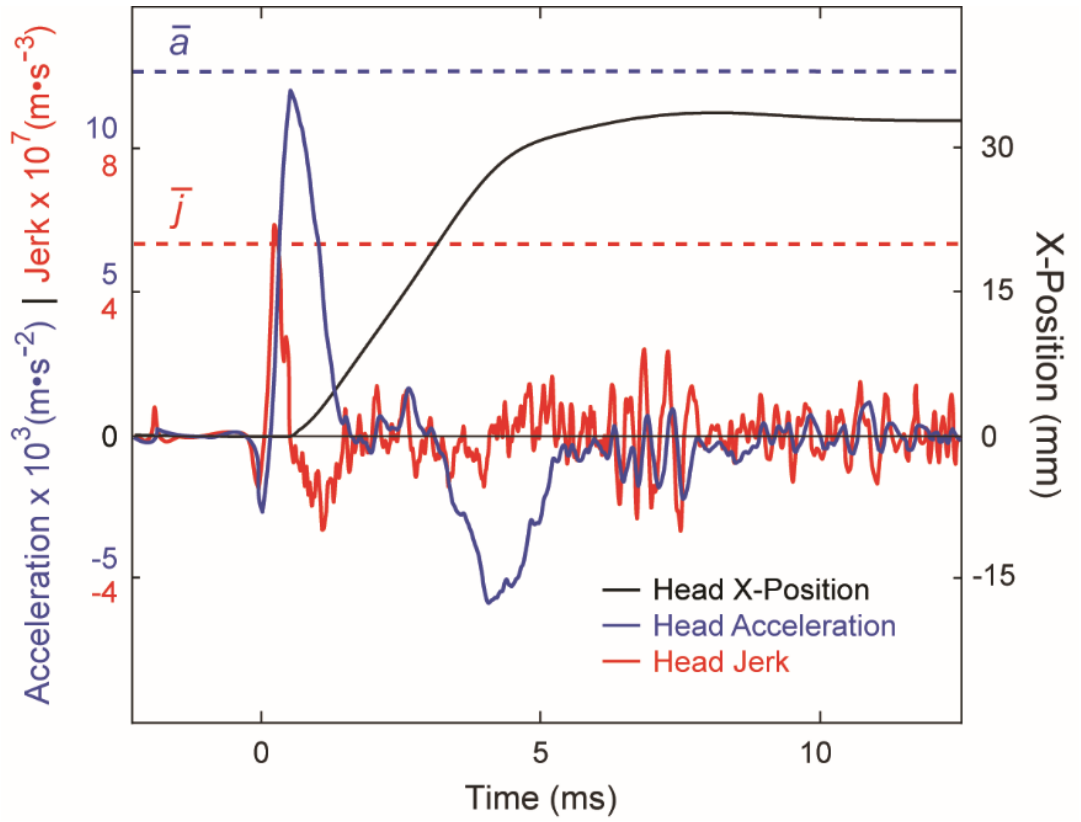

Figure 3.4: Representative kinematic plot of head motion in an awake mouse.
The impact neurotrauma model was designed to induce rapid head acceleration. High-speed videography (Chapter 2) head motion validates the design of the impact model.

To investigate concussion following impact TBI, each animal received a baseline, post-injury1, post-injury 2, and recovery BUCS score. We found that mean comparison over all time points between injury groups was significantly different ($p<0.001$). Comparison within the impact group showed the effect of impact neurotrauma on BUCS scores, with significant decrease from a baseline mean of 14.9 ± 0.02 to a post-injury 1 mean of 11.6 ± 0.2 (Baseline to Impact 1; $p < 0.001$, mean ± SEM). After the second hit, a further decrement in mean BUCS score (10.1 ± 0.2) was found compared to the

previous post-injury 1 mean (Impact 1 to Impact 2; $p < 0.05$, mean ± SEM). After 3 hours, mice fully recovered with significant increase from mean post-injury score to mean recovery score (10.1 ± 0.2 impact 2, 14.7 ± 0.04 recovery; $p < 0.001$, mean ± SEM) with no significant difference between mean recovery score and baseline score (14.9 ± 0.02 baseline, 14.7 ± 0.04 recovery; no significance; mean ± SEM). For control mice no significant difference was found between baseline, post-sham-1, post-sham-2, and recovery (Figure 3.5 and Figure 3.6).

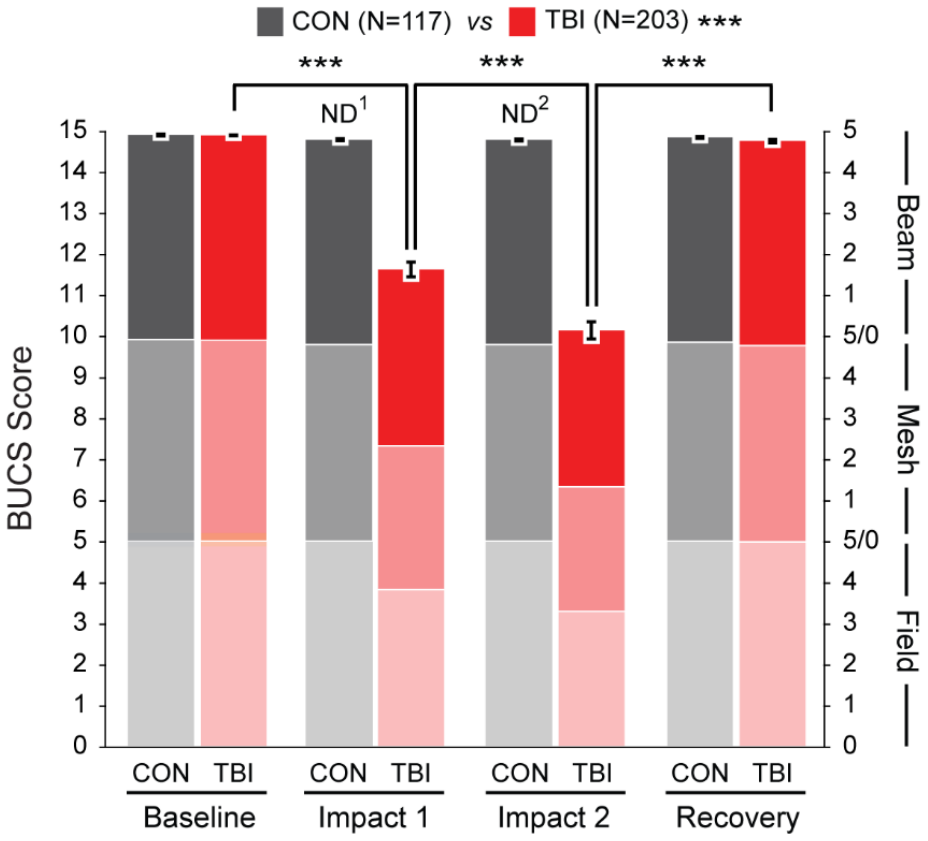

Figure 3.5: Boston University Concussion Scale (BUCS-3r) in mice.
A baseline BUCS assessment occurs before impact or control injury after injection of analgesic. Following impact injury the BUCS score drops measuring concussion and the BUCS score further lowers signifying an increase in concussion signs following 2nd hit. After 3 hours post-injury the impact mice completely recover from mTBI and return to baseline score. The BUCS design captures and measures the signs and severity of concussion. Control animals show no decrease in BUSC score over the different time assessments.

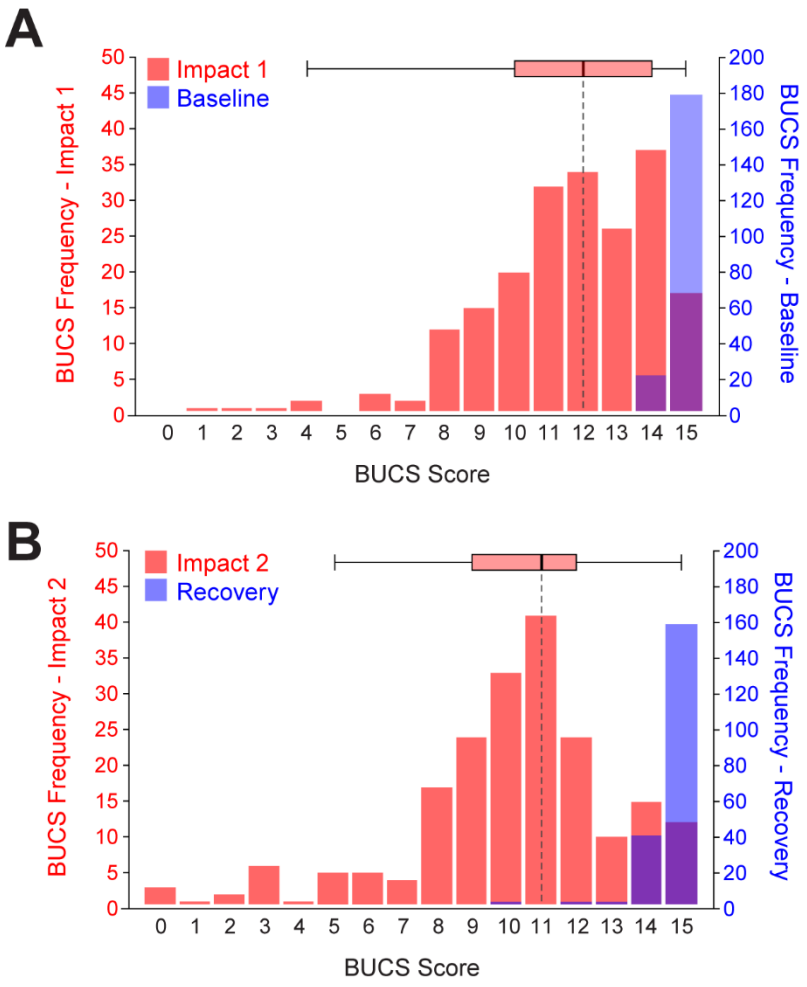

Figure 3.6: Individual phenotypic variation following impact neurotrauma.
Controlling for weight, age and genetics concussion varies based on individual mice.

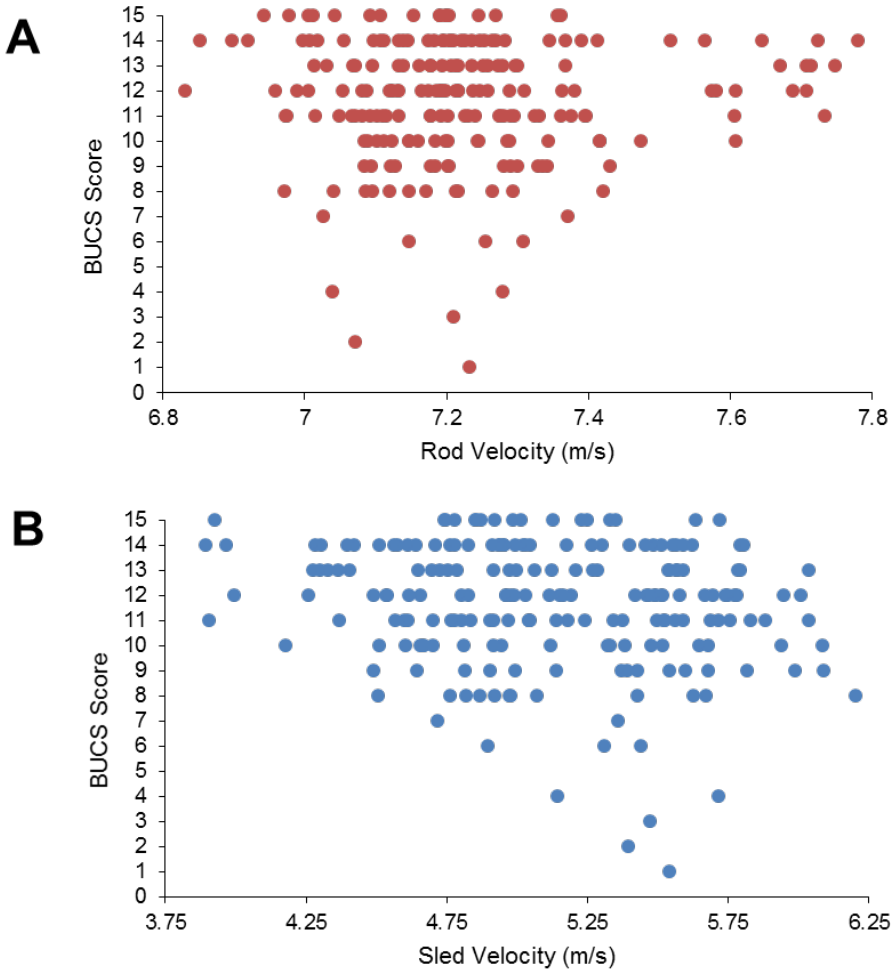

Figure 3.7: Rod and sled velocity does not correlate to BUCS hit 1 score.
Injury parameters do not correlate with resulting BUCS scores following exposure to initial impact neurotrauma. A) The graph shows no correlation between rod velocity and BUCS score (N=203). No correlation is also seen with sled velocity and BUCS score (N=203).

Symptoms of weakness, locomotion, and balance have been reported in athletes following concussive head injury (Guskiewicz, 2011; McCrory, Meeuwisse, Aubry, et al., 2013). The BUCS score accurately captured locomotion deficits and lateralized limb/grip weakness in mouse following impact neurotrauma. Using the Proc Mixed model, we found the amount of points lost between hit 1 and hit 2 differed for the open-field, mesh, and beam tests. The steepness of the slope between hit 1 and hit 2 provided

insights into where the decrease in BUCS points occur. The steepest slope between hit 1 and hit 2 was observed for the inverted mesh test. The difference in slope steepness for each subtest can be interpreted as an indicator of relative sensitivity for detection of transient post-traumatic neurological impairment (rank order: inverted mesh test > open field test > balance beam test).

Mice were impacted with an average sled velocity of 5.08 ± 0.5 m/s. However, we observed that the BUCS score distribution varied widely between animals. This observation is surprising given the tight control of the experimental injury (i.e., tank pressure, rod and sled velocities), animal subjects (e.g., matched for age, sex, weight, and genetics by strain), and large number of subjects in this study. These results underscore the wide variation in phenotypic response ("output") to what would appear to be similar if not identical injury conditions (input). This experimental observation comports well with the findings in numerous studies of human athletes that show wide variation in concussion threshold despite similar injury mechanisms, conditions, and kinematics (Guskiewicz, 2011; Guskiewicz et al., 2007; McCaffrey, Mihalik, Crowell, Shields, & Guskiewicz, 2007). In addition, we found no correlation between rod or sled velocity and BUCS score (Figure 3.7). Furthermore, no correlation was found between time of analgesic injection and BUCS score following hit 1 (N = 203) (Figure 3.8).

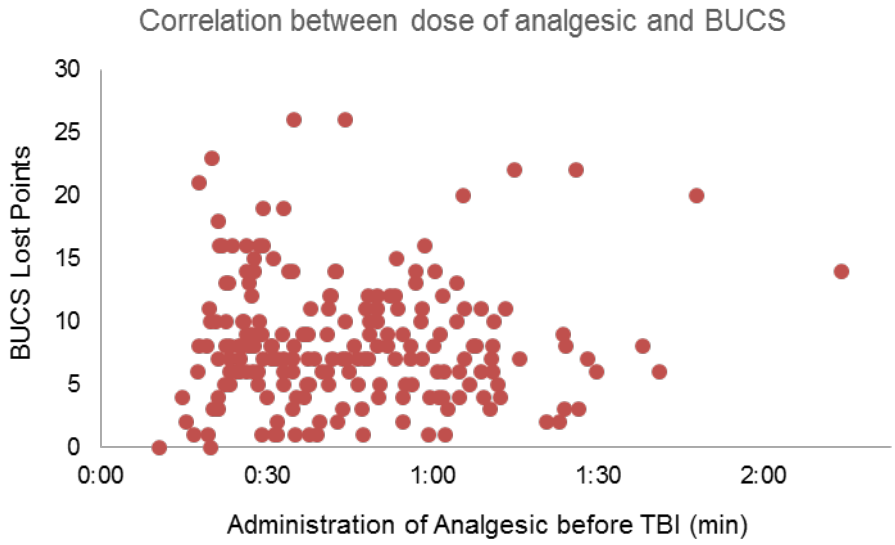

Figure 3.8: No correlation between injection of analgesic and BUCS score after hit 1. Mice are injected with analgesic before baseline BUCS test and are hit a minimum of 15 minutes after injection. The graph is scaled in hours, not minutes. This needs to be corrected.

3.4 Discussion

3.4.1 Validation of impact concussion model

Previous animal TBI models have been developed with the purpose of recreating different types of mild, moderate, or severe TBI (Cernak, 2005; Viano et al., 2012; Xiong et al., 2013). Classifying the severity of these injuries has most commonly relied on specific behavioral test such as the righting reflex or and composite scores such as the NSS (Alder et al., 2011; Beni-Adani et al., 2001; Y. Chen et al., 1996; Dixon et al., 1987; Eakin et al., 2014; Flierl et al., 2009; G. B. FOX et al., 1998; G. B. FOX et al., 1999; Fujimoto et al., 2004; Gennarelli, 1994; Hamm, 2001; Shapira et al., 1988; Shohami et al., 1988; Shohami et al., 1989; Stahel et al., 2000; Tsenter et al., 2008). A challenge in

current TBI research has been the misclassification of mild TBI as concussion without any pathobiological or neurobehavioral evidence to support this conjunction. To provide clinical validity to our impact neurotrauma model, we developed a novel impact neurotrauma model to induce transient lateralized neurological signs that recapitulate core clinical features of sports-related concussion in humans. To assess concussion in mice following closed-head impact injury, we developed and validated the Boston University Concussion Scale (BUCS) to enable rapid and objective assessment of transient neurological deficits that mirror those observed in concussed athletes (McCrory, Meeuwisse, Aubry, et al., 2013).

To date, most animal TBI models are conducted while the animal subject is deeply anesthetized. The clinical relevance of our mouse model depends on the biofidelity of the experimental-induced neurological deficits with respect to those observed in humans following an analogous head injury. General anesthesia and other neuropharmacological interventions that profoundly alter the sensorium introduce a serious confounding factor in any experimental TBI model used to study concussion. From a clinical perspective, the presence of mental status-altering drugs renders the GCS uninterpretable (Graham Teasdale et al., 2014). The requirement for conducting impact injury and neurological testing in non-anaesthetized mice represent critical components in the experimental design of the studies in this dissertation.

The overwhelming majority of TBI animal studies published to date have used anesthesia during experimental injury. Anesthetic pretreatment not only confounds post-traumatic neurobehavioral testing, but also influences brain injury outcomes. For

example, seven commonly used anesthetic agents differentially influenced cognitive recovery in a rat TBI model (Statler, Alexander, Vagni, et al., 2006; Statler, Alexander, Vayni, et al., 2006). Other studies have reported that anesthetic agents alter core body temperature, lipid peroxidation, and other key physiological factors that contribute to neurological recovery (Luh et al., 2011; Yurdakoc, Gunday, & Memis, 2008)(Planel et al., 2007). More worrying are the confounding effects of anesthesia on TBI-linked brain pathology, including anesthetic-induced persistent tau phosphorylation (Le Freche et al., 2012), induction of neuroinflammation (Luh et al., 2011), and changes in cerebral hemodynamics and cerebrovascular reactivity (Bowles & Gold, 2012). For these reasons it is not only necessary but experimentally imperative to conduct preclinical studies that target investigation of acute and chronic effects of neurotrauma in non-anesthetized animals.

3.4.2 Murine Concussion after Experimental Closed-Head Impact Injury

In McCrory *et al.* consensus statement on concussion in sport, concussion has been stated as to result in a rapid onset of short-lived impairments of neurological function that resolves spontaneously (McCrory, Meeuwisse, Aubry, et al., 2013; McCrory et al., 2009). The BUCS captured the observable impairments of locomotion, weakness, and balance that is often observed clinically after impact neurotrauma in humans. In our model, head injured mice transiently exhibited acute neurological signs that strikingly recapitulate concussion in humans. Moreover, as in sport-related head injuries, we observed further decrements in neurological function following a second impact of comparable intensity. In our model system, impact injury targeted the left-

lateral zygomatic region of the head. Predictably, post-injury BUCS testing revealed peripheral incoordination and weakness of the contralateral side of the body. Right-sided neurological deficits were also observed in the open-field test (i.e., clockwise rotation, right-sided upper extremity and paw grip weakness, and right-sided truncal asymmetry). Mice exhibited weakness on the contralateral side by showing incoordination in straight locomotion (counter-clockwise only motion) and inability to grasp mesh. On the beam test, static and balance deficits were observed with control mice finishing the test with the use of all paws, while concussed mice exhibited loss of balance and incoordination leading to the contralateral paws slipping off the beam, and in more severe cases, loss of static balance and truncal asymmetry leading to falls from the beam. Although these signs are easily observable following injury, all mice spontaneously recovered to baseline neurological function within 3 hours of injury. We did not observe any evidence of persistent locomotor deficits, weakness, or balance/gait impairments. In the clinic, the effects of concussion observed through the signs and symptoms vary greatly and are heterogeneous (Moser & Schatz, 2002) while in the animal model there appears to be highly consistence contralateral weakness and specific movements, suggesting specific impairments to locomotion, weakness and balance deficits are dependent on location of impact injury and suggest a similar mechanism which is investigated in Chapter 5. While the BUCS score was designed to capture specific domain deficits, the neurological impairments captured by the BUCS are consistent with analogous neurological signs associated with acute concussion and recovery in humans (Guskiewicz, 2011; McCrory, Meeuwisse, Aubry, et al., 2013; McCrory, Meeuwisse, Echemendia, et al., 2013;

McCrory et al., 2009).

The Question of Concussion Threshold

The diagnosis and definition of concussion are equally elusive. Much work has been done to understand the relationship between concussion and impact biomechanics with the goal of uncovering a threshold for concussion. To investigate this relationship, the leading hypothesis has been that linear and angular acceleration are the primary factors leading to concussion following an impact (Guskiewicz & Mihalik, 2011). In-helmet accelerometers have been developed and used to measure the linear and angular accelerations following a hit in different sport and different professional levels (Duma et al., 2005; Guskiewicz et al., 2003; Guskiewicz et al., 2000; McCaffrey et al., 2007; Mihalik, Bell, Marshall, & Guskiewicz, 2007; Mihalik et al., 2010; Naunheim, Standeven, Richter, & Lewis, 2000). Data from the accelerometers proved to be inconclusive in determining the magnitude needed to sustain a concussion (Guskiewicz & Mihalik, 2011; Guskiewicz et al., 2007). In our work, even with tight experimental control of the impact injury, including repeatable head kinematics and genetic homogeneity, we observed a highly variable concussion response measured by BUCS. Our experiments show no correlation between sled speed and BUCS, a finding consistent with the results of numerous studies of concussion in athletes outfitted with accelerometers during contact sport play (Guskiewicz & Mihalik, 2011; McCaffrey et al., 2007). As in our animal studies, a threshold for concussion cannot be precisely defined by injury kinematic parameters. Future studies should aim to vary impact severity, change padding material, and observe kinematics and BUCS deficits to further elucidate

biomedical inputs and the relationship to concussion.

3.4.3 Pain Medication and Concussion

Warner and colleagues sought to describe nonsteroidal anti-inflammatory drug (NSAID) use among high school football players (Warner, Schnepf, Barrett, Dian, & Swigonski, 2002). Their study reported 15% of the subjects surveyed were daily users. Reporting on these daily user's attitudes showed a perceived advantage in taking NSAID to block pain before it occurred with 91% reporting a perceived advantage in improved performance. In 2000, a survey given to NFL medical staff sought to determine the use of an injectable NSAID, called ketorolac tromethamine (brand name: Toradol) (Powell, Tokish, & Hawkins, 2002). Powell *et al.* found 28 of the 30 teams used ketorolac with an average of 15 players treated per team. Out of the 28 teams using Ketorolac, 93% reported the use of the medication on game day. A descriptive epidemiology study found in a collegiate population 53% believed injection of Ketorolac improved function and 38% thought it accelerated return to play (Sawyer, Anderson, Raukar, & Fadale, 2012). These findings suggest use of pain medication occurs at all sport levels ranging from high school to professional level and are taken to mask pain and aid in return to play (Powell et al., 2002; Sawyer et al., 2012; Warner et al., 2002). Studies investigating the effects pain medication on sideline assessments for concussion or neuropsychological testing has not been fully investigated as execution of such task would be difficult due to the prolific use of pain medication in sports.

In our animal model, prior to injury, mice received a dose of buprenorphine (0.2 mg/kg), a semisynthetic opioid with a half-life of 2.9 hours in a mouse (Yu et al., 2006).

Protocols for the impact require a minimum of 15-minute circulation time before injury. During these 15 minutes the mice undergo their baseline BUCS assessment. Our results showed no correlation between BUCS score and analgesic injection time. However, the use of an analgesic could possibly confound the BUCS score after impact by reducing pain and masking observable deficits in locomotion, balance, and grip strength. The prevalence of chronic pain medication in sport-athletes and its possible confounding effect in suppressing concussion signs and symptoms poses a serious concern. The development of this model and BUCS assessment provides the tools to investigate if a relationship exists between BUCS and pain medication in mice.

3.5 Assessment of Blood-Brain Barrier Disruption (Traumatic Microvascular Injury)

3.5.1 Motivation

The blood-brain barrier (BBB) plays an integral role in brain homeostasis. The BBB acts as a protective barrier by preventing neurotoxins from entering the brain while regulating the transportation of ions, neurotransmitters, and macromolecules (Abbott, Patabendige, Dolman, Yusof, & Begley, 2010). BBB dysfunction has been linked to many different neurological pathologies, including Alzheimer disease (Shlosberg, Benifla, Kaufer, & Friedman, 2010; Zlokovic, 2008); epilepsy (Remy & Beck, 2006); multiple sclerosis (Correale & Villa, 2007); hypoxia and ischemia (Kaur & Ling, 2008), and cerebral edema (Rosenberg & Yang, 2007).

Research on CTE pathology has shown that the early stage of the disease is

characterized by focal perivascular tau lesions (L. E. Goldstein et al., 2012; McKee et al., 2009; McKee et al., 2010; McKee et al., 2013). A recent NIH-sponsored consensus conference determined the pathognomonic signature of CTE was abnormal perivascular accumulation of phosphorylated tau protein in neurons and glia, in an irregular, focal pattern at the depths of the cortical sulci (NIH- Report First NIH Consensus Conference on CTE) (McKee et al., 2015).

These findings point to the possible involvement of BBB disruption and CTE pathogenesis. We hypothesis that impact concussion would induce traumatic BBB disruption (i.e., traumatic microvascular injury, TMI). To test this hypothesis, we designed an experiment to inject a serum albumin-binding dye (Evans Blue) prior to impact concussion and measure the fluorescence signal to determine the extent of extravasation of blood protein (i.e., albumin, the most abundant serum protein) across the BBB into the brain. Leakage of blood proteins into the brain parenchyma does not occur under normal physiological conditions when the BBB is intact. Compromise of BBB functional integrity is the pathogenic sine qua non of TMI.

3.5.2 Methods

Animal subjects

Animal subjects were subjected to experimental concussive impact injury or sham (no impact) control condition as explained in section 3.2.1. To assess BBB disruption, 1 hour before injury the mice received an intraperitoneal injection of a 2% weight-by-volume solution of Evan Blue (4 ml/kg of body weight), with the rationale that 1-hour

post-injection circulation time resulted in brain accumulation of EB following intracranial injection of collagenase (Manaenko, Chen, Kammer, Zhang, & Tang, 2011). The animals underwent the same impact/control injury and BUCS testing as before. Control mice underwent the same procedure but without impact injury.

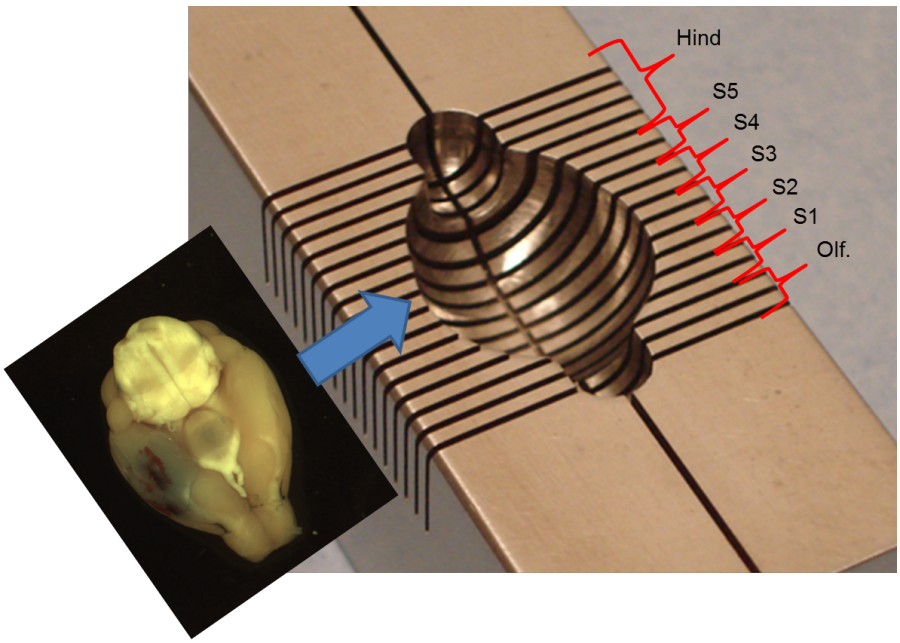

Figure 3.9: Slicing of the brain for BBB disruption.
Using a tissue block, the brain was placed and cut into 2 mm slices. The olfactory bulbs were not used (Olf) nor was the hindbrain (Hind.) For EB extravasation analysis only Slice 1-4 was used. (S1-S4)

To assess acute Evans Blue extravasation into the BBB, the mice were euthanized by CO2 asphyxiation according to IACUC-approved protocol followed by transcardially-gravity perfusion with phosphate-buffered saline. The brains were rapidly removed from the calvarium and gross pathology photos were taken with a cross-polarization camera set-up with a Nikon D5200.

Afterward, the brains were imaged using the IVIS Spectrum preclinical imaging system (Perkin-Elmer). Using the Living Image software (Perkin-Elmer), the excitation

filter was set at 535 nm and 14 fluorescence images were taken at emission filters set at 580, 600, 620, 640, 660, 680, 700, 720, 740, 760, 780, 800, 820, 840nm. The exposure time for each image was set at 0.5 seconds. The dorsal and ventral sides of the brain were imaged. The brains were sectioned coronally into 2 mm thick slices using a tissue block, rostral to caudal (Figure 3.9). Taking multiple images at different emission filters, the auto-fluorescence signal from the tissue was removed using a spectral unmixing feature available in the Living Image Software (Perkin-Elmer). To quantify regions of interest, the unmixed, calibrated images were saved and masked using Photoshop (Figure 3.10). A custom-written script developed by Ms. Amanda Guadreau-Balladrama (ECE) outputted raw pixel data from masks and fluorescence images. Data were further processed to prepare for data analysis. To calculate fluorescence signal, intensity was normalized to pixel area for each masked region and grouped by side, injury, and laterality. Percent of EB extravasation pixels was calculated by taking the mean 95^{th} percentile of all the counts per control slice and defined the value as the threshold. The threshold was applied across all brain slices and corresponds to EB extravasation (Weissberg et al., 2014). Grouping of EB extravasation pixel percentage was performed using a Gaussian mixture model (Matlab). Masking data measured by the IVIS are reported in counts/pixel. Linear mixed-effects regression analyses were used to test for the group differences for EB extravasation and to test the association between laterality and slices. We allowed for outcome-specific fixed effects and subject-specific random effects. Outcomes of the same mice were correlated using a single between-subject correlation by applying a compound-symmetry model for the covariance matrix. Spearman's rank order correlation

was performed for correlation analysis between BUCS and fluorescent sign and percent BBB disruption. Levels of analysis between BUCS and fluorescent sign and percent BBB disruption. Levels of significance were indicated as follows: *, $P < 0.05$; **, $P < 0.001$; < 0.001. Statistical significance was set at $P < 0.05$.

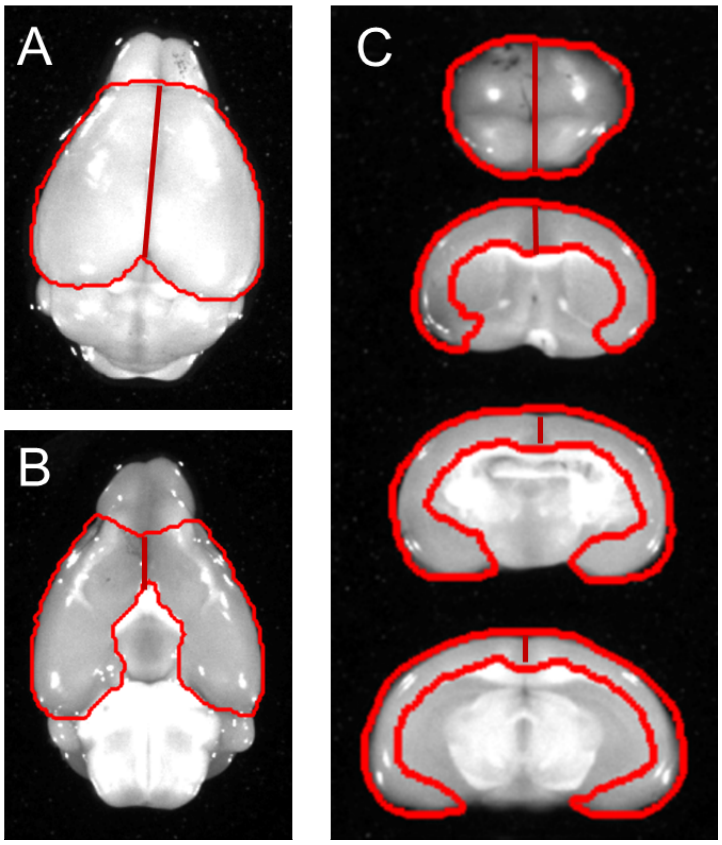

Figure 3.10: Masking protocol for EB fluorescence images.
A) Masking protocol was to only include the cortex of the dorsal surface, excluding the cerebellum and olfactory bulbs. B) Masking the ventral surface. Masking protocol was to segment only the cortex, removing the hypothalamus, brain stem, and the olfactory bulbs. C) Slices 1 to 4 were used. The first slice contained the pre-frontal cortex and was segmented along the surface and split into left and right sections. Slice 2, was masked to only contain the surface of the cortex, and following along external capsule until reaching the anterior commissure, where the mask would extend perpendicular from the brain surface. Slice 3, masked the surface of the cortex and followed the external capsule and contains the amygdala. Slice 4, masked the surface of the cortex and followed the external capsule.

3.5.3 Results

BBB disruption in impact concussion model

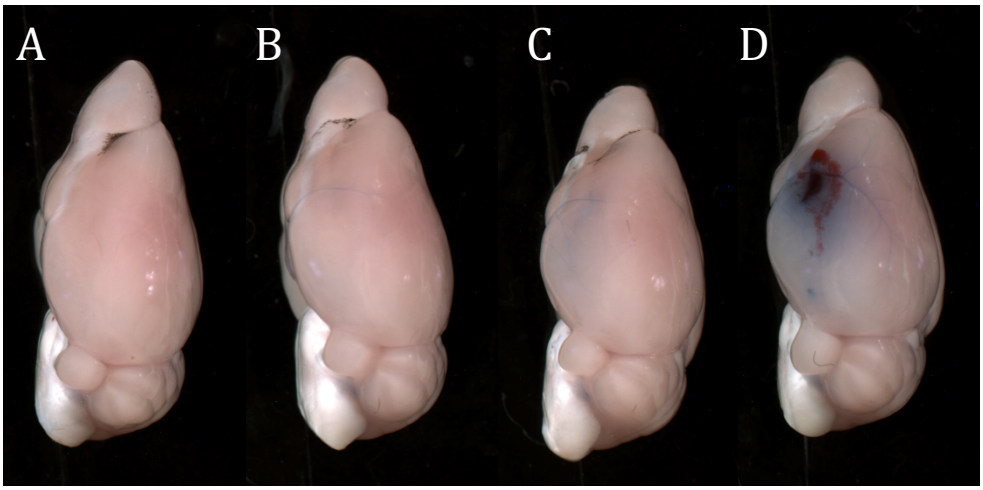

Figure 3.11: Gross pathology of brains 24 hours after injury.
A) Control brain with no signs of EB. B) Impact brain with no visible signs of BBB disruption. C) Impact brain with slightly visible EB. D) Impact, large area of EB extravasation and contusion.

Gross pathology observation of the control brains showed no signs of EB extravasation. Impact gross pathology showed a range of severity and were classified through a graded scale. Grade 0 has no visible EB (Figure 3.11-A,B); grade I has visible EB (Figure 3.11-C) and grade II has visible signs of EB and contusion (Figure 3.11-D). No gross pathology was observed on the contralateral side.

We used the IVIS Spectrum preclinical imaging system (Perkin Elmer) to measure the fluorescence signal on the dorsal and ventral surface of the brain. Spectral un-mixing removed endogenous tissue auto-fluorescence and was performed with a function in the Living Image software. Images of the dorsal and ventral surfaces revealed increased counts on the left-lateral side. The IVIS images (Figure 3.12 and Figure 3.13) correspond to the gross pathology images (Figure 3.11). After imaging the dorsal and

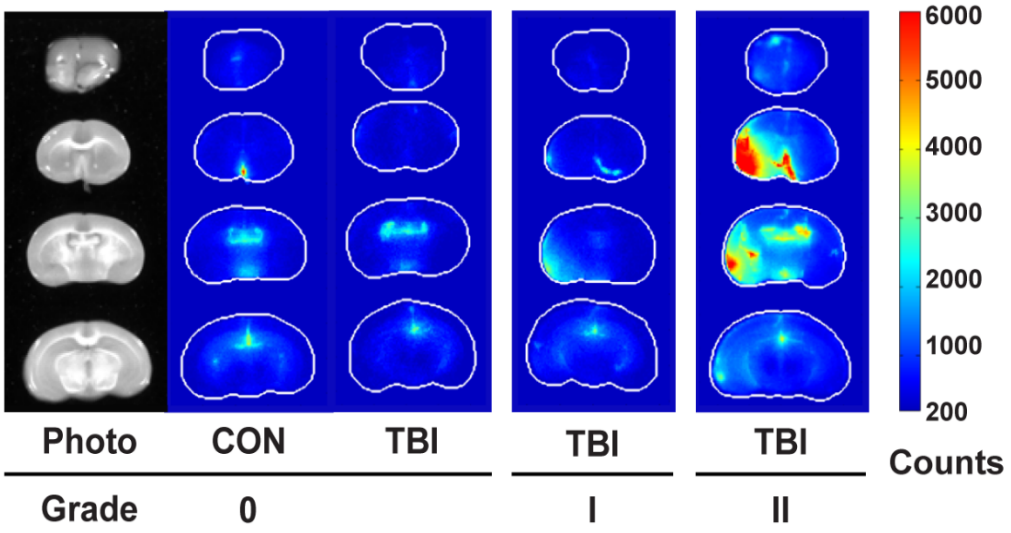

Figure 3.12: Fluorescence signal of EB extravasation by slice.
For quantitative assessment of EB signal, the brains were sliced into 2 mm thick slices and imaged with the IVIS imaging system at 24 hours. Fluorescence images were graded based on intensity. Grade 0 – contains all the control brains. Some impact brains were classified as grade 0. Grade I – contained only impact brains and had no high fluorescence signal (red), Grade II – contained high fluorescence signal. Grade 3 gross pathology showed BBB breakdown, blood and contusion.

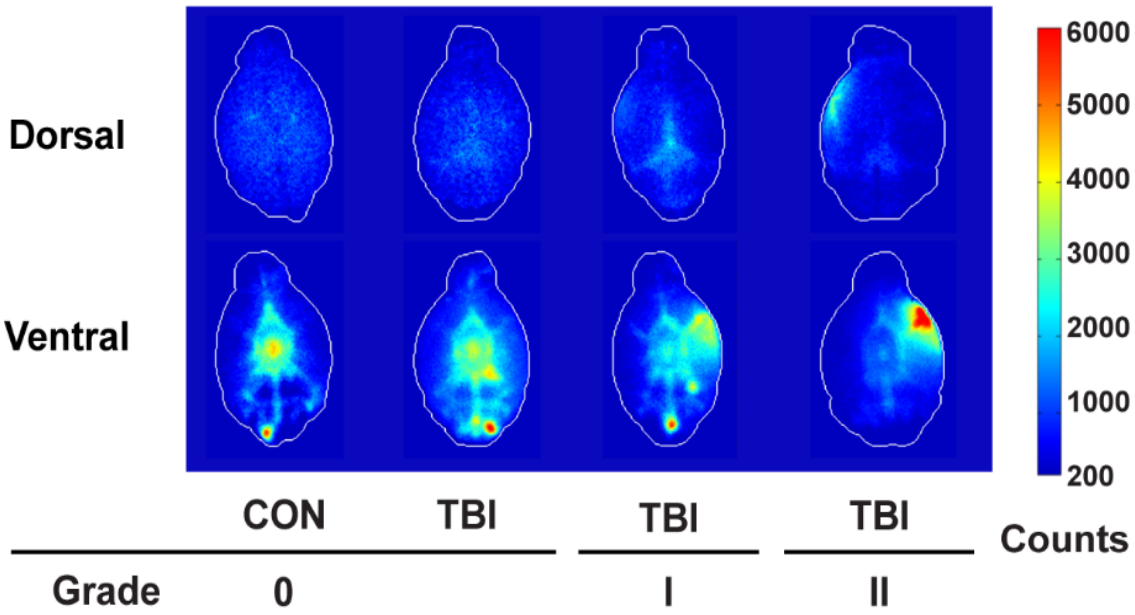

Figure 3.13: Fluorescence signal of EB extravasation for dorsal and ventral surface.
Brain surfaces correspond to gross pathology images in Figure 3.11.

ventral side with IVIS, each brain was sliced into 2 mm thick sections to characterize the focal distribution of fluorescence signal. Our Proc Mixed model revealed signal intensities for the control slices were comparable across all slices (1–4) and were not significantly different between ipsilateral and contralateral sides (Figure 3.14). Comparison between all ipsilateral impact slices revealed an increase in estimated marginal mean (EMM) signal intensity compared to ipsilateral control slices ($p = 0.003$, $F(15,118) = 410$) and an increase in signal intensity was seen between the ipsilateral impact slices compared to the contralateral impact slices ($p<0.0001$, $F(15,118) = 381$). Comparison between impact slices revealed a significant EMM increase from slice 1 to slice 2 ($p < 0.0001$, $F(15,118) = 408$), slice 1 to slice 3 ($p = 0.002$, $F(15,118) = 277$), slice 4 to slice 2 ($p = 0.0003$, $F(15,118) = 323$), and slice 4 to slice 3 ($p = 0.03$, $F(15,118) = 192$). EMM signal intensity comparisons within slice 2 showed a significant increase on the ipsilateral impact side compared to slice 2 controls ($p < 0.0001$ $F(15,118) = 763$) and a significant higher EMM signal on the ipsilateral impact side compared to the contralateral impact side ($p < 0.0001$ $F(15,118) = 670$). Significant EMM differences were similar for slice 3, with a significant increase on the ipsilateral impact side compared to slice 3 controls ($p = 0.003$, $F(15,118) = 502$) and a significantly higher EMM signal on the ipsilateral impact side compared to the impact contralateral side ($p < 0.0001$, $F(15,118) = 532$). Comparison between impact ipsilateral slices showed a significant EMM increase from slice 1 to slice 2 ($p < 0.0001$, $F(15,118) = 717$) and a significant EMM difference between slice 1 and slice 3 ($p < 0.0001$, $F(15,118) = 503$), while noting a significant EMM decrease between slice 3 to slice 4 ($p = 0.006$, $F(15,118)$

= 349) and a significant EMM difference between slice 2 and slice 4 ($p < 0.0001$, $F(15,118) = 563$). Greater signal in the impact slice-2 and slice-3 compared to slice-1 and slice-2 reveals a focal distribution. Also note that the impact contralateral sides showed

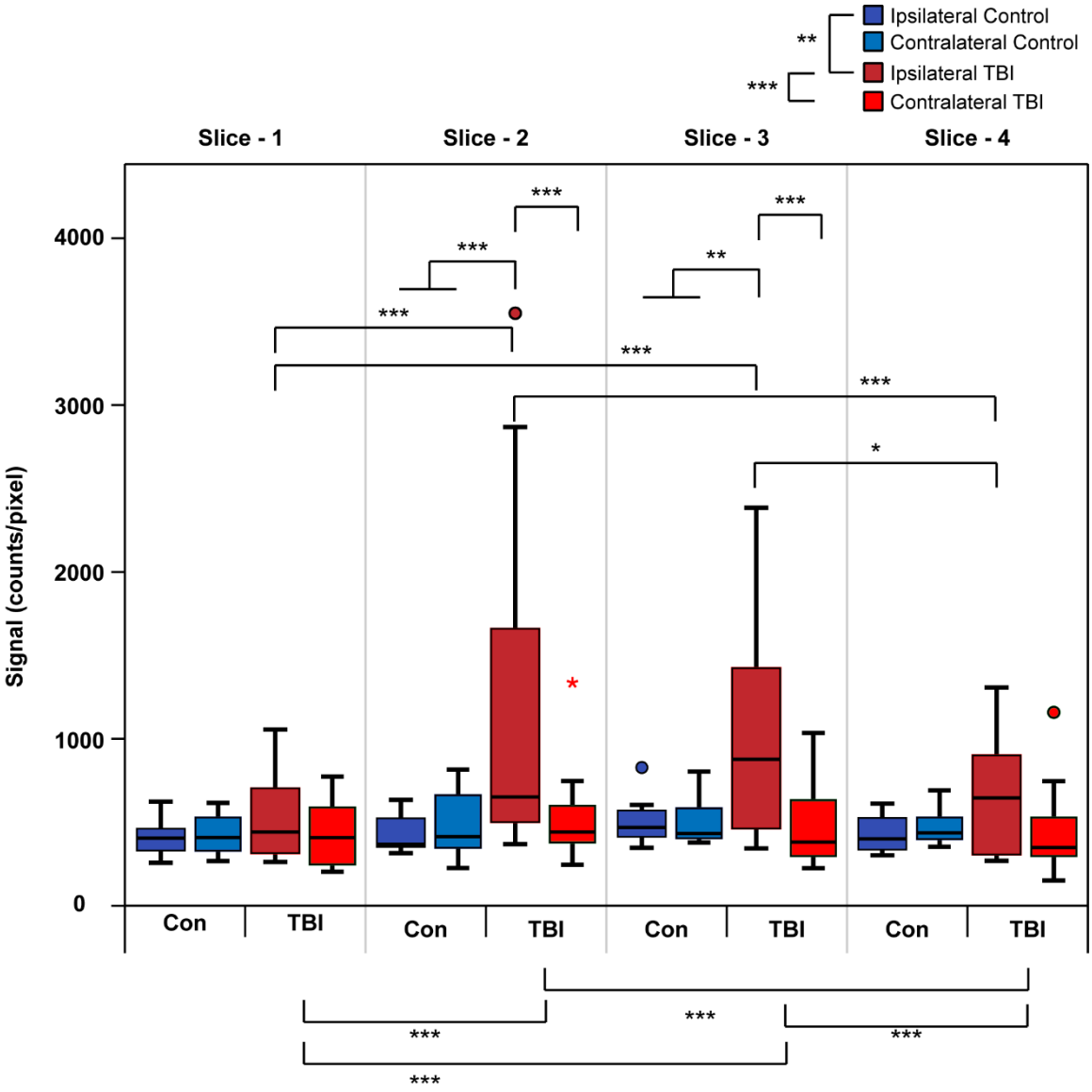

Figure 3.14: Concussive impact neurotrauma induces heterogeneous EB extravasation. Box plots of signal intensity normalized to pixel area for each masked region. Circles designate outliers and colored stars designate extreme outliers. Levels of significance were indicated as follows: *, $p < 0.05$; **, $p < 0.001$; ***, $p < 0.0001$

no significant difference between any control slices, suggesting for our model BBB disruption occurs only on the side of impact.

We used a defined threshold similar to a method reported by Weissberg *et al*. to calculate EB extravasation pixels (Weissberg et al., 2014). The method proposed by Weissberg *et al.* calculated BBB-disrupted voxels in American football players using dynamic contrast-enhanced magnetic resonance imaging (DCE-MRI). To compare our results to the clinical data, we calculated the mean 95^{th} percentile for all control slices for use as the threshold for EB extravasation into the parenchyma. Number of pixels above threshold in a slice was divided by the total pixels in the slice and was reported as percent of EB extravasation pixels. EB extravasation pixel data was plotted as box plots (Figure 3.15), analyzed using the same Proc Mixed model (SAS) and indicated a significant difference between all ipsilateral impact slices and all ipsilateral control slices ($p = 0.004$, $F(15,118) = 23.2$) and a significant increase between ipsilateral impact to contralateral impact ($p < 0.0001$, $F(15,118) = 16.9$). Comparison between impact slices reported a significant EMM percentage increase between slice 1 to slice 2 ($p = 0.01$, $F(15,118) = 9.5$) and slice 1 to slice 3 ($p = 0.0003$, $F(15,118) = 13.7$). A significant EMM percentage decrease was seen between slice 3 and slice 4 ($p = 0.02$, $F(15,118) = 8.8$). EMM percentage disruption compared within slice 2 showed a significant increase on the ipsilateral impact side compared to slice 2 controls ($p = 0.002$, $F(15,118) = 28.6$) and a significant higher EMM percentage on the ipsilateral impact side compared to the contralateral side ($p < 0.0001$, $F(15,118) = 21.1$). The same was seen for slice 3 with a significant increase on the ipsilateral impact side compared to slice 3 controls ($p =$

0.0003, F(15,118) = 33.5) and a higher EMM percentage on the ipsilateral impact side compared to the contralateral impact side ($p < 0.0001$, F(15,118) = 26.7). For slice 4,

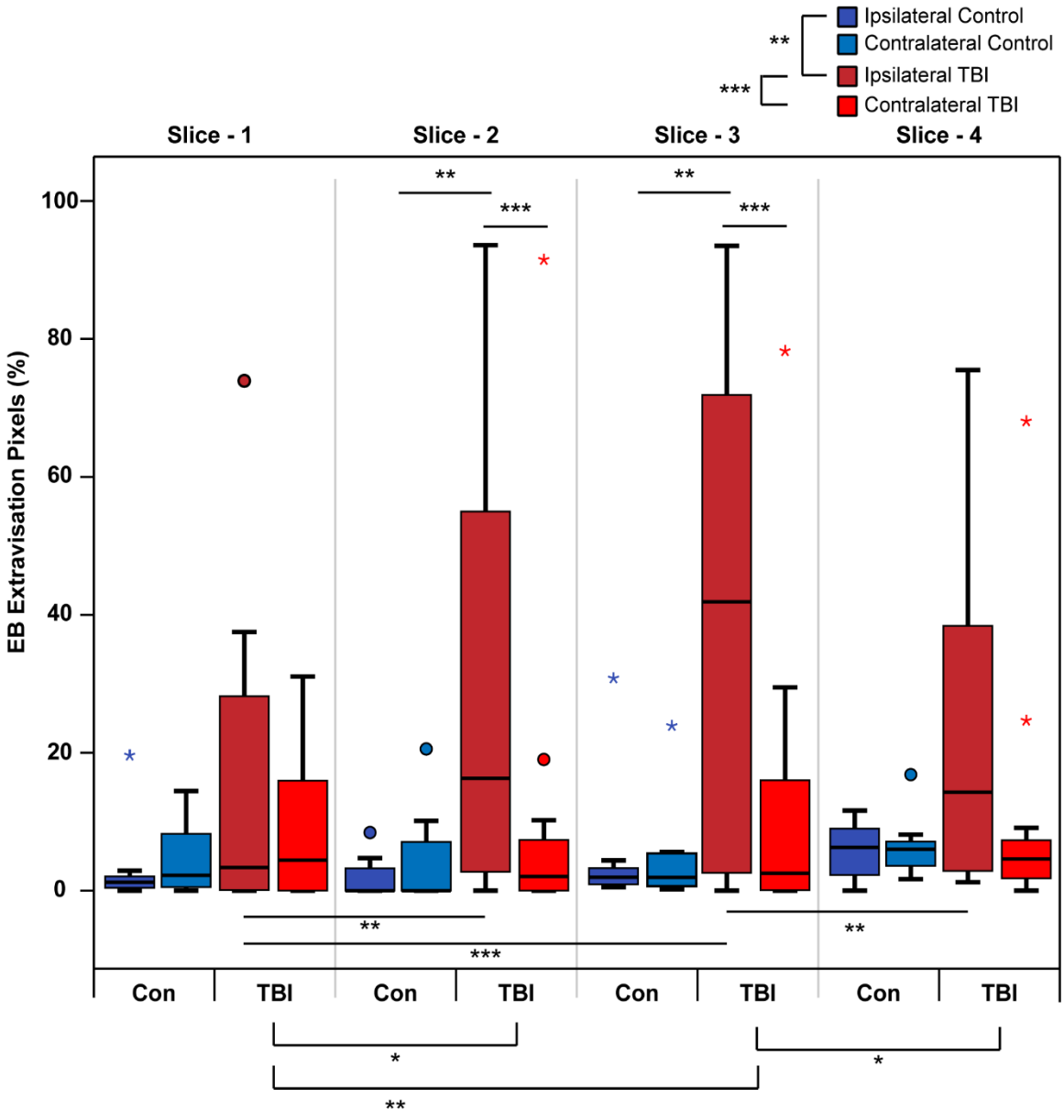

Figure 3.15: Concussive impact neurotrauma induces heterogeneous distribution measured by percent EB extravasated pixels.
Threshold of Evans Blue extravasated pixels was determined by calculating the mean 95th percentile of all the counts per control slice. Circles designate outliers and colored stars designate extreme outliers. Levels of significance were indicated as follows: *, $p < 0.05$; **, $p < 0.001$; ***, $p < 0.0001$

EMM percentage was higher on the ipsilateral impact side compared to contralateral impact side ($p = 0.02$, $F(15,118) = 12.6$). Comparison between ipsilateral impact sides showed a significantly higher EMM percentage disruption from slice 1 to slice 2 ($p = 0.002$, $F(15,118) = 16.5$) and a significant EMM difference between slice 1 and slice 3 ($p < 0.0001$, $F(15,118) = 23.5$). No significant difference was found between the ipsilateral impact side for slice 2 and slice 3, while a significant mean decrease was found between slice 3 and slice 4 ($p = 0.003$, $F(15,118) = 15.8$). Review of impact slice-1 contralateral side showed some impact slices contained a small fluorescence hot spot probably due to dura attached to the surface effecting the percent of EB extravasation for that slice.

Combining all slices by injury group, we calculated the total percentage of EB extravasation pixels for each animal. Automatic Gaussian clustering of the animals revealed 3 subgroups: a group with low percentage containing 6 control animals and 5 impact animals, a group with medium percentage containing 1 control and 5 impact animals, and a high percentage consisting of 2 impact animals. Gaussian grouping by EB extravasation corresponds to the observed gross surface pathology grading. In grade I and grade II, all EB extravasation pixels were found in the left-lateral slices, except for the control grade I brain and EB extravasation was found in slice-1 and slice-2 on the contralateral sides (Figure 3.16).

Each impact animal had a BUCS assessment with a baseline, post-hit 1, post-hit 2, and recovery score. BUCS lost points reflects the points lost after both post injury assessments. We assessed possible correlation between BUCS lost points and fluorescence signal or percentage of EB extravasation (n=11). Spearman's rank-order

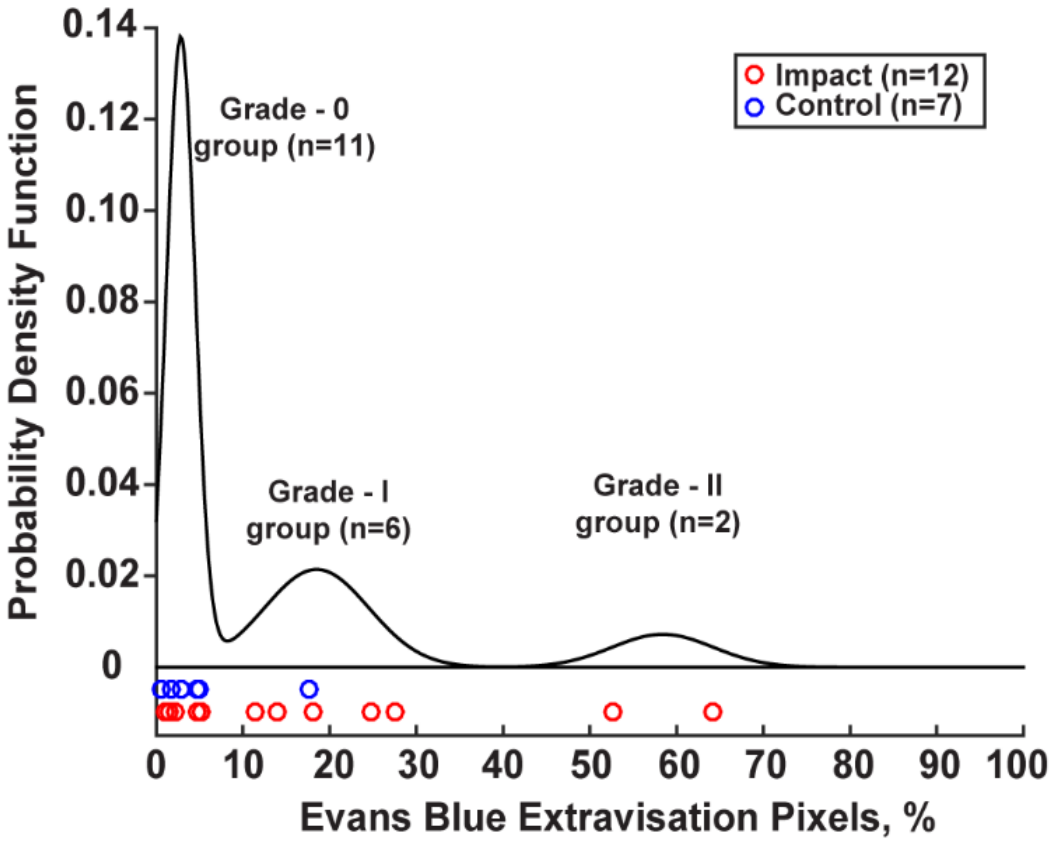

Figure 3.16: Clustering of mice based on percent Evans Blue extravasation pixels. Percent Evans Blue (EB) extravasation pixel was calculated by applying a threshold (mean 95th percentile of all control slices) which defined a pixel with no EB extravasation. Percentage of extravasation pixel above threshold were clustered using a Gaussian mixture model.

correlation revealed no correlation between any whole brain signal and whole brain percentage with BUCS lost points. No correlation was present between both the left and the right side for counts and percentage (Figure 3.17). Analysis for individual slices revealed no correlation for counts or percentage (n = 11) (Figure 3.18).

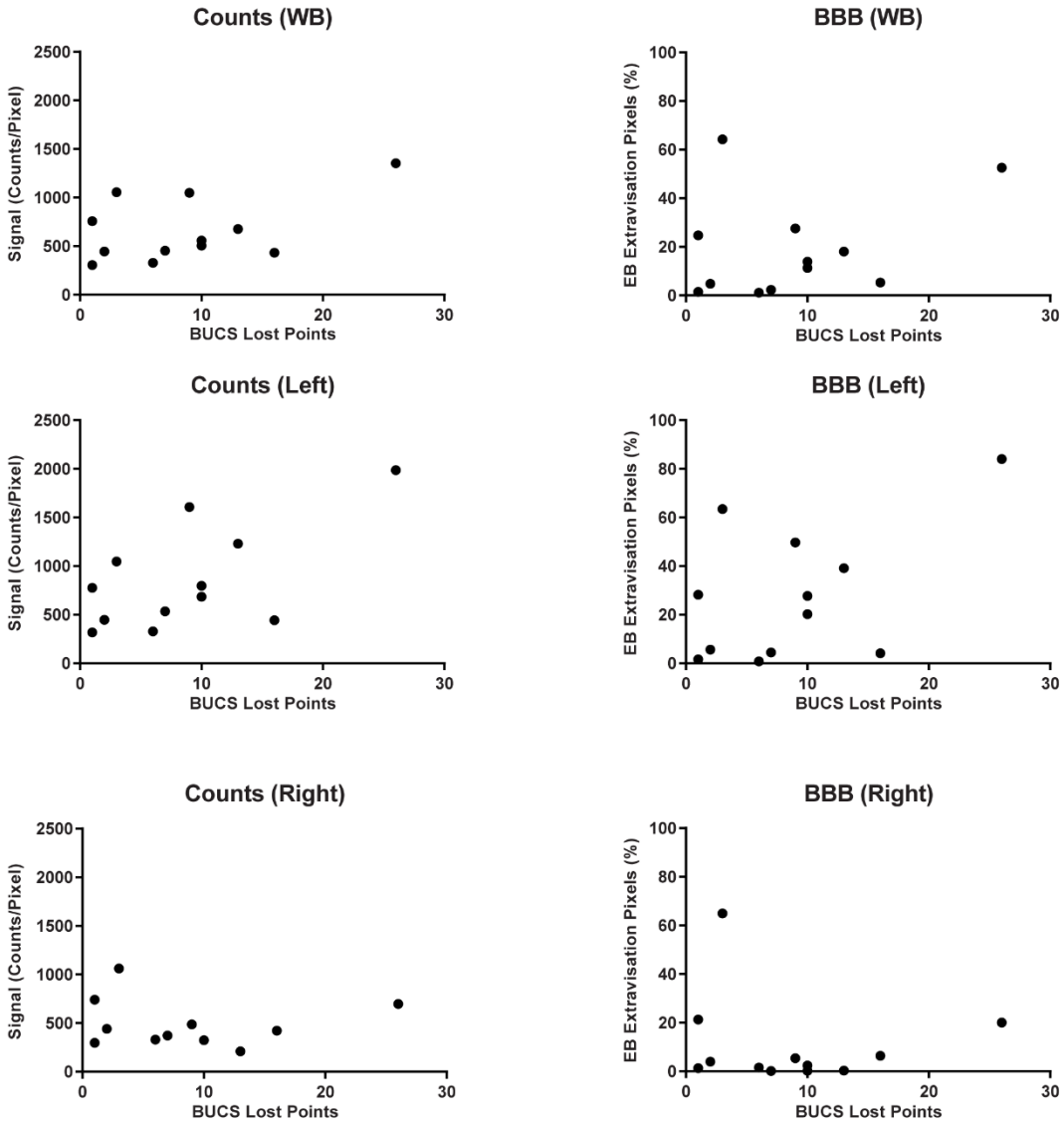

Figure 3.17: Correlation analysis for counts and percent of Evans Blue extravasation.
Correlation analysis for whole brain (WB) and ipsilateral (Left) and contralateral (Right) side.

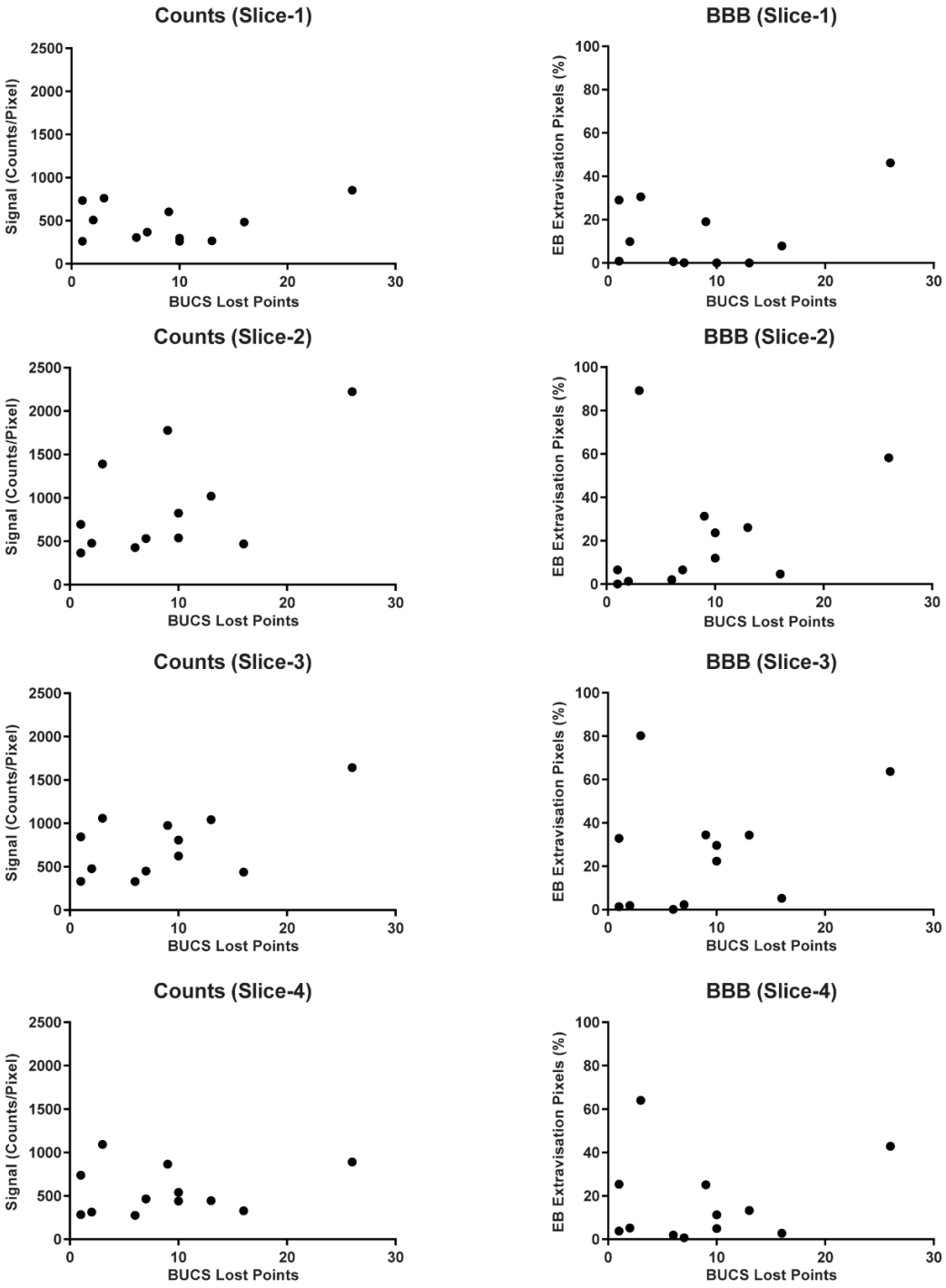

Figure 3.18: Correlation analysis for counts and percent of Evans Blue extravasation for each slice.

3.5.4 Discussion

Evans Blue assay is a commonly used technique to evaluate BBB disruption as this dye binds serum albumin (Gregersen & Rawson, 1943). By using EB fluorescence, a common technique to determine BBB disruption relies on the use of a spectrophotometer to measure the amount of EB dye in a homogenized brain (Ballabh, Braun, & Nedergaard, 2004). Limitations in sensitivity to detect EB and inability to globally assess location of the dye led Jaffer and colleagues to develop an optical imaging method to map vascular leakage in a rat stroke model (Jaffer, Adjei, & Labhasetwar, 2013). The same group used this method to assess vascular leakage following blast TBI (Kabu et al., 2015). To evaluate the extent and location of EB extravasation into the brain parenchyma after closed-head impact injury, we optically imaged the surface and slices of impact and control brains using the Boston University Medical Campus IVIS Imaging Core.

In this experiment, fluorescent imaging using the IVIS system was able to reveal a varying extent of BBB disruption at 24 hours in impact animals. Of the impact group, 5 of 12 were classified as intact BBB (Group 0), 5 of 12 were classified with visible BBB, (Group I) and 2 of 12 were classified with high BBB disruption with contusion (Group II). Impact groups were confirmed by gross pathology and Gaussian analysis. In the control group, 6 of 7 were classified as having intact BBB with 1 of 7 in the visible BBB group. Review of all acquired fluorescence images revealed possible confounding contamination on two contralateral slices by residual dura mater, which remained highly perfused with EB dye after 24 hours.

BBB disruption following TBI has been garnered from previous animal models

using controlled-cortical impact (Y. Chen et al., 1996; Flierl et al., 2009; Stahel et al., 2000) and weight-drop methods (Habgood et al., 2007; Hellal et al., 2004; Zohar et al., 2003). However, these models were primarily designed to investigate moderate to severe TBI with prominent diffuse axonal injuries. Interpretation of the results of these studies is confounded by craniotomy and crush injury, both factors that alter BBB structure and function. Clinical analysis using DCE-MRI revealed 40% of imaged football players had BBB pathology (Weissberg et al., 2014). BBB lesions occurred focally and without correlation between concussion and BBB pathology. Our results revealed BBB disruption is most prominent on the ipsilaterally cortex near the site of impact. We did not detect significant correlation between BUCS lost points and EB extravasation. Furthermore, impact injury resulted in a heterogeneous distribution of BBB disruption among injured animals, while possible explanations could include the injury mechanism such as positioning the animal during impact and variation of impact parameters. Biological differences such as slight variations in blood vessel and capillary anatomy could also influence BBB disruption when impact energy is transferred to the skull. To further elucidate the distribution of BBB disruption in an impact concussion group, further studies with larger samples sized are required.

Review of the unique pathological features of CTE suggests BBB disruption plays a role in the development of CTE (L. E. Goldstein et al., 2012; McKee et al., 2009; McKee et al., 2010; McKee et al., 2013). Research following football players who were exposed to multiple hits but reported no concussions revealed increased serum astrocytic protein S100Bs, suggesting BBB disruption (Marchi et al., 2013). Although this imaging

technique captured macroscopic disruption and gross pathological changes, we have reported that BBB disruption occurs at the ultrastructural level in our blast TBI animal model (L. E. Goldstein et al., 2012). Investigating ultrastructural BBB disruption after concussion impact is under active investigation in our laboratory. Other animal studies have reported BBB disruption occurs with rapid onset, increases permeability of the BBB, and declines with a delayed phase 3 to 7 days post injury in controlled-cortical impact animal model and found BBB leakage persisted from days to weeks (Baskaya, Rao, Dogan, Donaldson, & Dempsey, 1997; Shapira, Setton, Artru, & Shohami, 1993; Shlosberg et al., 2010).

We have reported that BBB disruption occurs at the macroscopic scale in a focal region after concussion impact injury and found no correlation between BUCS lost points and BBB disruption. However, the extent of BBB damage was found to be heterogeneous within the injured group and consistent with the clinical spectrum of BBB disruption in sport-related impact injuries. Understanding the acute and long-term sequelae of BBB disruption after impact injury for both concussive and sub-concussive hits remains undetermined and warrants further investigation. This impact model, which can induce concussion injuries, could contribute to our understanding into the possible mechanistic role BBB disruption plays in the formation of the pathognomonic, focal, perivascular pathology of CTE.

3.6 Detection of Traumatic Microvascular Injury In-Vivo

3.6.1 Motivation

Current neuroimaging techniques rely on the use computer tomography (CT) and magnetic resonance imaging (MRI). After brain injury, neuroimaging provides essential clinical information to identify macroscopic abnormalities and to determine the severity of brain injury. MRI is more sensitive than CT for detecting brain abnormalities in TBI patients (Lee et al., 2008). Assessment of structural damage (e.g., contusions, hematomas, hemorrhage) by neuroimaging has become an integral part of TBI classification (Maas et al., 2008). However, neuroimaging with conventional CT and MRI commonly reveals no structural abnormalities in mild TBI patients (Shenton et al., 2012). Yet, a clinical study of 47 mild TBI cases found that 27.7% of these patients showed intracranial abnormalities by conventional neuroimaging (e.g., CT or MRI) (Iverson et al., 2012).

Difficulties in diagnosing mild TBI has led to the development of advanced neuroimaging techniques with the purpose of characterizing abnormalities (i.g. micro-hemorrhages), increasing the sensitivity of observing microstructure changes, and measuring brain function with the motivation to develop neuroimaging biomarkers following injury (Shenton et al., 2012). One such structural imaging technique is diffusion tensor imaging (DTI), a relatively new technique that has been used to investigate white matter changes following TBI (Bazarian, Blyth, & Cimpello, 2006). DTI has been performed in athletes (Koerte, Ertl-Wagner, Reiser, Zafonte, & Shenton, 2012; McAllister et al., 2014) and while these findings suggest diffusivity changes

following injury (Shenton et al., 2012), it should be noted that DTI studies rely on group comparisons and as a consequence are of limited clinical value in identifying TBI-linked brain abnormalities in individual patients (Bazarian, Zhu, Blyth, Borrino, & Zhong, 2012). Functional MRI (fMRI) has been used to measure brain function through the association of oxygen consumption (Han, Bangen, & Bondi, 2009). Application of this technique in mild TBI patients has focused on investigating working memory (Jantzen, Anderson, Steinberg, & Kelso, 2004; McAllister et al., 1999; McAllister et al., 2001) and researchers have suggested correlations between fMRI abnormalities and post-concussion symptoms (J. K. Chen et al., 2004; Lovell et al., 2007). As with DTI, fMRI suffers from the same issue regarding single-subject analysis. While these neuroimaging techniques hold promise as possible research biomarkers for brain injury, further studies are needed to validate the utility and efficacy of these diagnostic imaging modalities for routine clinical care.

Results from our previous BBB experiment provided evidence of BBB disruption following concussion impact, but only assessed the injury at a single time point. In order to detect alterations in the BBB associated with concussion impact, serial dynamic contracts-enhanced (DCE) MRI scans were performed at 3, 24, 72 hours, and 1 week post-injury. An albumin-binding gadolinium based contrast agent (Gadofosveset Trisodium, Ablavar) was injected during each scan. In these experiments, we sought to investigate the ability of DCE-MRI to detect subject-specific changes in BBB disruption following closed-head concussive impact injury in a mouse.

3.6.2 Materials and methods

Imaging Protocol

MRI imaging was performed by the Boston University Medical Center MRI/NMR High Field Imaging Core. Animal subjects were subjected to experimental concussive impact or sham (no impact) conditions. Mice were injected with analgesic (buprenorphine, 0.2 mg/kg, i.p.) *but without anesthesia* before receiving a baseline BUCS score. BUCS scores were assessed after each injury as previously described. Imaging was performed using 11.7 T MRI (Bruker, Ettlingen, Germany) at Boston University Medical Center (BUMS). Anatomical images were acquired using T1-weighted sequence (axial multi-slice multi-echo, TR/TE = 450/9 msec, in-plane resolution: 0.1x0.1 mm, slice thickness: 1 mm, acquisition matrix size: 220x220, 16 averages), and T2-weighted sequence (axial turbo spin echo RARE sequence, TR/TE = 3000/56 msec, in-plane resolution: 0.1x0.1 mm, slice thickness: 1 mm, acquisition matrix size: 220x220, 10 averages). Dynamic contrast-enhanced images (DCE-MRI) were acquired using T1-weighted gradient echo images (fast low angle shot sequence (FLASH)) with the following parameters: TR/TE = 102/1.9 msec, flip angle: 20˚, in-plane resolution: 0.17x0.17 mm, slice thickness: 1 mm, acquisition matrix size: 128x128, scan interval: 13 sec, 150 repetitions). During the dynamic sequence, 0.1 ml Ablavar (Gadofosveset Trisodium) was injected into the tail vein after five scans, followed by additional 145 scans (31 minutes). Data was analyzed from treated (N=3) mice scanned at four time points (3, 24, 72 hours and one week after the impact) and matched controls (N=3).

Image analysis

DCE-MRI and image analysis was performed in collaboration between the Goldstein laboratory, BUSM, and Dr. Alon Friedman, Dalhousie University, Halifax, Canada. Analysis was performed as previously reported (Chassidim et al., 2013; Weissberg et al., 2014) using in-house MATLAB scripts (Mathworks, USA). In short, a linear curve was used to fit the time-series of each voxel: $s(t) = A \cdot t + B$, where s(t) is the fitted signal. A, the slope of the linear fit, reflecting accumulation of the contrast agent within the brain is referred to as permeability index. It has units of intensity/time and serves as a measure of BBB permeability. Permeability index was compared between hemispheres in a region-of-interest (ROI) within the concussed temporal lobe (volume of approximately 4 mm^3). In addition, the percentage of voxels with abnormal permeability was calculated for each ROI in every scan. The threshold to define a voxel as "highly permeable" was determined by are the mean and standard deviation of the slope in the ROI on the right (contralateral) hemisphere.

3.6.3 Results

Enhancement on T1 images after the injection of Ablavar reflecting BBB disruption was clearly observed within the left temporal lobe (Figure 3.19-A). Permeability maps demonstrated that BBB dysfunction was most prominent at 72 hours after the impact (Figure 3.19-B) and a significant increase was observed for all early time points ($p=0.001$, 0.006, 10^{-25}, for 3, 24, 72 hours, respectively). The percentage of voxels with abnormally high permeability in each ROI was calculated for all mice, demonstrating higher values in the ipsilateral side to the impact (left hemisphere) for all

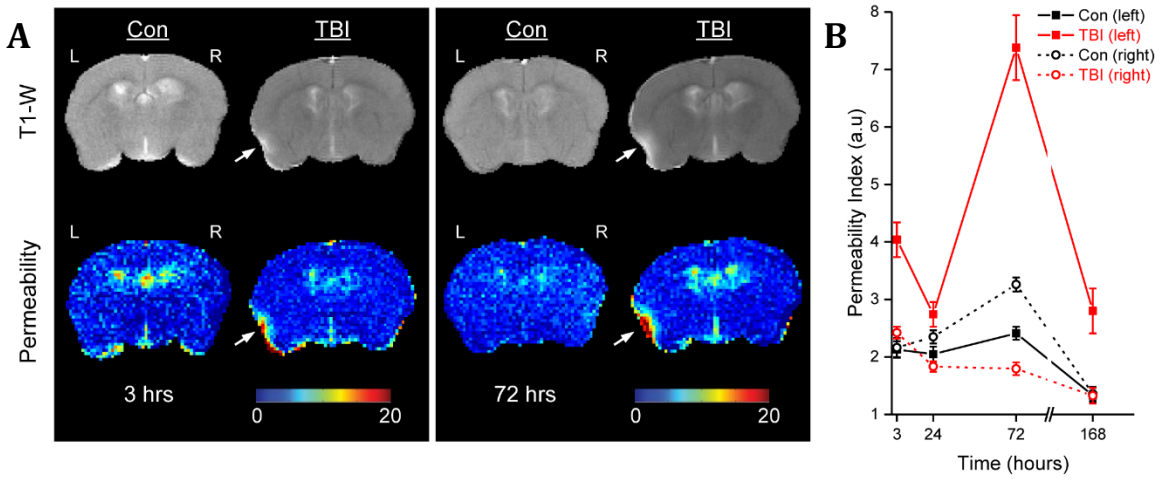

Figure 3.19: TBI-induced blood-brain barrier disruption
(A) Comparison of control and TBI mice, at 3 and 72 hours following TBI. Top: T1-weighted images following injection of Ablavar (Gadofosveset Trisodium). Bottom: colored coded maps showing permeability value for each voxel. (B) Comparison of permeability index in a ROI within the temporal lobe of each hemisphere (left: solid, right: dash) in control (black) and treated (red) mice. Data is displayed as mean ± SEM of permeability index in selected ROI. T=0 is impact time for treated mice.

time points consistent with our EB experiments.

The percentage of permeable voxels on the left side (impact side) was: at 3 hours post-impact: 1.25±0.91 (control group), 22.12±10.86 (TBI group); at 24 hours: 4.00±2.23 (control), 8.7±2.92 (TBI); at 72 hours: 5.48±3.66 (control), 22.58±16.67 (TBI); at 1 week: 2.71±0.65 (control), 9.32±2.5 (TBI). On the right side: at 3 hours: 1.25±0.26 (control), 1.9±0.89 (TBI); at 24 hours: 3.51±0.24 (control), 2.73±0.27 (TBI); at 72 hours: 1.74±0.24 (control), 1.72±0.49 (TBI); at 1 week: 0.98±0.26 (control), 1.44±0.4 (TBI). Data is reported as mean± standard error of mean.

3.6.4 Discussion

Recent work using dynamic contract-enhanced magnetic resonance imaging (DCE-MRI) revealed BBB pathology in football players (Weissberg et al., 2014). The study demonstrated the ability of DCE-MRI to visualize, map, and quantify BBB disruption. We utilized this same technique to investigate the dynamics of BBB disruption in our concussion impact model. Previous work with animal models reported BBB disruption occurs at a rapid onset, increasing the permeability of the BBB (Baskaya et al., 1997; Shapira et al., 1993; Shlosberg et al., 2010). Wei *et al.* reported BBB peaked 3 days post injury using DCE-MRI (Wei, Zhang, Li, Li, & Li, 2012). These studies relied on control-cortical impact or weight drop methods to induce TBI. The mice subjected to a close-head concussive impact injury in this study revealed similar initial BBB permeability on the ipsilateral side at 3 hours post-injury for impact mice and measured permeability peaked at 72 hours post-injury. Also, the initial increase in BBB permeability at 3 hours suggests the energy transferred during injury could provide a mechanism and substrate leading to microvascular injury and BBB disruption. Depending on the severity of the functional or mechanical disruption, BBB breakdown could allow blood constituents (i.e., albumin, platelets, red blood cells) to enter the brain parenchyma, thereby initiating neuroinflammatory responses during the peri-acute stage following TBI (Abbott et al., 2010). As our experiment relied on an albumin-binding gadolinium contrast agent or dye, our results from DCE-MRI and EB experiment suggest that this abundant serum protein entered into brain parenchyma after the initial injury. Albumin has been found to increase proliferation of microglia (Hooper, Taylor, & Pocock, 2005)

and increase IL-1beta and production of TNF-alpha, both associated with neuroinflammation (Hooper et al., 2009) and oxidative stress (Hooper et al., 2009). While our results suggest albumin influx following concussion, it is possible that other blood components (e.g., fibrinogen, thrombin, red-blood cells, glutamate, Ca^{2+}) may also be involved (Chodobski, Zink, & Szmydynger-Chodobska, 2011).

After the initial increase in BBB permeability at 3 hours, we found permeability peaked 3 days post-injury suggesting a secondary influx of albumin-binding gadolinium contrast agent. Our findings support other animal models results which have shown albumin and other proteins peaking 2–3 days after injury (Baldwin, Fugaccia, Brown, Brown, & Scheff, 1996; Baskaya et al., 1997). The mechanism leading to this secondary influx remains unclear in the literature (Chodobski et al., 2011). However, the fact that we observed this secondary peak permeability at 72 hours suggests investigation at this time point could provide insights into the mechanism and pathophysiology following concussion impact and long-term sequelae.

Contrary to other advanced neuroimaging technique, our results suggest DCE-MRI with albumin-binding gadolinium contrast agent can differentiate acute BBB disruption following concussion impact injury in a single individual subject. These results established the possibly of DCE-MRI as a diagnostic biomarker tool. However, validating studies are needed to confirm the T1-weighted abnormalities reflect gadolinium and albumin influx into the brain parenchyma. Ongoing studies in the Goldstein laboratory are using metallomic imaging mass spectrometrometry (MIMS) to confirm these findings.

3.7 Limitations and Conclusions

In the proceeding chapter, we have noted the need to develop a clinically-relevant concussion impact neurotrauma model. The impact model was designed to allow a full range of motion of the cervical spine and induce kinematic comparable head motion to our blast neurotrauma mouse model (L. E. Goldstein et al., 2012) (see Chapter 1 and 2).

In this chapter, the development and rationale behind the Boston University Concussion Scale (BUCS) was examined. Concussion signs and symptoms following impact neurotrauma with non-anesthetized mice showed locomotion, weakness, and balance deficits after injury and recovery occurring 3 hours post-injury. Full BUCS assessments have been performed on over 200 injured and 100 control mice. Ongoing research using the BUCS system is focused on establishing intra- and inter-rater reliability and other quality control metrics. Working with the BUCS has highlighted limitations of the instruments that require adjustment for accurate assessment of heavier mice (~40 grams), differences in mouse strains, possible sex-related effects, and grader bias. Furthermore, the BUCS has only been assessed in mice subjected to impact injury and blast neurotrauma. BUCS assessment was designed to detect gross neurological deficits following impact injury and although the mice recover after 3 hours, detailed quantifiable analysis of locomotion has not been performed. As with the GCS, the BUCS relies on a graded scale and introduces limitations regarding the scalable weight of a lost point.

Studies investigating BBB disruption following concussion impact injury utilized an optical fluorescence technique using EB dye. Results suggest BBB damage occurs

after initial concussion injury in a focal distribution and within the impact group heterogeneous BBB was observed. Limitations of this study included the semi-quantitative nature of the recorded fluorescence signal, the possibility of dura mater confounding tissue slices, and reliance of manually masking region of interest. Raw fluorescence data were confounded by tissue auto-fluorescence that required removal using an automated script in the Living Image Software (Perkin-Elmer). Validation of this technique was not formally investigated. Slice analysis focused on specific regions in the cortex and excluded regions with high signal intensity due to ventricles and dura mater. The hippocampal region was not investigated, but in our blast neurotrauma model BBB disruption was observed (L. E. Goldstein et al., 2012).

DCE-MRI enable serial assessments of BBB permeability. Findings from this study suggested initial BBB disruption due to impact injury and the peak permeability occurs 72 hours after injury. For this study 3 impact and 3 control animals were serially scanned, and 1 of 3 animals showed observable T1-weighted enhanced abnormality. Limitations of this study included the small sample size, lack of baseline scans, and use of anesthetic during imaging. Further studies are needed to investigate the dosage of Ablavar and the effects on image enhancement. Also, the study assumed the enhancement seen with DCE-MRI is the accumulation of the bound fraction of Ablavar to albumin rather than the unbound fraction.

In summary, our impact neurotrauma model induces a clinically-relevant closed-head concussive impact injury that can be used to advance our understanding concerning the driving forces of BBB disruption in the development of acute and long-term sequelae

following concussion injury and aid in the development of imaging biomarkers.

Chapter 4: Chronic Sequelae and Brain Pathologies Following Closed-Head Concussive Impact Injury in Mice

4.1 Purpose

The pathogenesis of acute concussion and CTE are unknown. In the previous chapters we described our impact neurotrauma model, BUCS, and showed acute BBB disruptions following closed-head concussive impact. In this chapter, we hypothesize that closed-head concussive impact recapitulates acute and long-term pathobiology seen in sport-concussed athletes.

4.1.1 Clinical Motivation

Each year, over 1.7 million Americans sustain a traumatic brain injury (TBI) (Faul et al., 2010) of which an estimated 75% are classified as mild TBI (Report to Congress on Mild Traumatic Brain Injury in the United States, CDC). These statistics likely underestimate the true incidence as these estimates include only those head-injured individuals who sought medical care. One study estimated that ~75% of individuals who sustain a TBI do not seek medical attention (Willer & Leddy, 2006). An incident research study based on high school sports reported 2651 concussions observed in roughly 11 million athlete exposures, with 1 athlete-exposure equaling a single athlete participation in a practice or game (Lincoln et al., 2011). Although concussion rates increased in all sports during the study possibly attributed to greater concussion awareness and detection, current understanding of the long-term effects of concussion and mild TBI on the brain remain unknown.

4.2 Materials and methods

4.2.1 Animal Subjects

Adult wild-type C57BL/6 male mice 10–12 weeks-of-age (Charles River Laboratories) were group housed in cage at the Laboratory Animal Science Center at Boston University School of Medicine (BUSM). All animal experiments utilized 2.5-month-old mice. Animal housing and experimentation were conducted in accordance with guidelines from the Association for Assessment and Accreditation of Laboratory Animal Care (AAALAC). Animal experimentation was under an active protocol approved by Institutional Animal Care and Use Committees at BUSM.

4.2.2 Closed-Head Concussive Impact Neurotrauma Mouse Model

Mice were weighted and received an intraperitoneal injection of analgesic (buprenorphine, 0.2 mg/kg, i.p.) but no anesthesia before receiving a baseline BUCS score. Assessment of the BUCS score followed the protocol outlined in Section 3.1.4. Mice were secured in the prone position with a modified DecapiCone (Braintree Scientific) such that the head and cervical spine extended outside the plastic restraint. A Velcro strap was used to secure the torso while allowing lateral flexion. If the front paws extended beyond the distal end of the cone, the mouse was removed and repositioned. The head was positioned on the sled with the padding in contact with the left-lateral zygomatic region of the head. Experimental parameters were optimized to model impact injury conditions in humans and head kinematics in our blast neurotrauma mouse model (L. E. Goldstein et al., 2012). Fire pressure was 19.12 ± 1.26 (psi), slug velocity was

25.38 ± 0.72 (m/s), rod velocity was 7.20 ± 0.28 (m/s), and sled velocity was 5.08 ± 0.05 (m/s) (mean ± SD). Concussive impact in our mouse model was compatible with 100% survival and with no evidence of skull flexure, fracture, or crush injury* (*dynamic modeling indicated no more than ~10 microns of skull flexure; see Chapter 5). Non-anesthetized mice were exposed to two impacts separated by 15:00 ± 3:36 (mean ± SD) minutes between experimental impact injuries. The rationale for this experimental design was to model injury conditions associated with repetitive mild TBI—in this case, closed-head concussive impact injury—as might be experienced during contact-sport play (Crisco et al., 2010; Wong, Wong, & Bailes, 2014). Sham (control) mice did not receive impact injury but were otherwise subjected to exactly the same procedures as the impact group (i.e., analgesic injection and placement in cone restraint). The experimental impact injury parameters were compatible with 100% survival with no evidence of skull crush injury. As described in Chapter 2, all impact parameters were recorded after each impact. Following injury, mice were removed from the cone and evaluated using the BUCS test (Chapter 3). A total of 217 impact and 117 control mice were assessed immediately prior to experimental injury (baseline), after the first impact injury (Impact 1), after the second injury (Impact 2), and 3 hours post 2nd injury (Recovery).

4.2.3 Histopathological Analyses

Brains were harvested from mice subjected to experimental concussive impact or sham (no impact) control condition. Mice were euthanized by CO_2 asphyxiation followed by gravity-driven transcardial perfusion with phosphate-buffered saline (PBS). Whole brains were removed and pre-fixed in 10% neutral buffered formalin, block sectioned

into 2 mm coronal slabs, post-fixed in 4% paraformaldehyde, paraffin embedded, and serially sectioned at 10 μm. A battery of primary detection antibodies (SMI-34, GFAP, Iba-1, CP13) was used for immunohistopathological analyses performed as part of an ongoing collaboration between the laboratories of Lee Goldstein, MD, PhD (Boston University School of Medicine, College of Engineering) and Ann McKee, MD (Boston VA Healthcare System).

4.2.4 Quantitative Assessment of Phosphorylated and Total Tau Protein.

Brains were harvested from mice subjected to experimental concussive impact or sham (no impact) control conditions. For immunoblot analysis, left and right hemisected brain samples were obtained from ice-cold, PBS-perfused mice 2 weeks after impact concussion injury or sham. Snap frozen hemisected brain specimens were thawed and resuspended in 0.7 ml protease-phosphatase inhibitor buffer as previously described (Saman et al., 2012). Equal volumes of homogenized samples were subjected to standard polyacrylamide gel electrophoresis in duplicate and immunoblotted with monoclonal antibody CP-13 (Dr. Peter Davies, Albert Einstein College of Medicine, Manhasset, NY, USA) directed against tau protein phosphorylated at serine-202 (pS202), or monoclonal antibody Tau 5 (Dr. Lester Binder, Northwestern University Medical School, Chicago, IL, USA) directed at phosphorylation-independent tau protein (total tau). In order to compare the Tau 5 immunolabeling between the experimental and control samples, triplicate densitometry measurements were conducted on bands (maximum for each band) and summed. An Enzyme-Linked ImmunoSorbent Assay (ELISA) kit (Invitrogen, Carlsbad, CA, USA) was used to quantitate murine-specific tau protein phosphorylated at

serine 199. Frozen brain samples were homogenized in eight volumes of 5 M guanidine-HCl 50 mM Tris (pH 8) followed by five passes in a glass teflon homogenizer. Homogenates were mixed for 3 hrs, diluted into PBS containing protease inhibitors, and centrifuged for 20 min at 16,000 g. Supernatants were diluted and assayed in quadruplicate for phosphorylated tau according to the manufacturer's instructions. These analyses were performed as part of an ongoing collaboration between the laboratories of Dr. Goldstein and Dr. Garth Hall, University of Massachusetts Lowell.

4.2.5 Flow Cytometry

Brains were harvested from mice subjected to experimental concussive impact or sham (no impact) control conditions. Flow cytometry was performed using homogenized brain single-cell suspensions. Cells were separated with a 30%/70% Percoll® (GE Healthcare, NJ, USA) gradient as previously reported (Pino & Cardona, 2011). Single cell suspensions were stained with anti-CD45-APC (1: 100; BioLegend), anti-CD11b-Efluo450 (1:200; eBioscience), anti-Ly-6G-FITC (1:1000; Biolegend), anti-Ly-6C-PE/Cy7 (1:200; Biolegend) and Trem2-PE (1:100; R&D System). Cell populations were defined as follows: $CD45^{+}$ as inflammatory cells, $CD45^{low}CD11b^{+}$ as microglia, $CD45^{high}CD11b^{+}Ly\text{-}6G^{-}$ as monocytes. Ly-6C was used to define subpopulations of monocytes, which were $Ly\text{-}6C^{high}$, $Ly\text{-}6C^{middle}$ and $Ly\text{-}6C^{low}$ monocytes. For Trem2 expression experiments, Fluorescence Minus One (FMO) was used to assess $Trem2^{+}$ cells. The percentage of cells from each population was determined by flow cytometry (Flow Cytometry Core, BUSM), and the absolute number of each cell population was calculated by using the percentage number multiplied by the isolated cells per brain. Cells

were analyzed on a LSR-II (BD Biosciences, CA, USA), and all analyses were performed using FlowJo software (TreesStar, OR, USA). These analyses were performed as part of ongoing collaboration between the laboratories of Dr. Goldstein and Drs. Bruce Lamb, PhD and Richard Ransohoff, MD, Cleveland Clinic Foundation.

4.2.6 Hippocampal and Prefrontal Cortical Electrophysiology

Prepared brains harvested from mice were subjected to experimental concussive impact or sham (no impact) control conditions. Mice were decapitated under deep isoflurane anesthesia and the brains were quickly removed, hemisected, and sliced with a Leica model VT 1200S vibratome at 350 μm thickness. Slices were fixed to a stage with cyanoacrylate adhesive and immersed in oxygenated artificial cerebrospinal fluid (ACSF composition: NaCl, 126 mM; KCl, 3 mM; NaH2PO4,1.25 mM; MgCl, 1.3 mM; CaCl2, 2.5 mM; NaHCO3, 26 mM; glucose, 10 mM; saturated with 95% O2 and 5% CO2) maintained at 32º C. Axonal conduction velocity was assessed with a recording electrode placed in CA1 *stratum alveus*. Schaffer collateral-CA1 synaptic transmission and plasticity was assessed using a recording electrode in the CA1 *stratum radiatum*. Comparisons of axonal conduction velocity and LTP magnitude were conducted using repeated-measures multi-factorial ANOVA with Bonferroni-Dunn post-hoc correction. Statistical significance was pre-set at $P < 0.05$. These analyses were performed in collaboration between the Goldstein Laboratory, BUSM, and Dr. Patrick Stanton, New York Medical College.

4.3 Results

4.3.1 Neuropathology in a Mouse Model of Closed-Head Concussive Impact Injury

We developed an impact concussion neurotrauma model to investigate the mechanistic linkage between concussion impact injury and CTE-linked neuropathology (Chapter 2). In Chapter 3, we reported similar kinematics between impact injury and the blast injury. We hypothesized that direct impact injury would induce head acceleration-deceleration of sufficient intensity to cause detectable neuropathology in the acute period after the inciting trauma and recapitulate CTE-linked pathology. To evaluate this hypothesis, brains from mice were studied 24 hours, 72 hours, and 2 weeks after impact. At 24 hours post injury, we reported Evans Blue (EB) extravasation within the impact-concussion group. The gross pathology revealed a heterogeneous distribution of blood brain barrier (BBB) disruption ranging from no visible gross pathology to more severe pathologies, including petechial hemorrhage and frank contusion. Analysis of EB fluorescence which measures albumin extravasation into the parenchyma of the brain revealed similarly variable outcomes ranging from no measurable difference of EB compared to sham, to slight increase of EB with the most severe injury showing diffuse BBB disruption across multiple brain slices and lateralization on the side of impact. Immunohistochemical and biochemical analyses (Figure 4.1) revealed a temporal progression of neuropathological changes in the impact-concussed mice at 24 hours, 72 hours, and 2 weeks post-injury. These brains demonstrated an ipsilateral appearance variation in density of staining and pyknotic neurons with nuclear and cytoplasmic smudging at 24 hours (Figure 4.1-A, black arrows). At 72 hours, impact-concussed brains

exhibited notable signs of neurodegeneration (Figure 4.1-B). Hemosiderin accumulation was observed 2 weeks post-injury in the ipsilateral cortex only, and suggests microhemorrhage related to phagocytosis of red blood cells and hemoglobin. Impact-concussed mice demonstrated acute increase in phosphorylatedneurofilament protein at 24 hours that was also evident at 72 hours. Reactive astrocytosis was evident at 24 hours and peaked at 72 hours and decreased but remains present at 2 weeks. Activated microglia revealed barely visible staining at 24 hours. At 72 hours a marked increase in neuroinflammatory response was present and decreased at 2 weeks.

Immunoblot analysis of mouse brain homogenates 2 weeks after impact-concussion showed a significant impact-related elevation of phosphorylated tau protein (monoclonal antibody CP-13: pSer202;) known to be associated with early neurodegenerative tau misprocessing compared to sham control (Figure 4.2). An enzyme-linked assay of whole brain homogenates prepared from impact-concussed mice demonstrated elevated integrated band density (Tau 5 and CP-13) compared to sham impact control mice (Tau 5, $p < 0.005$; CP-13, $p < 0.05$; two-tailed Student's t-test), along with elevated band area for impact-concussed mice compared to sham impact control mice (Tau 5, $p < 0.05$; CP-13, $p < 0.001$; two-tailed Student's t-test) (Figure 4.3). Total tau protein immunoblots (Tau 5) and tau phosphorylation protein immunoblots (CP-13) revealed an apparent impact-related alteration in tau protein isoform distribution. Note that increased immunolabelling for phospho-tau epitopes (CP-13) was detected diffusely in both hemispheres, suggesting tau proteinopathy is not dependent on the lateral-location of the injury (Figure 4.2).

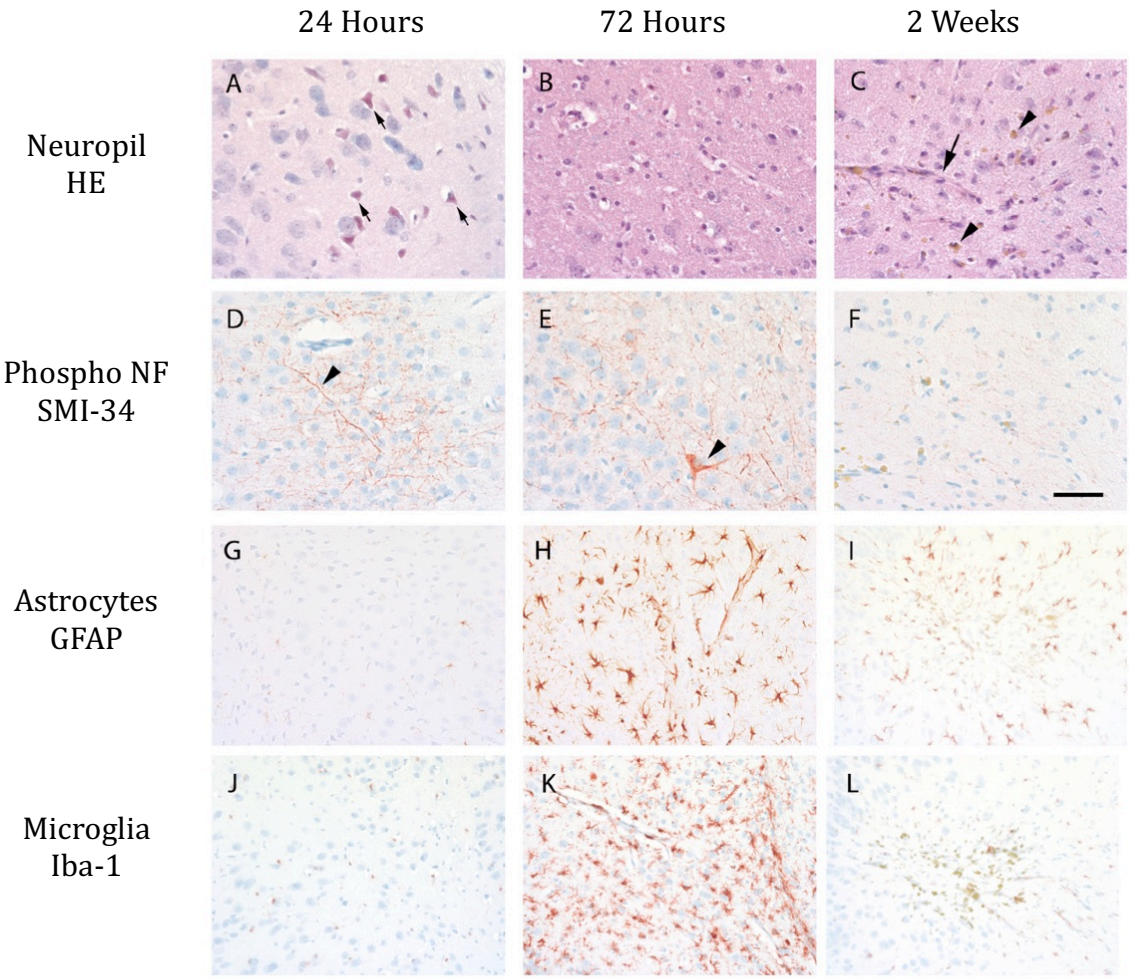

Figure 4.1: Neuropathology in wild-type C57BL/6 mice 24 hours, 72 hours and 2 weeks after impact concussion injury.
(A-C) Hematoxylin and eosin strain (HE), dark neuros visible at 24 hours (A, arrows) and increased at 72 hours. Eosinophilic neuron (arrow heads) and capillary disruption (arrow) at 2 weeks. (D-F) Increase phosphorylated neurofilament (NF) immunostaining at 24 hours, 72 hours, and 2 weeks post injury with detectable axonal injury. (G-H) Astrocytic glial fibrillary acidic protein (GFAP) immunoreactivity peaks at 72 hours. (J-L) Microglia specific ionized calcium-binding adapter molecule 1 (Iba-1) immunoreactivity also peaks at 72 hours.

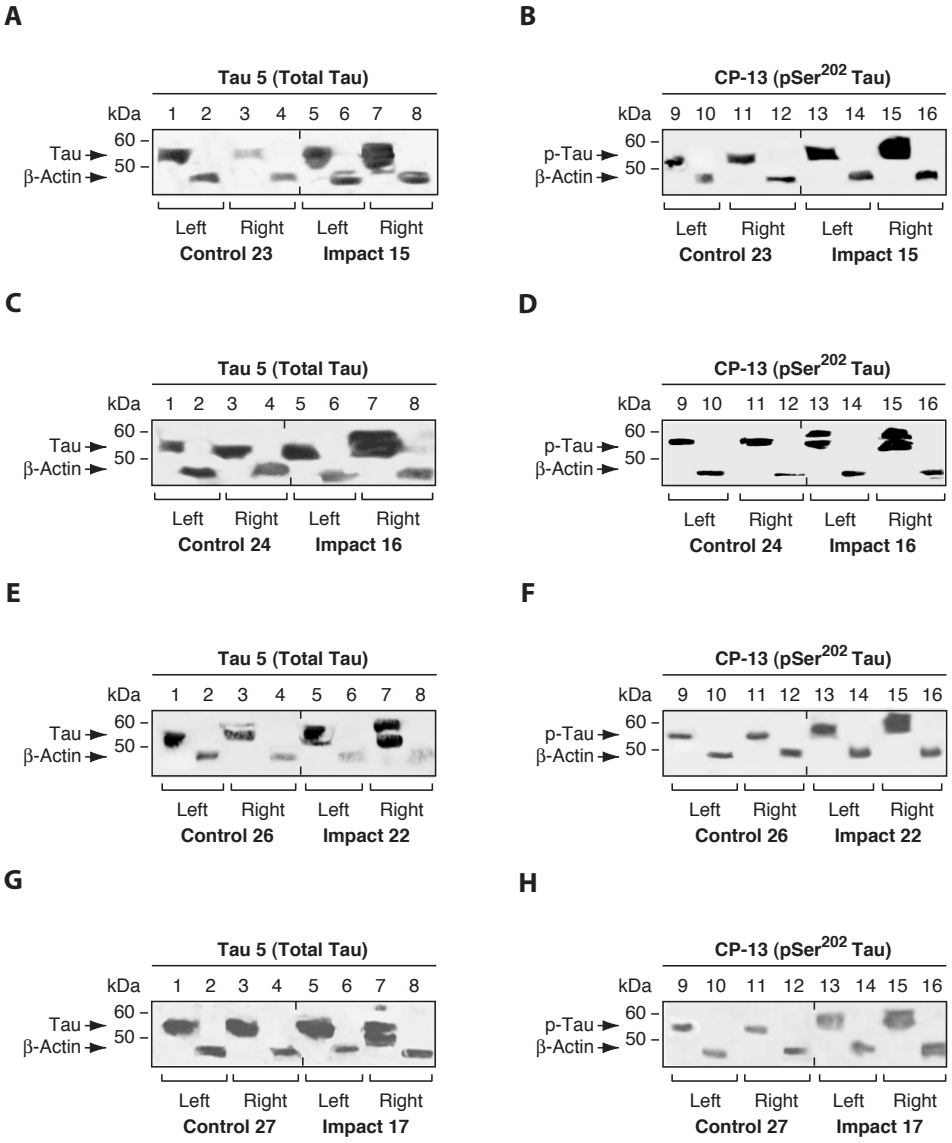

Figure 4.2: Increased tau protein phosphorylation in the brains of C57BL/6 mice 2 weeks after impact concussion injury.

Brain homogenate were prepared two weeks after impact or sham injury and assayed by quantitative immunoblot analysis using phosphorylation-independent total tau epitope antibody Tau 5(A,C,E,G) and antibody directed against phosphorylation site. CP-13 ($pSer^{202}$), (B,D,F,H). Note increased band density and band area for both left and right hemispheres of impact concussion mice. Proteins concentration were determined by quantitative densitometry (Image J) and normalized relative to background level across all immunoblots.

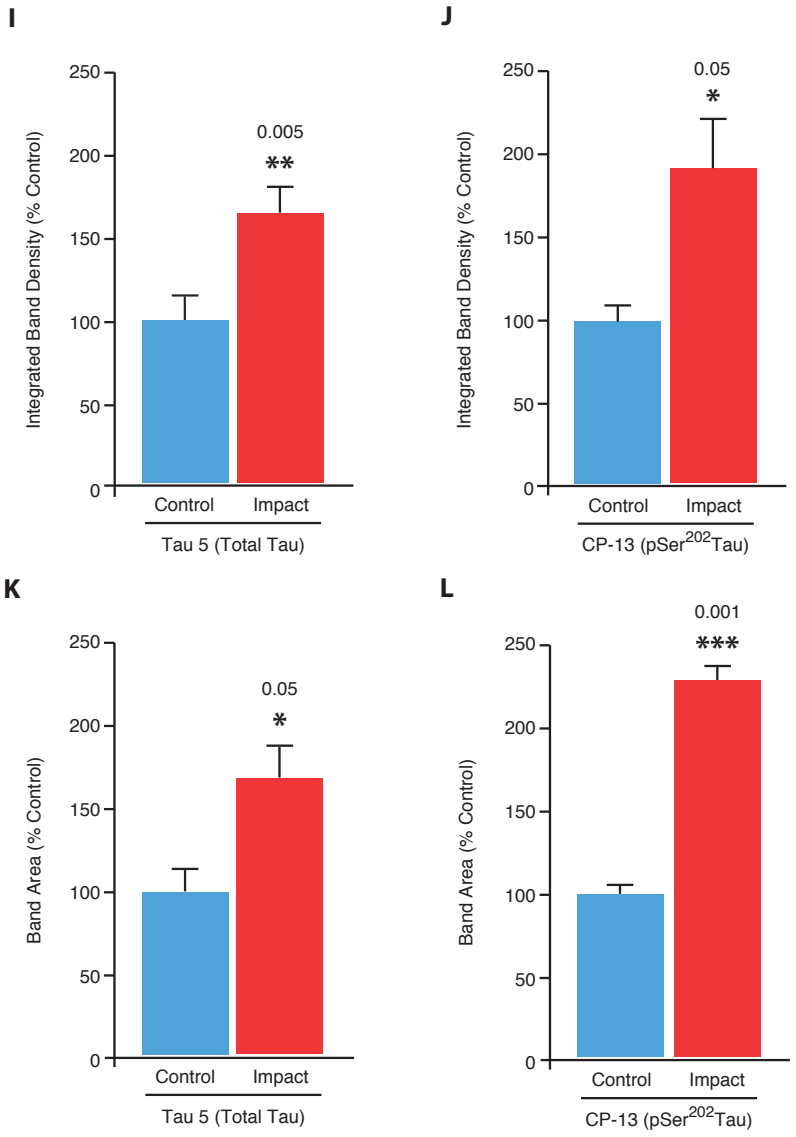

Figure 4.3: Quantitation of total tau and phosphorylation tau protein 2 weeks following impact concussion injury.

(I,K) Tau 5 integrated band density and band area revealed significant increase in the brain of mice impacted compared to control mice (density, $p < 0.005$; area, $p < 0.05$; two-tailed Student's t-test mean ± S.D.). (J,L) CP-13 integrated band density and band area also revealed significant increase in the brain of mice impacted compared to control mice (density, $p < 0.05$; area, $p < 0.001$; two-tailed Student's t-test mean ± S.D.).

4.3.2 Inflammatory cells accumulate in the brain following impact-concussion injury

Neuroinflammation was quantified following impact-concussion injury. Flow cytometry measured that number of $CD45^+$ inflammatory cells significantly increased most prominently at 72 hours after impact compared to sham impact ($p = 0.05$) and a significant increase was observed when compared to 24 hour impact ($p = 0.05$) and 24 hour sham ($p = 0.05$). Number of $CD45^+$ cells ($x10^4$) measured at 24 hours post injury (Impact: 18.3±3.8, Sham: 19.2±2.3); at 72 hours post injury (Impact: 27.6±3.6, Sham: 18.7±9.3); and at 2 weeks post injury (Impact: 23.0±1.9, Sham: 18.7±5.7). Microglia with $CD45^{high}$-$CD11b^+$ increased significantly at 72 hours for impact-concussion injury compared to 24 hour impact brain ($p < 0.01$) and 24 hour sham brain ($p < 0.05$). Microglia number ($x10^4$) were quantified at 24 hours post injury (Impact: 12.4±3.4, Sham: 13.7±2.8); at 72 hours post injury (Impact: 22.7±2.7, Sham: 16.3±8.5); and at 2 weeks post injury (Impact: 17.6±3.0, Sham: 14.7±5.0). Also infiltrating monocytes exhibit significant accumulation in impact-concussed mice at 72 hours compared to sham at the same time point ($p < 0.05$) and were quantified (cells $x10^4$) at 24 hours post injury (Impact: 1.7±1.0, Sham: 1.4±0.5); at 72 hours post injury (Impact: 1.9±0.8, Sham: 0.8±0.4); and at 2 weeks post injury (Impact: 1.4±0.4, Sham: 1.1±0.6; all data reported mean ± SD). Further analysis revealed all subpopulation of monocytes significantly increased at 72 hour post injury in the impact-concussion mice compared to the sham injury ($Ly\text{-}6C^{high}$, $p < 0.001$; $Ly\text{-}6C^{middle}$, $p < 0.001$; $Ly\text{-}6C^{low}$, $p < 0.001$).

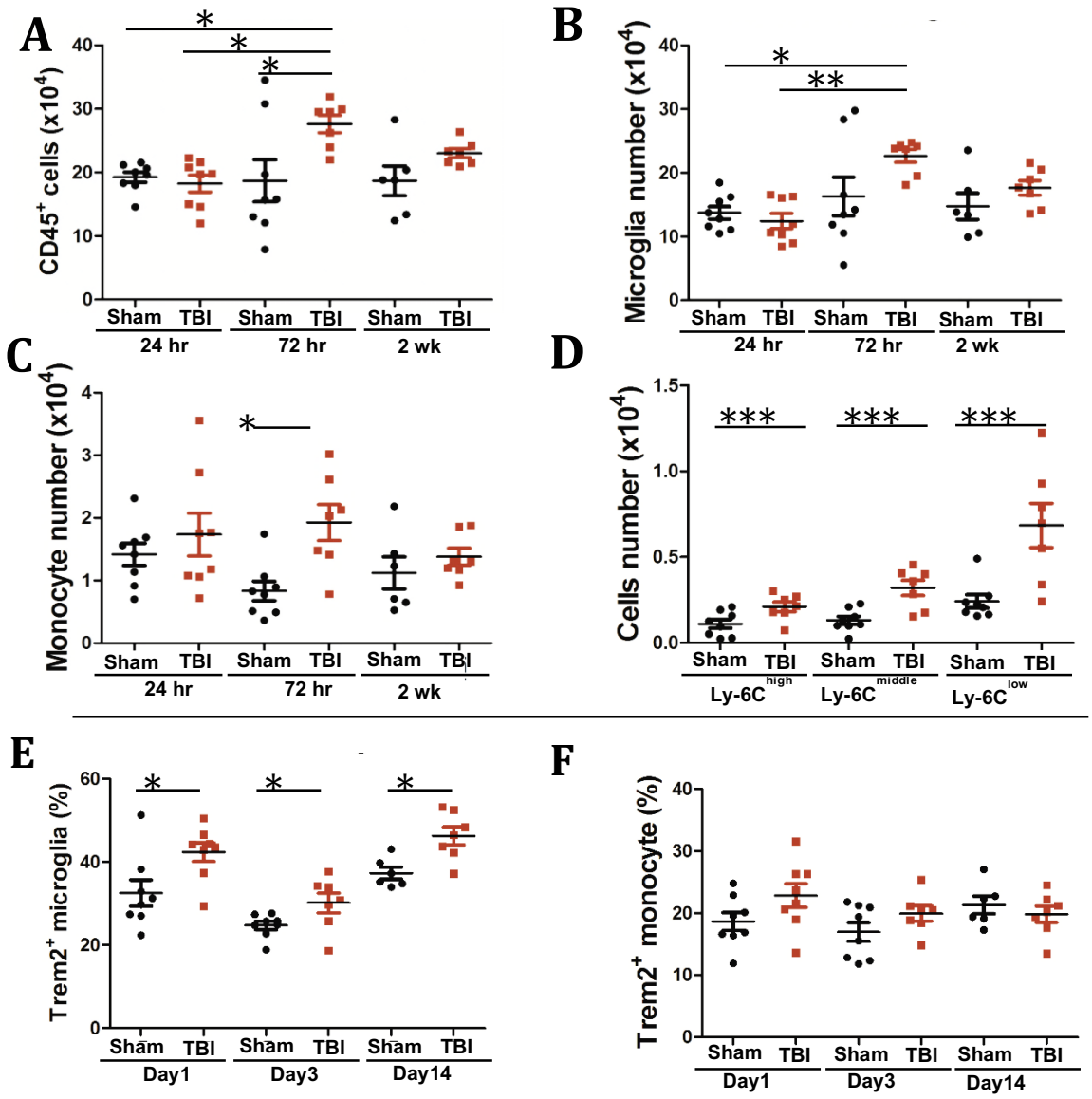

Figure 4.4 Inflammatory cell accumulation in the brain 24 hours, 72 hour and 2 weeks after impact concussion injury.

A) Flow cytometry showed that number of $CD45^{+}$ inflammatory cells increased at 72 hours post-TBI (A) with $CD45^{low}CD11b^{+}$ microglia expansion at 72 hours post-TBI (B). $CD45^{high}CD11b^{+}Ly\text{-}6G^{-}$ monocytes also exhibit accumulation at 72 hours post-TBI (C) showing the increasing in each subpopulation of $Ly\text{-}6C^{high}$, $Ly\text{-}6C^{middle}$ and $Ly\text{-}6C^{low}$ monocytes (D). B. Flow cytometry showed upregulation of Trem2 expression by microglia at 24 hours, 72 hours, and 2 weeks post-TBI (a-b), but not by monocytes at each time point (E,F).

Trem2^{+} inflammatory cells have been shown to be negative regulators of inflammation (Ford & McVicar, 2009). TREM2 expression is also linked to Alzheimer's disease risk and pathogenesis (Tanzi, 2015). To investigate the TREM2+ subpopulation of microglia and monocytes, we conducted flow cytometry analysis using the Fluorescence Minus One (FMO) method to quantify the percentage of Trem2^{+} cells. Flow cytometry revealed a significant upregulation of Trem2^{+} expression in microglia for impact mice compared to sham mice at each time point (24 hours, $p < 0.05$; 72 hours, $p < 0.05$; 2 weeks, $p < 0.05$). No significance was found for Trem2^{+} monocytes at any time point.

4.3.3 Impact-concussion injury induces persistent hippocampal and medial prefrontal cortical electrophysiological deficits

Working memory and learning deficits have been shown to persist in athletes following concussions (De Beaumont et al., 2009; Guskiewicz et al., 2007; Guskiewicz et al., 2001). However, current imaging techniques to measure functional deficits with functional magnetic resonance imaging (fMRI) or diffusion tensor imaging (DTI) have proven unsuccessful detecting functional changes following concussion (Mayer, Bellgowan, & Hanlon, 2015; K. Zhang et al., 2010). To investigate the possible effect impact-concussion might have on the impairment of hippocampal and medial prefrontal cortex neurophysiology over time, analysis of axonal conduction velocity of CA1 pyramidal cell compound action potentials was conducted in the *stratum alveus* and revealed significantly slowed velocity acutely in impact concussed mice at 24 hours post injury in both the left and right hippocampus (HC) compared to control (left HC, $p <$

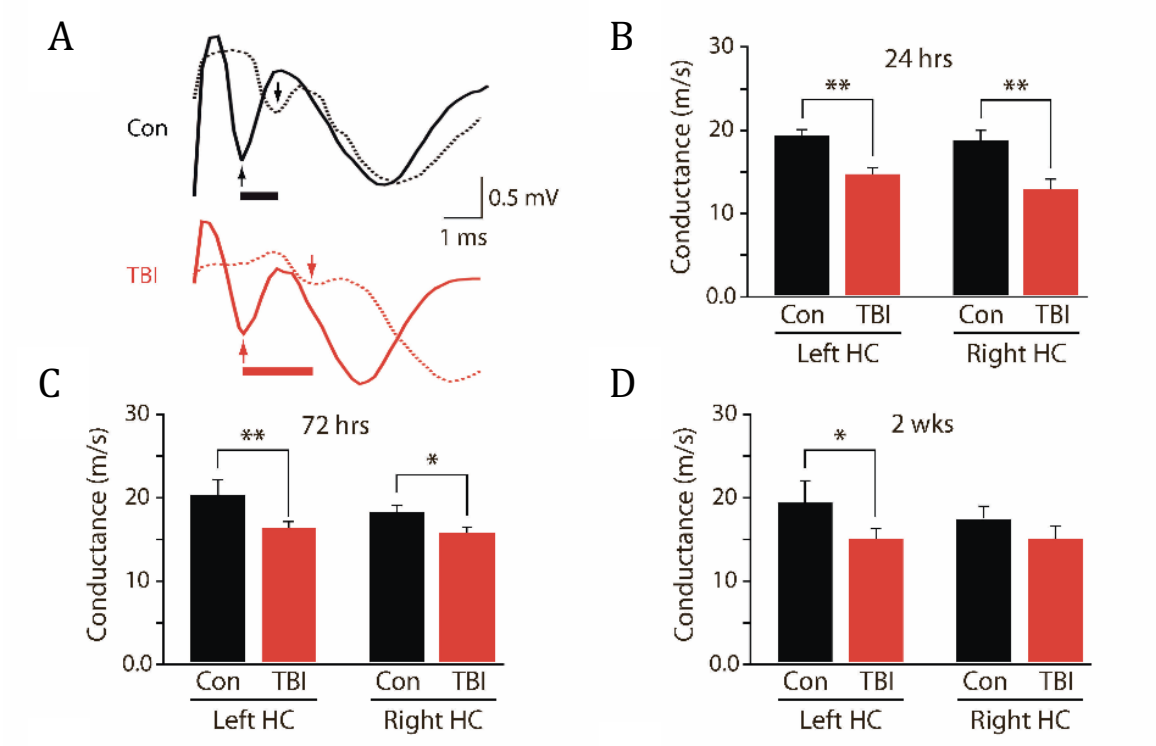

Figure 4.5: Persistent impairments in axonal conduction velocity in impact concussion mice at 24 hours, 72 hours, and 2 weeks.
A) Representative stimulus-evoked compound action potential at proximal (solid lines) and distal (hashed lines) recording sites in hippocampal slices from impact mice (red) and control mice (black). Arrows indicate peak negatives used to calculate conduction velocity. B-C) Conduction velocity measured in left and right hippocampus (HC) for control and impact injury at 24 hours, 72 hours and 2 weeks (mean ± S.E.M., Student's t-test)

0.005; right HC, $p < 0.005$). Axonal conduction velocity remained significantly slower for impact concussed mice at 72 hours post injury in both left and right hippocampus (left HC, $p < 0.005$; right HC, $p < 0.05$). Two weeks post injury conduction velocity deficit persisted significantly only in the left HC for impact concussed mice compared to sham (Left HC, $p < 0.05$), but not in the right HC (not significant) (Figure 4.5).

The effect of impact concussion on stimulus-evoked long-term potentiation (LTP) in the medial prefrontal cortex (mPFC) was also investigated. Marked impairments of stimulus-evoked LTP were observed in impact concussed mice in both the left and right

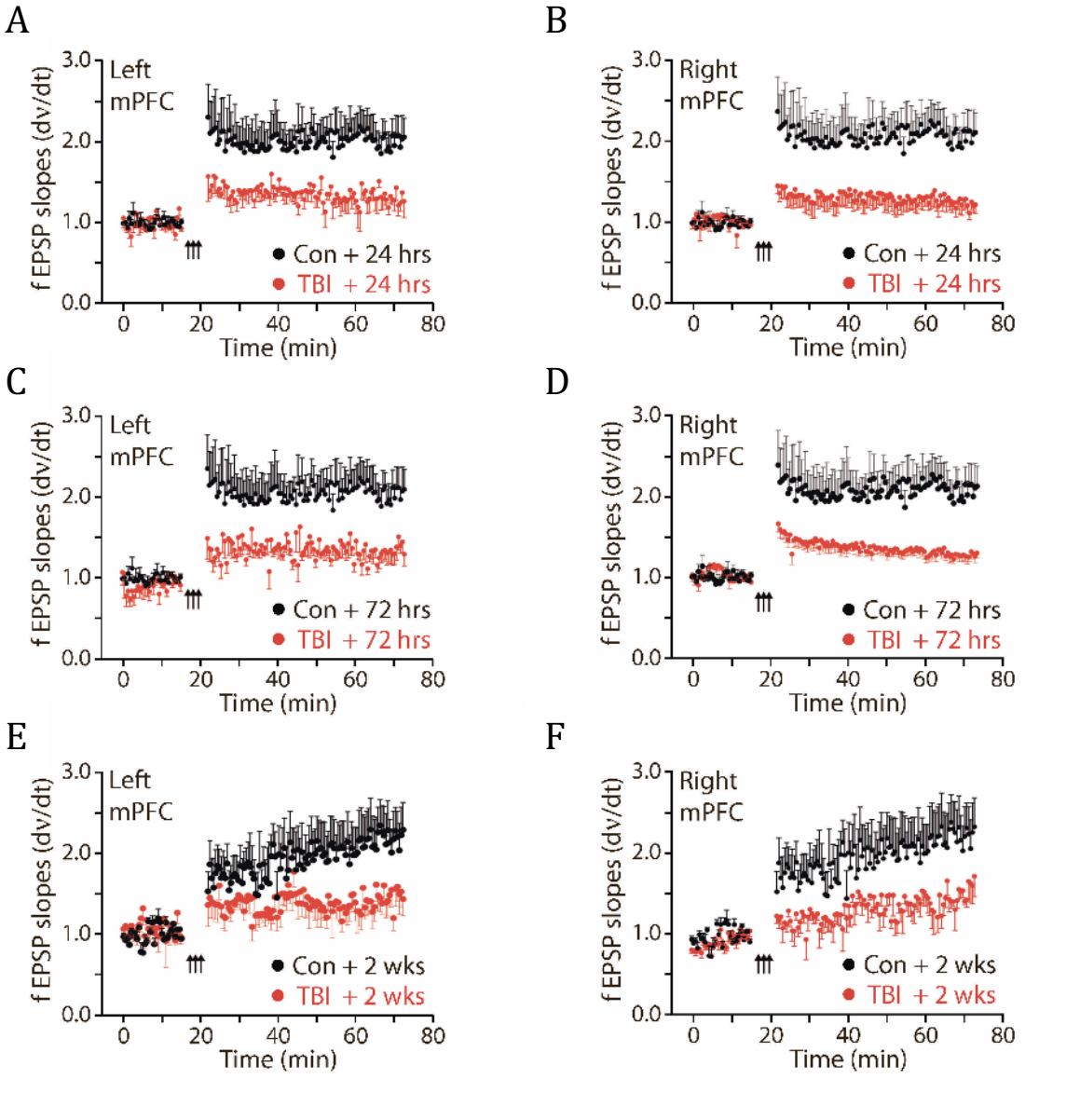

Figure 4.6: Time course of long-term potentiation (LTP) evoked by theta-burst stimulation in impact and control mice at 24 hours, 72 hours, and 2 weeks post injury.
A-B) LTP time course in left and right medial prefrontal cortex (mPFC) 24 hours post injury. C-D) LTP time course at 72 hours. E-F) LTP time course at 2 weeks. Each point mean ± S.E.M. fEPSP slope of n slices.

mPFC compared to control mice at 24 hours following impact injury (left mPFC, $p < 0.05$; right mPFC, $p < 0.05$; Repeated-measures multi-factorial ANOVA). Stimulus-

evoked LTP persisted bilaterally in impact concussed mice at 72 hours (left mPFC, $p < 0.05$; right mPFC, $p < 0.05$; Repeated-measures multi-factorial ANOVA) and at 2 weeks following injury (left mPFC, $p < 0.05$; right mPFC, $p < 0.05$; Repeated-measures multi-factorial ANOVA). These results indicate that exposure to impact concussion impairs hippocampal conduction velocity and long-term, activity-dependent synaptic plasticity for at least 2 weeks after impact in our model system (Figure 4.6).

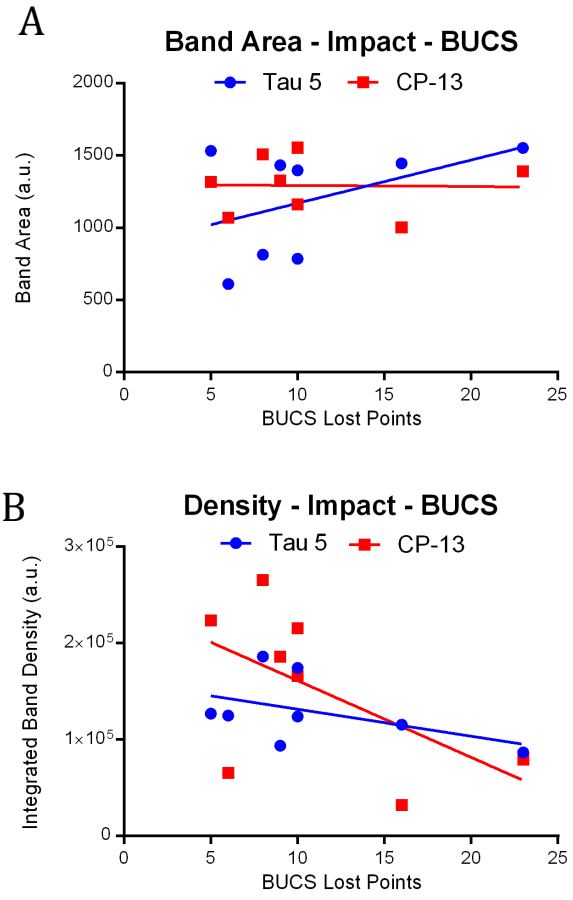

Figure 4.7: Correlation of 2 week post-TBI whole brain tauopathy.
Correlation graphs for the chronic end points of protein tauopathy. Integrated band density and band area for Tau 5 and CP-13 show no correlation between BUCS lost points (**A-B**).

4.3.4 Correlation between Acute Concussion Severity and Chronic Sequelae

Concussion severity measured by BUCS did not correlate with impact-induced head acceleration (see Chapter 3). Immunoblot analysis of mouse brain homogenates was performed in 8 impact-concussed mice 2 weeks following injury (Figure 4.7). Phosphorylated tau (CP-13) and total tau (Tau 5) band area and integrated density were quantitated for each mouse. BUCS assessment occurred after each hit and total lost points were calculated. Spearman's correlation analysis revealed no correlation between band area (Tau 5 or CP-13) and band density (Tau 5 or CP-13).

Flow analysis revealed peak neuroinflammation occurs at 72 hours post injury. Impact concussed mice (N=7) $CD45^{+}$, microglia, and monocyte cell counts were compared to the BUCS lost points. Spearman's correlation revealed no correlation at 72 hours post injury (Figure 4.8).

Correlation of axonal conduction in the hippocampus to BUCS for impact mice required the use of a linear mixed-effects regression model by applying a variance components model for the covariance matrix. The mixed effects analysis was required because multiple hippocampal slices were analyzed from a single animal, violating the Spearman's correlation assumption of sample independence. Analysis from the linear mixed-effects regression model showed no correlation ($p < 0.05$) for all combinations of impact-laterality (left and right) at the different time points (24 hours, 72 hours, and 2 weeks) and BUCS lost points.

Correlation of LTP measurements used the same linear mixed-effects regression model as the axonal conduction analysis. The model showed no correlation ($p < 0.05$)

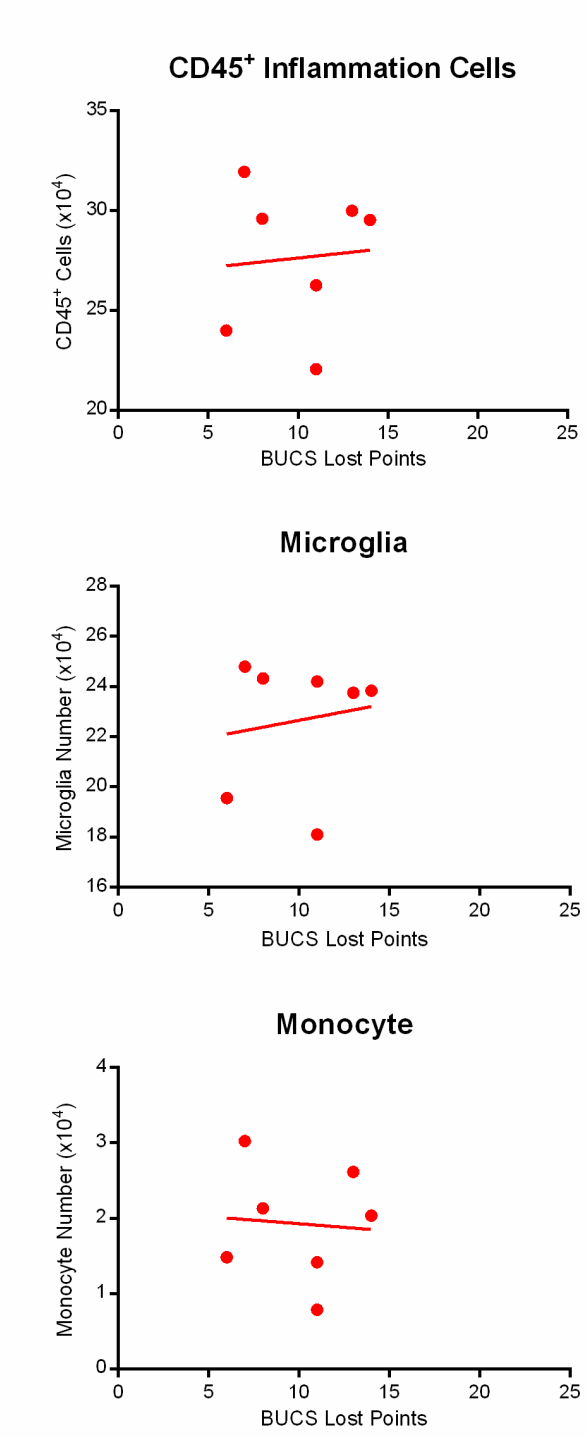

Figure 4.8 Correlation of neuroinflammation.
Correlation graphs for inflammatory cells accumulated in the brain 72 hours post-TBI. Concussion (BUCS Lost Points) showed no correlation between $CD45^{+}$, microglia and monocyte cell population.

between BUCS lost points and impact laterality (left and right) at the 24 hour and 72 hour time points. At the 2 week time point the model showed a positive estimated slope for both the left and right mPFC-LTP (Left: 0.03 estimated slope, DF=7, p = 0.04; Right: 0.04, DF=7, p=0.04). The model results suggest that as BUCS points are lost (greater severity of signs) LTP increases in impacted mice. This runs contradictory to the proposition that as more BUCS points are lost LTP decreases (negative estimated slope).

4.4 Discussion

In the previous chapters (Chapters 2–3) the design of the impact concussion model relied on specific injury requirements to recapitulate sport-related concussions and allow for comparison between blast neurotrauma and impact neurotrauma. Injury intensity was not arbitrarily chosen, but was determined based on our previous work using our blast neurotrauma experiments, which revealed angular acceleration induced CTE-linked pathology in a mouse after a single blast exposure (L. E. Goldstein et al., 2012). Through novel designs and adaptations, this model induced comparable head kinematics to blast neurotrauma (Chapter 2). The rationale for this experimental design was to model injury conditions associated with repetitive mild TBI—in this case, closed-head concussive impact injury— as might be experienced during contact-sport play (Crisco et al., 2010; Wong et al., 2014). In Chapter 3, we described the development of the Boston University Concussion Scale (BUCS) and reported impact neurotrauma induces concussion-like signs such as postural incoordination, weakness, and balance dysfunction (Cavanaugh et al., 2005; Cavanaugh et al., 2006; Z. G. Fox, Mihalik,

Blackburn, Battaglini, & Guskiewicz, 2008; McCrea et al., 2005; McLeod & Leach, 2012). Furthermore, mice were hit twice and showed a significant decrease in BUCS score from the first hit to the second hit, consistent with published research reporting previous history of concussion increases the likelihood of a future concussion (Guskiewicz et al., 2003). Concussion assessment 3 hours post-injury revealed concussed mice recovered to baseline BUCS score, highlighting the transient nature of this injury and similarity to concussion resolution in sport-athletes (McCrea et al., 2003; Meehan et al., 2011). Ability to assess these transient concussion signs and symptoms required mice to be unanesthestized during injury.

Histopathological analysis showed a temporal progression of neuropathology. Hematoxylin and eosin examination of brains at 24 hours showed neuronal cell death and loss of structure, at 72 hours neuronal loss and micro-vacuolation, and at 2 weeks hemosiderin-laden macrophages evidence of BBB disruption. Cytoskeleton proteins provide neuronal structure and function (Drake & Lasek, 1984). Phosphorylated neurofilament-h pNFH antibody (SMI-34) was used to assess axonal injury and showed an axonal damage occurred at 24 hours with axonal varicosities and irregularities. SMI-34 immunostaining at 72 hours was found to have increased axonal varicosities and irregularities with perikaryal accumulation of pNFH. By 2 weeks SMI-34 immunostaining showed a marked reduction in axonal staining. Temporal progression of neuroinflammation showed astrocytosis and microgliosis was not present until 72 hours post injury, corresponding to the peak BBB disruption measured with DCE-MRI (see Chapter 3). Neuroinflammation decreased at 2 weeks but hemosiderin staining persisted

indicating neuroinflammation occurred in regions of micro contusions.

Overall, these neuropathological observations are consistent with early CTE-linked neuropathology in the brains of young adult athletes with repetitive concussive injury and military veterans with blast exposure (L. E. Goldstein et al., 2012; McKee et al., 2014) and correspond to neuropathology findings in blast exposed mice (L. E. Goldstein et al., 2012). These finds suggest a common mechanism of head acceleration-deceleration that lead to pathogenic shearing strain imposed on the cranial contents (Gennarelli & Meaney, 1996; Holbourn, 1943; J. Zhang, Yoganandan, Pintar, & Gennarelli, 2006). Recent studies have investigated the effects of strain amplification near tissue heterogeneities in the brain specifically around micro vessels (Cloots, Gervaise, van Dommelen, & Geers, 2008; Cloots, van Dommelen, Kleiven, & Geers, 2013; Povlishock, 1993). Our studies with EB and DCE-MRI have shown BBB disruption at 24 hours post injury and increased permeability at 72 hours. These findings, along with the temporal neuropathological progress, parallels results from animal models and clinical data suggests that BBB disruption can be induced from contact head injury (Korn, Golan, Melamed, Pascual-Marqui, & Friedman, 2005; Tomkins et al., 2008) and a secondary delayed phase occurs 3–7 days following injury (Cernak, 2005; Shapira et al., 1993).

Our impact concussion injury model recapitulates many key features of acute human concussion and chronic brain pathologies and dysfunction associated with repetitive closed-head concussive impact injury, including cellular accumulation of diffuse phosphorylated tau protein for both left and right hemispheres of impact

concussed mice. It is notable that no neurofibrillary tangles (NFT) were detected by CP-13 antibody in brains of impact concussed mice. Recent work by Kondo *et al.* reported that *cis* hypophosphorylated tau (P-tau), an early tau epitope found in animal and human TBI brains, plays a major role in the pathogenesis of the tauopathy in CTE (Kondo et al., 2015). TBI mouse models showed *Cis* P-tau was present at 48 hours post-injury before the detection of other tau oligomers, aggregation, or tau tangle epitopes and suggest an association with axonal injury, microtubules, and mitochondria disruption. Furthermore, human CTE brain tissue revealed *cis* P-tau to be concentrated near blood vessels. These results suggest early tau epitopes are elevated after TBI and possibly act as a contributing mechanism in neurodegeneration and formation of NFT in CTE.

Activated microglia has been reported in acute concussion cases (McKee et al., 2014). Flow cytometry analysis revealed impact-concussion injury induces neuroinflammation composed of infiltrating monocytes and activated microglia and observed similar temporal progression between the flow experiment and histological staining. At the early acute time point (24 hours) we found no significant increase in activated microglia or infiltrating monocytes. However, at 72 hours post-injury infiltrating monocytes and activated microglia significantly increased and inflammation did not fully resolve by 2 weeks. The delay in infiltrating monocytes has been shown to occur 3 and 4 days after contusive TBI (Clark, Schiding, Kaczorowski, Marion, & Kochanek, 1994; Holmin, Soderlund, Biberfeld, & Mathiesen, 1998). Our findings indicated an increase in Ly-6C^{high}, Ly-6C^{middle} and Ly-6C^{low} monocytes populations and peripheral Ly-6c^{low} monocytes significantly increased after impact-concussion injury and

corresponded to an increase in activated microglia. In mice, monocytes population contain two subsets, Ly-6C^{high} which are classified as inflammatory (Serbina, Jia, Hohl, & Pamer, 2008), and Ly-6C^{low} or patrolling monocytes which migrate along the surface of small blood vessels (Auffray et al., 2007). How these subsets of infiltrating monocytes once in the brain parenchyma influence chronic neuroinflammation, react after repetitive hits and their role in the development of tauopathies remains unknown. We also observed significant upregulation of TREM2^{+} microglia at all three time points, however no significant upregulation in the monocyte population. The triggering receptor expressed on myeloid cells 2 (TREM2) has been shown to be expressed by microglia and monocytes (Wang et al., 2015) and if mutated, increases the risk of developing Alzheimer's disease (Guerreiro et al., 2013; Jonsson et al., 2013). Function of TREM2 on microglia has been shown to influence phagocytosis activity and decrease pro-inflammatory response (Rohn, 2013). A recent study found TREM2 activation is caused by damage-induced lipid release, which leads to reactive microgliosis (Wang et al., 2015) and suggests TREM2 upregulation is associated with neuronal damage and loss caused by concussive injury. TREM2 functions with regards to chronic neuroinflammation and neuroprotection is poorly understood; however, it appears impact concussion injury induces TREM2 upregulation and warrants further investigation (Tanzi, 2015).

Hippocampal conduction velocity and LTP in the mPFC abnormalities are substantial. Impact injury was sufficient to induce persistent conduction velocity impairment on both hemispheres and after 2 weeks only the right hemisphere conduction velocity showed no significance. During the same time course, LTP in the mPFC does

not return to control levels. The persistent findings may indicate mechanisms underpinning postconcussive syndrome seen in the clinic regrading cognitive deficits (Bohnen, Jolles, Twijnstra, Mellink, & Wijnen, 1995), working memory (McAllister et al., 1999), and processing speed (Cicerone, 1996).

The BUCS score was designed to assess the severity of concussion. We reported no correlation between impact input (rod and sled velocity) and BUCS score. No correlation was revealed when compared to tau, inflammation, or conduction velocity. LTP at 2 weeks showed a positive estimated slope with BUCS lost points and no correlation at 24 hours and 72 hours.

Our findings indicate that impact concussive injury induces brain injury in the peri-acute period following injury. Our study raises concern that severity of concussion does not correlate with brain injury. Although the signs of concussion resolved, the brain might not have healed from the insult. The delayed neuroinflammation response and persistence of LTP provided new insights into the pathogenesis of concussive impact injury. The availability of a neuropathologically-validated murine model with correspondence to human CTE is expected to open new avenues for investigation of mechanisms, biomarkers, and risk factors relevant to concussive injury.

Chapter 5: Mechanism of concussion

The injury mechanism of acute concussion is unknown. In this chapter we compare BUCS scores between our blast and impact model and present results obtained from computer simulations performed in collaboration with Dr. Willy Moss at Lawrence Livermore National Laboratory, Livermore CA. The chapter concludes with a summary of the thesis findings and implications.

5.1 Concussion Injury and Biomechanics for Acute Concussion

The definition of concussion continues to be refined by professional groups, governmental bodies, and consensus groups (Christopher C Giza et al., 2013; McCrory, Meeuwisse, Aubry, et al., 2013). Some of the refinements to the definition of concussion have included the addition of clinical features (i.e., headache and nausea) (Guskiewicz, Bruce, Cantu, Ferrara, Kelly, McCrea, Putukian, & McLeod, 2004) and the removal of loss of consciousness as a requirement for concussion (McCrory, Meeuwisse, Aubry, et al., 2013). However, even with these refinements the understanding of concussion remains similar to the 1966 definition by the Committee on Head Injury Nomenclature of the congress of Neurological Surgeon which defined concussion as "a clinical syndrome characterized by immediate and transient impairment of neural functions, such as alteration of consciousness, disturbance of vision, equilibrium, etc. due to mechanical forces." [Emphasis added] (Committee of Head Injury, 1966 quotes in (Guskiewicz, Bruce, Cantu, Ferrara, Kelly, McCrea, Putukian, & Valovich McLeod, 2004).

Mild TBI (mTBI) and concussion are commonly interchanged in the literature.

The American Medical Society for Sports Medicine position statement on concussion in sport defined concussion as a subset of mTBI within the severity spectrum of traumatic brain injury (Harmon et al., 2013). The Fourth International Conference on Concussion in Sport has defined concussion as a brain injury (McCrory, Meeuwisse, Aubry, et al., 2013), and reports by the Department of Defense equate concussion and mTBI (VA/DoD, 2009). While disagreement exists where concussion resides on the TBI severity scale, it appears to be a consensus that concussion should be viewed as part of the continuum of brain injury: mild, moderate and severe. The implications of this association suggest that concussion signs and symptoms are induced by the same mechanism responsible for objective pathobiological injury.

Previous work investigating the injury mechanism of TBI has provided evidence that angular acceleration or inertial loading to the brain produce shear strains capable of inducing tissue damage (Gennarelli et al., 1982; Holbourn, 1943; Ommaya & Gennarelli, 1974). Using a primate inertial animal model, it was revealed that angular acceleration induces paralytic coma (Ommaya & Gennarelli, 1974) (see section 1.6.2). This work produced a hypothesis that angular acceleration induces shear strains that affect level of consciousness. These shear strains affect both function and structure starting at the cortex and with more severe injuries extend inward damaging the reticular activating system leading to coma (Ommaya & Gennarelli, 1974). In other words, this hypothesis for the syndromes of concussion scale with the primary injury of angular acceleration (Ommaya & Gennarelli, 1974).

In mTBI, the extent of objective pathobiological injury and its relationship to the

observed clinical syndrome of concussion is not clearly understood. However, experimental data presented in chapters 3 and chapters 4 revealed no correlation between BUCS/insult intensity (rod and sled speed), BUCS/BBB disruption, BUCS/Tau proteinopathy, and BUCS/neuroinflammation. These results suggest concussion or the acute effects of closed-head neurotrauma are an insufficient metric in determining the extent of the long-term pathobiological effects. Furthermore, we hypothesize that acute concussion and chronic sequelae are engaged through different mechanisms.

5.2 BUCS Comparison between Blast and Impact Neurotrauma

Adult C57BL/6 mice, 10–12 weeks-of-age (Taconic) were subjected to either blast or impact neurotrauma. Blast neurotrauma model delivered a blast shock wave, which measured blast overpressure at 72.3 ± 2.8 kPag (mean, S.D.), which induced a reproducible left-lateral closed-head blast injury to awake mice. Mice were injected with buprenorphine (0.2 mg/kg, i.p.) and secured in the prone position with a modified DecapiCone (Braintree Scientific) such that the head and cervical spine extended outside the plastic restraint and placed in a thoracic-protected restrain system inside the shock tube (L. E. Goldstein et al., 2012). BUCS was scored at baseline, 2 minutes post-injury and at the 3 hour recovery time.

Impact neurotrauma model with a fire pressure of 19.1 ± 1.3 psig (mean, S.D.) resulted in a 7.2 ± 0.3 m/s (mean, S.D.) rod speed and 5.08 ± 0.50 m/s (mean, S.D.) sled speed, which delivered a reproducible left-lateral closed-head impact injury to awake mice. Mice were injected with buprenorphine (0.2 mg/kg, i.p.) and secured in the prone

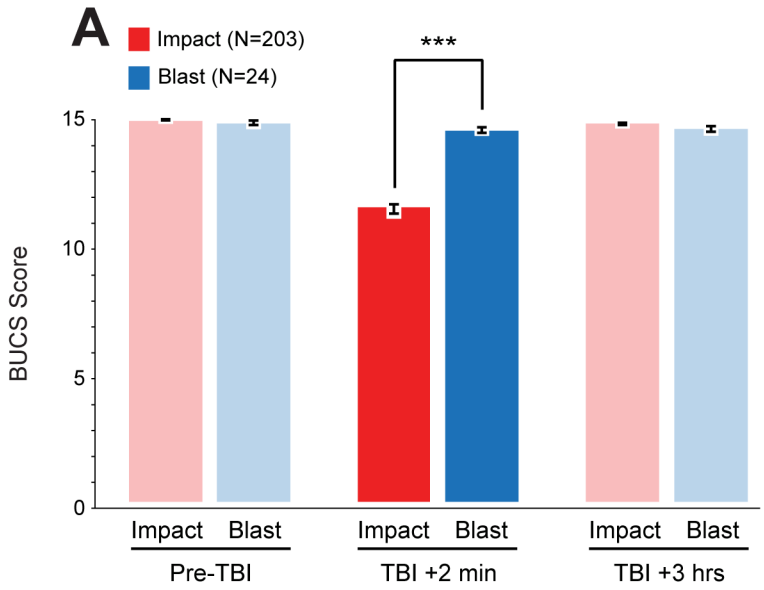

Figure 5.1: Neurological Impairments differ after blast-exposed injury and closed-head impact injury.
BUCS assessment after injury revealed significant difference between impact neurotrauma and blast neurotrauma ($P<0.001$). No significant difference between blast pre-TBI, TBI + 2 min, and TBI + 3 hours.

position with a modified DecapiCone (Braintree Scientific) such that the head and cervical spine extended outside the plastic restraint and a Velcro strap was used to secure the torso.

Analysis of the BUCS scores for the blast-exposed mice (N=12) revealed no significant difference between baseline, post blast exposure, and recovery (Figure 5.1). After mice were removed from the restraint cone, normal locomotion, exploration and balance was observed in the open-field test, wire-mesh and beam-walk tests. These blast-exposed BUCS scores were compared to the experimental impact neurotrauma group (N=203). Statistical analysis was performed using a mixed linear model for repeated-measurements with significance set at $p < 0.5$, and found a significant difference between

impact and blast BUCS post injury. (see Chapter 2 – methods).

The impact model was designed to enable the comparison between blast and impact neurotrauma. Kinematic analysis revealed comparable kinematics between the two models (see – section 2.3.3). However, Figure 5.1 shows that the acute effects (i.e., "concussion") (2 minutes post-injury) are different and transient, in particular mice exposed to impact are concussed, whereas, the mice exposed to blast are not. As the gross motion for both models are comparable, the difference between neurological impairments measured by BUCS must be due to the method by which motion is established. Consequently, there must be details about the blast and impact loading conditions that

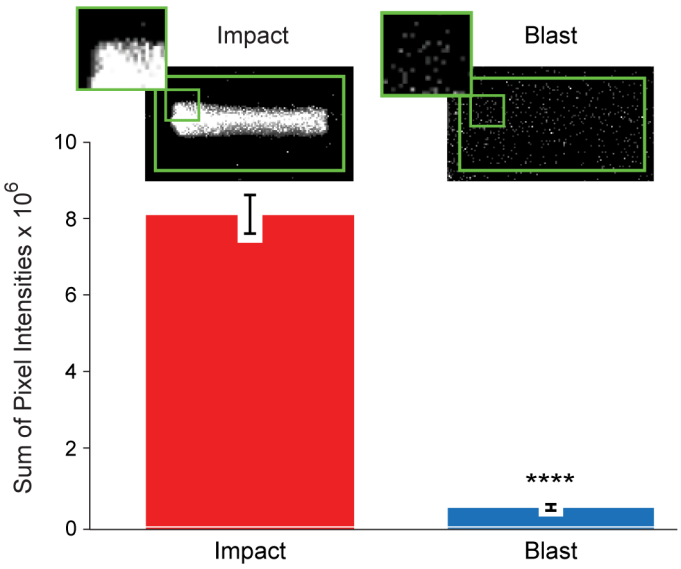

Figure 5.2: Significant difference in loading conditions between impact and blast neurotrauma.
Pressure film analysis revealed a significant difference between pixel intensity between blast and impact ($p < 0.0001$, Student's t-test). Note the focal distribution and dense pixel intensity in the impact film compared to speckled pixel intensity in the blast film.

differ but don't affect the gross motion.

An experiment investigating the loading conditions was performed with pressure indicating films (Fujifilm Prescale, pressure range 350 – 1,400 psi, "low" film type). The motivation was to determine the disruption of distribution of loading for each injury model. We hypothesized that impact neurotrauma would apply a higher pressure compared to blast neurotrauma. To observe the applied pressure during impact and blast, we attached the film to a 50 mL falcon tubes that were filled with 10% gelatin. The diameter of the tube closely approximated the height of a mouse head. Film was exposed to same injury intensity as the mice. Andrew Fisher scanned and calculated pixel intensity.

Comparison between the total pixel intensity revealed a stark difference ($p<0.0001$, Student's t-test). Visual comparison showed a focal loading during impact injury compared to blast injury (Figure 5.2). These results suggest examining how the mechanical loads couple to the head during blast and impact could further elucidate the resulting mechanical response in the brain.

5.3 Numerical Simulation of Blast and Impact Neurotrauma

From the previous experiments we have shown that impact neurotrauma induce neurological deficits in mice while blast neurotrauma show no discernable deficits. The loading of forces to the brain differs between the two models; however, the resulting head motion is comparable. To investigate a detailed spatial and temporal evolution of stresses in the brain, an experiment would require copious experimental data from instrumented

mouse brains and is beyond the scope of this thesis. Therefore, we collaborated with with Dr. Willy Moss at Lawrence Livermore National Laboratory, Livermore CA. and used a numerical simulation.

Simulation Parameters	Thickness	Density
Brain (diameter, density)	10.0 mm	1.04 g•cm^{-3}
CSF (thickness, density)	0.2 mm	1.00 g•cm^{-3}
Skull (thickness, density)	0.2 mm	1.70 g•cm^{-3}

Simulation Results	Impact	Blast
Peak Acceleration (m•s^{-2})	10404	10611
Head Injury Criterion (HIC)	6021	6723

Figure 5.3: Simulation Parameters and simulation results for blast and impact simulated neurotrauma.

We used the arbitrary Lagrangian-Eulerian hydrostructural finite element code ALE3D to simulate the both the blast tube and the impactor described previously (see Chapter 2). We assume a spherical mouse head consisting of a 20 mm OD brain, 0.2 mm thick CSF, and 0.2 mm thick skull (Figure 5.3). Although an exact representation of the head would be desirable, the spherical approximation is sufficient to compare the effects of blast- and impact-induced tissue deformation.

We require that the blast- and impact-induced center-of-geometry motions be similar to each other and representative of the experimental data in order to contrast details of the tissue response. Figure 5.4 shows time-dependent blast- and impact-induced accelerations at the center of the brain. The blast simulation was initialized with 172kPag He overpressure in the driver chamber. The agreement of the blast simulation with the

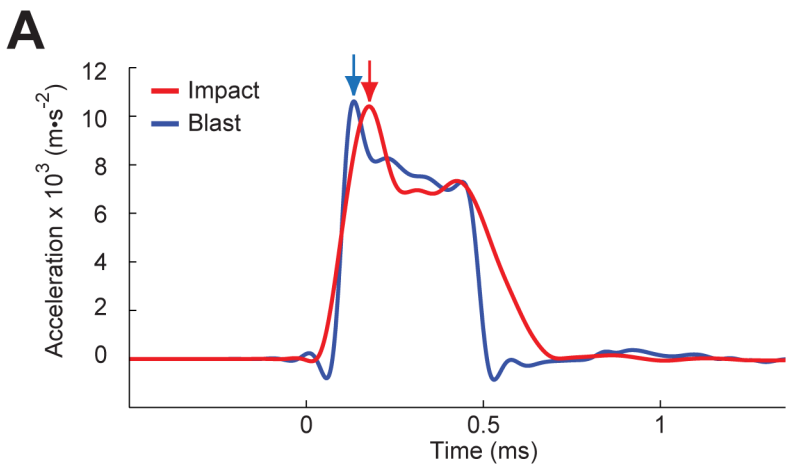

Figure 5.4: Time-dependent blast- and impact-induced accelerations at the center of the brain.

experimental data (see Figure 5.1), due in part to the ratio of the head area to the head mass in the simulation being similar to the experimental value, provides sufficient validation for the remaining comparisons. The spherical head mass is less than the experimental (actual) value, so the impactor velocity in the impact simulation was scaled from the 7.2m/s experimental value to 2.6m/s to obtain a peak acceleration similar to that calculated for blast. The peak accelerations and calculated HICs are shown in Figure 5.3, providing additional confirmation of the kinematic similarity of the blast and impact results.

Our first hypothesis was that pressure in the brain accounts for the difference in neurological deficits between impact and blast neurotrauma. However, after correcting the impact simulation speed to produce a comparable accelerations curve (Figure 5.4), the calculated overpressures in the brain (not shown) were ~50kPa larger for blast than for impact. If overpressure was a dominant concussion-generating mechanism, we would

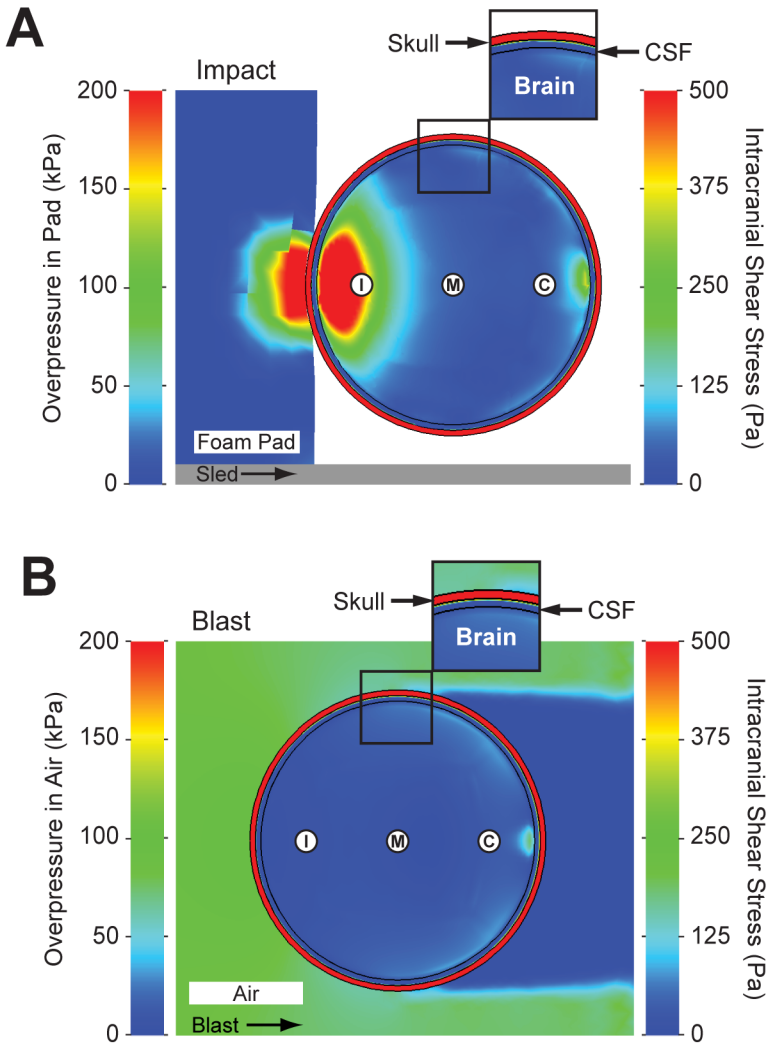

Figure 5.5: Numerical simulation of shear stress.
Numerical simulation of shear stress is increased in impact simulation on left-lateral side consistent with right-sided weakness observed in BUCS assessments. Blast simulation shows no increase in shear stress compared to impact simulation. A) Impact simulation (2D slice) showing overpressure in the foam (left scale) and shear stress in the head (right scale) at the time of peak acceleration; B) blast simulation showing overpressure in the air (left scale) and shear stress in the head (right scale) at the time of peak acceleration.

expect the blast exposed mice to be more concussed than those exposed to impact, but the opposite was observed.

These results required an adjustment of our hypothesis and we hypothesized shear

stress as the concussion-generating mechanism. Figure 5.5 shows cross sections through the center of the impacted and blasted spheres at the time of peak acceleration in Figure 5.4. Overpressure (left scale) is shown in the foam pad (impact) and air surrounding the sphere (blast), whereas, the von Mises or equivalent stress, labeled shear stress (right scale) is shown in the skull, CSF, and brain. The dynamic air pressure (not shown in Figure 5.5-B) is approximately one-fifth the value of the static pressure. In Figure. 5.5-B, the blast wave approached from the left and exited to the right. Reynolds number for this (nonsteady) flow is $\sim 10^5$, so the flow field is turbulent. Modeling of the turbulent wake is outside the scope of this study and therefore the flow in the wake was modeled as a region of still air at ambient pressure. The blue shaded region to the right of the sphere is maintained at ambient pressure, effectively a numerically enforced representation of the turbulent wake, as the actual non-steady turbulence effects are at best extremely difficult to simulate. The light-blue region of shear stress in Figure 5.5-B is due to wave coalescence as the blast sweeps over the head and subsequent ringing. It arises 25us after the blast reaches the front of the skull and dissipates 85us later.

Figures 5.6-A,B show time histories of the shear stresses at the ipsilateral, medial, and contralateral locations identified in Figures 5.5-A,B. The plot of time histories demonstrate that the shear stress in the brain tissue is more widely distributed and an order of magnitude higher in amplitude for the impact case in comparison to the blast case. Figure 5.5 and Figure 5.6 demonstrate that the difference in the shear stresses generated by the blast and impact is profound, despite the fact that the gross motion and pressure are similar. The genesis for the difference can be understood from Figure 5.5-B,

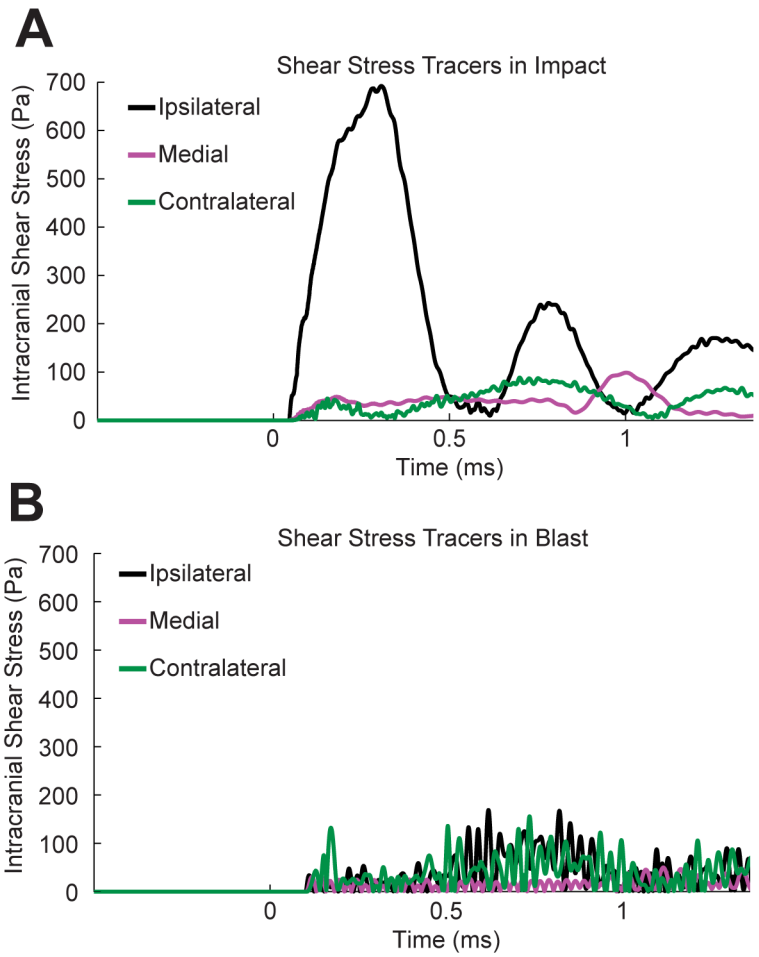

Figure 5.6: Temporal histories shear stress for impact and blast simulations.
A) impact simulation showing the temporal variation of shear stresses at the left, right, and center points labeled in Figure 5.5-A ; B) same as Figure 5.5-B, but for blast.

which shows that after the initial passage of the blast front, the loading around the head is fairly uniform, except at the turbulent wake boundary. Even though the magnitude of the pressure in the flow behind the blast wave is decreasing with time, the spatial gradients across the head are small, as shown in the figure. Consequently, this spatially uniform loading does not generate significant shear stress. In contrast, impact results in a more concentrated loading, through a small contact patch (Fig. 5.5-A), and the large spatial

gradients will result in significant shear stress. We note that shear stresses predicted by the model are on the order of hundreds of pascals (Pa). This value is less than the 6–10 kPa (L. Zhang et al., 2004) that has been reported to result in concussion in football players. However, the shear stresses are large enough and persist long enough, lasting a few milliseconds after exposure due to the viscoelastic properties of brain tissue, to disrupt neurochemical activity where shear stresses on the order of 1 Pa have been reported to result in calcium activity (Ravin et al., 2012).

Key Points:

1. Energy loading in the head assumed subsequent to head motion.
2. Energy loading is focal and asymmetric in impact neurotrauma, comparable to a diffuse and symmetric loading in blast neurotrauma.
3. Shear stress from impact neurotrauma is located on the side of injury in a focal manner.
4. Within the first millisecond of exposure, the head motion is less than 1mm, so that the mechanical insult occurs prior to “macroscopic” head motion.
5. Impact and blast neurotrauma induces long-term neurobiological sequelae.

The absence of concussion in the mice exposed to blast and the presence of concussion in the impacted mice, coupled with the simulation results allows us to hypothesize that concussion may result from early-time shear stresses generated by the impact.

5.4 Conclusions

The overarching goal of this thesis research was to design and develop a new murine impact neurotrauma model that could recapitulate acute clinical concussion and CTE-linked pathology.

Design of the impact model was based on specific user needs. The gas driven impactor allowed for scalability and reliability and allowed for easy modification. Incorporation of the rod allowed for a failure point and eliminated any free flying projectiles. The novel addition of the sled provided this model to induce a left-lateral hit with no skull crush. Through these design elements, all injury requirements were satisfied and allowed for comparable kinematic comparison between the two models.

To provide clinical validity to our impact neurotrauma model, we conducted all animal experiments without anesthesia. This allowed for the assessment of the transient lateralized neurological signs after impact neurotrauma and recapitulated core clinical features of sport-related concussion in humans. We developed the Boston University Concussion Scale to enable rapid and objective assessment of transient neurological deficits. Decreases in BUCS scores were observed after impact neurotrauma injury and further deficits observed following the second hit. These deficits recovered after 3 hours.

Investigation into the blood brain barrier (BBB) disruption following impact neurotrauma resulted in focal, lateral disruption and heterogeneous distribution of disruption within the impact injured group. These differences suggested the variability of impact neurotrauma in inducing macroscopic injury. We performed a serial MRI study investigating the temporal progression of BBB disruption in closed-head injured mice,

and showed the ability of DCE-MRI and Ablavar contrast agent as a possible candidate as a biomarker for concussion brain injury.

Concussed mice recovered neurological function within three hours, but demonstrated persistent myelinated axonopathy, microvasculopathy, neuroinflammation, and phosphorylated tauopathy consistent with early CTE. Concussive impact injury also induced blood-brain barrier disruption, neuroinflammation (including infiltration of CD45+ peripheral monocytes and activation of TREM2-expressing microglia), impaired hippocampal axonal conduction, and defective long-term potentiation (LTP) of synaptic transmission in medial prefrontal cortex.

However, the presence or degree of concussion measured by BUCS did not correlate with chronic sequelae. Moreover, concussion was observed following impact injury but not blast exposure under conditions that induce comparable head kinematics. Empirical pressure measurements and dynamic modeling revealed greater pressure on the head and compression wave loading in the brain during impact compared to blast neurotrauma. These findings indicate that acute concussion is triggered by efficient coupling and transmission of high-velocity compression waves that transit the brain before onset of macroscopic head motion. These results indicate that acute concussion and chronic sequelae may be triggered by the same insult injury but the mechanisms and time domains are distinct. Our results indicate that concussion is neither necessary nor sufficient to induce acute brain injury or chronic sequelae, including CTE. The development of the impact neurotrauma trauma model and BUCS, along with the blast neurotrauma model provide the necessary tools to further investigate biomechanical and

pathobiological determinants that link traumatic brain injury (TBI) with chronic traumatic encephalopathy (CTE).

Chapter 6: BIBLIOGRAPHY

Abbott, N. J., Patabendige, A. A., Dolman, D. E., Yusof, S. R., & Begley, D. J. (2010). Structure and function of the blood-brain barrier. *Neurobiology of Disease, 37*(1), 13–25. doi:10.1016/j.nbd.2009.07.030

Adams, J. H., Graham, D. I., & Gennarelli, T. A. (1983). Head injury in man and experimental animals: neuropathology. *Acta Neurochirurgica. Supplementum, 32*, 15–30. Retrieved from <Go to ISI>://MEDLINE:6581702

Alder, J., Fujioka, W., Lifshitz, J., Crockett, D. P., & Thakker-Varia, S. (2011). Lateral Fluid Percussion: Model of Traumatic Brain Injury in Mice. *Journal of Visualized Experiments: JoVE* (54). doi:10.3791/3063

Alla, S., Sullivan, S. J., Hale, L., & McCrory, P. (2009). Self-report scales/checklists for the measurement of concussion symptoms: a systematic review. *British Journal of Sports Medicine, 43*, I3–I12. doi:10.1136/bjsm.2009.058339

American Academy of Neurology, P. (1997). Practice Parameter: The management of concussion in sports (summary statement). *Neurology, 48*(3), 581–585.

Aubry, M., Cantu, R., Dvorak, J., Graf-Baumann, T., Johnston, K., Kelly, J., . . . Schamasch, P. (2002). Summary and agreement statement of the First International Conference on Concussion in Sport, Vienna 2001. Recommendations for the improvement of safety and health of athletes who may suffer concussive injuries. *British Journal of Sports Medicine, 36*(1), 6–10.

Auffray, C., Fogg, D., Garfa, M., Elain, G., Join-Lambert, O., Kayal, S., . . . Geissmann, F. (2007). Monitoring of blood vessels and tissues by a population of monocytes with patrolling behavior. *Science, 317*(5838), 666–670. doi:10.1126/science.1142883

Azevedo, F. A., Carvalho, L. R., Grinberg, L. T., Farfel, J. M., Ferretti, R. E., Leite, R. E., . . . Herculano-Houzel, S. (2009). Equal numbers of neuronal and nonneuronal cells make the human brain an isometrically scaled-up primate brain. *Journal of Comparative Neurology, 513*(5), 532–541. doi:10.1002/cne.21974

Bakay, L., Lee, J. C., Lee, G. C., & Peng, J. R. (1977). Experimental cerebral concussion 1. Electron-microscopic study. *Journal of Neurosurgery, 47*(4), 525–531. doi:10.3171/jns.1977.47.4.0525

Baldwin, S. A., Fugaccia, I., Brown, D. R., Brown, L. V., & Scheff, S. W. (1996). Blood-brain barrier breach following cortical contusion in the rat. *Journal of Neurosurgery, 85*(3), 476–481. doi:10.3171/jns.1996.85.3.0476

Ballabh, P., Braun, A., & Nedergaard, M. (2004). The blood-brain barrier: an overview: structure, regulation, and clinical implications. *Neurobiology of Disease, 16*(1), 1–13. doi:10.1016/j.nbd.2003.12.016

Bandak, F. A. (2005). Shaken baby syndrome: A biomechanics analysis of injury mechanisms. *Forensic Science International, 151*(1), 71–79. doi:10.1016/j.forsciint.2005.02.033

Baskaya, M. K., Rao, A. M., Dogan, A., Donaldson, D., & Dempsey, R. J. (1997). The biphasic opening of the blood-brain barrier in the cortex and hippocampus after traumatic brain injury in rats. *Neuroscience Letters, 226*(1), 33–36.

Bazarian, J. J., Blyth, B., & Cimpello, L. (2006). Bench to bedside: evidence for brain injury after concussion–looking beyond the computed tomography scan. *Academic Emergency Medicine, 13*(2), 199–214. doi:10.1197/j.aem.2005.07.031

Bazarian, J. J., Zhu, T., Blyth, B., Borrino, A., & Zhong, J. (2012). Subject-specific changes in brain white matter on diffusion tensor imaging after sports-related concussion. *Magnetic Resononance Imaging, 30*(2), 171–180. doi:10.1016/j.mri.2011.10.001

Beni-Adani, L., Gozes, I., Cohen, Y., Assaf, Y., Steingart, R. A., Brenneman, D. E., . . . Shohami, E. (2001). A peptide derived from activity-dependent neuroprotective protein (ADNP) ameliorates injury response in closed head injury in mice. *Journal of Pharmacology and Experimental Therapeutics, 296*(1), 57–63. Retrieved from <Go to ISI>://WOS:000165951800008 http://jpet.aspetjournals.org/content/296/1/57.full.pdf

Bhaskar, K., Hobbs, G. A., Yen, S. H., & Lee, G. (2010). Tyrosine phosphorylation of tau accompanies disease progression in transgenic mouse models of tauopathy. *Neuropathology and Applied Neurobiology, 36*(6), 462–477. doi:10.1111/j.1365-2990.2010.01103.x

Black, K. L., Hanks, R. A., Wood, D. L., Zafonte, R. D., Cullen, N., Cifu, D. X., . . . Francisco, G. E. (2002). Blunt versus penetrating violent traumatic brain injury: frequency and factors associated with secondary conditions and complications. *Journal of Head Trauma Rehabilitation, 17*(6), 489–496.

Bohnen, N. I., Jolles, J., Twijnstra, A., Mellink, R., & Wijnen, G. (1995). Late neurobehavioral symptoms after mild head-injury. *Brain Injury, 9*(1), 27–33. doi:10.3109/02699059509004568

Bolouri, H., & Zetterberg, H. (2015). Animal Models for Concussion: Molecular and Cognitive Assessments-Relevance to Sport and Military Concussions. In F. H. Kobeissy (Ed.), *Brain Neurotrauma: Molecular, Neuropsychological, and Rehabilitation Aspects*. Boca Raton (FL): CRC Press/Taylor & Francis.

Bowles, E. D., & Gold, M. E. (2012). Rethinking the paradigm: evaluation of ketamine as a neurosurgical anesthetic. *AANA Journal, 80*(6), 445–452. Retrieved from <Go to ISI>://MEDLINE:23409639

Boyd, C. R., Tolson, M. A., & Copes, W. S. (1987). Evaluating trauma care – the triss method. *Journal of Trauma-Injury Infection and Critical Care, 27*(4), 370–378. Retrieved from <Go to ISI>://WOS:A1987H090200005

Brody, D. L., Mac Donald, C., Kessens, C. C., Yuede, C., Parsadanian, M., Spinner, M., . . . Bayly, P. V. (2007). Electromagnetic controlled cortical impact device for precise, graded experimental traumatic brain injury. *Journal of Neurotrauma, 24*(4), 657–673. doi:10.1089/neu.2006.0011

Broglio, S. P., Schnebel, B., Sosnoff, J. J., Shin, S., Fend, X., He, X., & Zimmerman, J. (2010). Biomechanical properties of concussions in high school football. *Medicine and Science in Sports and Exercise, 42*(11), 2064–2071. doi:10.1249/MSS.0b013e3181dd9156

Cantu, R. C. (1986). Guidelines for return to contact sports after a cerebral concussion. *Physician and Sportsmedicine, 14*(10), 75–83. Retrieved from <Go to ISI>://WOS:A1986E206200005

Carroll, L., Cassidy, J. D., Peloso, P., Borg, J., x000F, rgen, . . . pin, M. (2004). Prognosis for mild traumatic brain injury: results of the who collaborating centre task force on mild traumatic brain injury. *Journal of Rehabilitation Medicine, 36*, 84–105. doi:10.1080/16501960410023859

Cavanaugh, J. T., Guskiewicz, K. M., Giuliani, C., Marshall, S., Mercer, V., & Stergiou, N. (2005). Detecting altered postural control after cerebral concussion in athletes with normal postural stability. *British Journal of Sports Medicine, 39*(11), 805–811. doi:10.1136/bjsm.2004.015909

Cavanaugh, J. T., Guskiewicz, K. M., Giuliani, C., Marshall, S., Mercer, V. S., & Stergiou, N. (2006). Recovery of postural control after cerebral concussion: new insights using approximate entropy. *Journal of Athletic Training, 41*(3), 305–313.

CDC. (2003). *Report to Congress on mild traumatic brain injury in the United States: Steps to prevent a serious public health problem*. Retrieved from: http://www.cdc.gov/TraumaticBrainInjury/factsheets_reports.html

Cernak, I. (2005). Animal Models of Head Trauma. *NeuroRx, 2*(3), 410–422. Retrieved from http://www.ncbi.nlm.nih.gov/pmc/articles/PMC1144485/

Champion, H. R., Copes, W. S., Sacco, W. J., Lawnick, M. M., Bain, L. W., Gann, D. S., . . . Schwaitzberg, S. (1990). A new characterization of injury severity. *Journal of Trauma-Injury Infection and Critical Care, 30*(5), 539–546. doi:10.1097/00005373-199005000-00003

Champion, H. R., Sacco, W. J., Copes, W. S., Gann, D. S., Gennarelli, T. A., & Flanagan, M. E. (1989). A revision of the trauma score. *Journal of Trauma-Injury Infection and Critical Care, 29*(5), 623–629. doi:10.1097/00005373-198905000-00017

Chassidim, Y., Veksler, R., Lublinsky, S., Pell, G. S., Friedman, A., & Shelef, I. (2013). Quantitative imaging assessment of blood-brain barrier permeability in humans. *Fluids and barriers of the CNS, 10*(1), 9. doi:10.1186/2045-8118-10-9

Chen, J. K., Johnston, K. M., Frey, S., Petrides, M., Worsley, K., & Ptito, A. (2004). Functional abnormalities in symptomatic concussed athletes: an fMRI study. *Neuroimage, 22*(1), 68–82. doi:10.1016/j.neuroimage.2003.12.032

Chen, Y., Constantini, S., Trembovler, V., Weinstock, M., & Shohami, E. (1996). An experimental model of closed head injury in mice: Pathophysiology, histopathology, and cognitive deficits. *Journal of Neurotrauma, 13*(10), 557–568. Retrieved from <Go to ISI>://A1996VQ83400002

Chodobski, A., Zink, B. J., & Szmydynger-Chodobska, J. (2011). Blood-brain barrier pathophysiology in traumatic brain injury. *Translational Stroke Research, 2*(4), 492–516. doi:10.1007/s12975-011-0125-x

Cicerone, K. D. (1996). Attention deficits and dual task demands after mild traumatic brain injury. *Brain Injury, 10*(2), 79–90.

Clark, R. S., Schiding, J. K., Kaczorowski, S. L., Marion, D. W., & Kochanek, P. M. (1994). Neutrophil accumulation after traumatic brain injury in rats: comparison of weight drop and controlled cortical impact models. *Journal of Neurotrauma, 11*(5), 499–506.

Cloots, R. J., Gervaise, H. M., van Dommelen, J. A., & Geers, M. G. (2008). Biomechanics of traumatic brain injury: influences of the morphologic heterogeneities of the cerebral cortex. *Annals of Biomedical Engineering, 36*(7), 1203–1215. doi:10.1007/s10439-008-9510-3

Cloots, R. J., van Dommelen, J. A., Kleiven, S., & Geers, M. G. (2013). Multi-scale mechanics of traumatic brain injury: predicting axonal strains from head loads.

Biomechanics and Modeling in Mechanobiology, 12(1), 137–150. doi:10.1007/s10237-012-0387-6

Cole, J. T., Yarnell, A., Kean, W. S., Gold, E., Lewis, B., Ren, M., . . . Watson, W. D. (2011). Craniotomy: true sham for traumatic brain injury, or a sham of a sham? *Journal of Neurotrauma, 28*(3), 359–369. doi:10.1089/neu.2010.1427

Collie, A., Darby, D., & Maruff, P. (2001). Computerised cognitive assessment of athletes with sports related head injury. *British Journal of Sports Medicine, 35*(5), 297–302.

Collie, A., Maruff, P., Makdissi, M., McCrory, P., McStephen, M., & Darby, D. (2003). CogSport: reliability and correlation with conventional cognitive tests used in postconcussion medical evaluations. *Clinical Journal of Sport Medicine, 13*(1), 28–32.

Collins, M. W., Iverson, G. L., Lovell, M. R., McKeag, D. B., Norwig, J., & Maroon, J. (2003). On-field predictors of neuropsychological and symptom deficit following sports-related concussion. *Clinical Journal of Sport Medicine, 13*(4), 222–229. doi:10.1097/00042752-200307000-00005

Correale, J., & Villa, A. (2007). The blood-brain-barrier in multiple sclerosis: functional roles and therapeutic targeting. *Autoimmunity, 40*(2), 148–160. doi:10.1080/08916930601183522

Crisco, J. J., Fiore, R., Beckwith, J. G., Chu, J. J., Brolinson, P. G., Duma, S., . . . Greenwald, R. M. (2010). Frequency and location of head impact exposures in individual collegiate football players. *Journal of Athletic Training, 45*(6), 549–559. doi:10.4085/1062-6050-45.6.549

De Beaumont, L., Theoret, H., Mongeon, D., Messier, J., Leclerc, S., Tremblay, S., . . . Lassonde, M. (2009). Brain function decline in healthy retired athletes who sustained their last sports concussion in early adulthood. *Brain, 132*(Pt 3), 695–708. doi:10.1093/brain/awn347

DeFord, S. M., Wilson, M. S., Rice, A. C., Clausen, T., Rice, L. K., Barabnova, A., . . . Hamm, R. J. (2002). Repeated mild brain injuries result in cognitive impairment in B6C3F1 mice. *Journal of Neurotrauma, 19*(4), 427–438. doi:10.1089/08977150252932389

Denny-Brown, D., & Russell, W. R. (1941). Experimental cerebral concussion. *Brain, 64*(2–3), 93–164.

Dixon, C. E., Lyeth, B. G., Povlishock, J. T., Findling, R. L., Hamm, R. J., Marmarou, A., . . . Hayes, R. L. (1987). A fluid percussion model of experimental brain

injury in the rat. *Journal of Neurosurgery, 67*(1), 110–119. doi:10.3171/jns.1987.67.1.0110

Drake, P. F., & Lasek, R. J. (1984). Regional differences in the neuronal cytoskeleton. *Journal of Neuroscience, 4*(5), 1173–1186.

Duma, S. M., Manoogian, S. J., Bussone, W. R., Brolinson, P. G., Goforth, M. W., Donnenwerth, J. J., . . . Crisco, J. J. (2005). Analysis of real-time head accelerations in collegiate football players. *Clinical Journal of Sport Medicine, 15*(1), 3–8. doi:10.1097/00042752-200501000-00002

Eakin, K., Baratz-Goldstein, R., Pick, C. G., Zindel, O., Balaban, C. D., Hoffer, M. E., . . Hoffer, B. J. (2014). Efficacy of N-Acetyl Cysteine in Traumatic Brain Injury. *PLoS One, 9*(4). doi:10.1371/journal.pone.0090617

Eckner, J. T., & Kutcher, J. S. (2010). Concussion Symptom Scales and Sideline Assessment Tools: A Critical Literature Update. *Current Sports Medicine Reports, 9*(1), 8–15. doi:10.1249/JSR.0b013e3181caa778

Erlanger, D., Kaushik, T., Cantu, R., Barth, J. T., Broshek, D. K., Freeman, J. R., & Webbe, F. M. (2003). Symptom-based assessment of the severity of a concussion. *Journal of Neurosurgery, 98*(3), 477–484. doi:10.3171/jns.2003.98.3.0477

Faul, M., Xu, L., Wald, M. M., & Coronado, V. (2010). Traumatic Brain Injury in the United States. Atlanta, GA: Centers for Disease Control and Prevention, National Center for Injury Prevention and Control.

Flierl, M. A., Stahel, P. F., Beauchamp, K. M., Morgan, S. J., Smith, W. R., & Shohami, E. (2009). Mouse closed head injury model induced by a weight-drop device. *Nature Protocols, 4*(9), 1328–1337. doi:10.1038/nprot.2009.148

Ford, J. W., & McVicar, D. W. (2009). TREM and TREM-like receptors in inflammation and disease. *Current Opinion in Immunology, 21*(1), 38–46. doi:10.1016/j.coi.2009.01.009

Fox, G. B., Fan, L., LeVasseur, R. A., & Faden, A. I. (1998). Sustained sensory/motor and cognitive deficits with neuronal apoptosis following controlled cortical impact brain injury in the mouse. *Journal of Neurotrauma, 15*(8), 599–614.

Fox, G. B., LeVasseur, R. A., & Faden, A. I. (1999). Behavioral responses of C57BL/6, FVB/N, and 129/SvEMS mouse strains to traumatic brain injury: implications for gene targeting approaches to neurotrauma. *Journal of Neurotrauma, 16*(5), 377–389.

Fox, Z. G., Mihalik, J. P., Blackburn, J. T., Battaglini, C. L., & Guskiewicz, K. M. (2008). Return of postural control to baseline after anaerobic and aerobic exercise protocols. *Journal of Athletic Training, 43*(5), 456–463. doi:10.4085/1062-6050-43.5.456

Fujimoto, S. T., Longhi, L., Saatman, K. E., & McIntosh, T. K. (2004). Motor and cognitive function evaluation following experimental traumatic brain injury. *Neuroscience & Biobehavioral Reviews, 28*(4), 365–378.

Fulton, J. F. (1942). Blast and concussion in the present war. *New England Journal of Medicine, 226*(1), 1–8.

Gelman, A., Hill, J., & Yajima, M. (2012). Why we (usually) don't have to worry about multiple comparisons. *Journal of Research on Educational Effectiveness, 5*(2), 189–211.

Gennarelli, T. A. (1994). Animate models of human head-injury. *Journal of Neurotrauma, 11*(4), 357–368. doi:10.1089/neu.1994.11.357

Gennarelli, T. A., & Meaney, D. F. (1996). Mechanisms of primary head injury. In R. H. Wilkins & S. S. Regachary (Eds.), *Neurosurgery* (Vol. 2, pp. 2611–2621). New York: McGraw-Hill.

Gennarelli, T. A., Ommaya, A. K., & Thibault, L. E. (1971). *Comparison of translational and rotational head motions in experimental cerebral concussion.* Paper presented at the Proc. 15th Stapp Car Crash Conference.

Gennarelli, T. A., Thibault, L., & Ommaya, A. K. (1972). *Pathophysiologic responses to rotational and translational accelerations of the head*. SAE Technical Paper 720970. doi:10.4271/720970.

Gennarelli, T. A., & Thibault, L. E. (1982). Biomechanics of acute subdural-hematoma. *Journal of Trauma-Injury Infection and Critical Care, 22*(8), 680–686. doi:10.1097/00005373-198208000-00005

Gennarelli, T. A., Thibault, L. E., Adams, J. H., Graham, D. I., Thompson, C. J., & Marcincin, R. P. (1982). Diffuse axonal injury and traumatic coma in the primate. *Annals of Neurology, 12*(6), 564–574. Retrieved from <Go to ISI>://A1982PU00300010

Gennarelli, T. A., Thibault, L. E., & Graham, D. I. (1998). Diffuse Axonal Injury: An Important Form of Traumatic Brain Damage. *Neuroscientist, 4*(3), 202–215. doi:10.1177/107385849800400316

Geurts, A. C., Ribbers, G. M., Knoop, J. A., & van Limbeek, J. (1996). Identification of static and dynamic postural instability following traumatic brain injury. *Archives of Physical Medicine and Rehabilitation, 77*(7), 639–644.

Gill, M. R., Reiley, D. G., & Green, S. M. (2004). Interrater reliability of Glasgow Coma Scale scores in the emergency department. *Annals of Emergency Medicine, 43*(2), 215–223. doi:10.1016/mem.2004.421

Giza, C. C., & Hovda, D. A. (2001). The Neurometabolic Cascade of Concussion. *Journal of Athletic Training, 36*(3), 228–235.

Giza, C. C., & Hovda, D. A. (2014). The new neurometabolic cascade of concussion. *Neurosurgery, 75 Suppl 4*, S24–33. doi:10.1227/neu.0000000000000505

Giza, C. C., Kutcher, J. S., Ashwal, S., Barth, J., Getchius, T. S., Gioia, G. A., . . . Manley, G. (2013). Summary of evidence-based guideline update: Evaluation and management of concussion in sports Report of the Guideline Development Subcommittee of the American Academy of Neurology. *Neurology, 80*(24), 2250–2257.

Goldstein, H. (2011). *Multilevel statistical models* (Vol. 922): John Wiley & Sons.

Goldstein, L. E., Fisher, A. M., Tagge, C. A., Zhang, X. L., Velisek, L., Sullivan, J. A., . . . McKee, A. C. (2012). Chronic traumatic encephalopathy in blast-exposed military veterans and a blast neurotrauma mouse model. *Science Translational Medicine, 4*(134), 16. doi:10.1126/scitranslmed.3003716

Goldstein, L. E., McKee, A. C., & Stanton, P. K. (2014). Considerations for animal models of blast-related traumatic brain injury and chronic traumatic encephalopathy. *Alzheimer's Research & Therapy, 6*(5), 64. doi:10.1186/s13195-014-0064-3

Granacher Jr, R. P. (2007). *Traumatic brain injury: Methods for clinical and forensic neuropsychiatric assessment*: CRC Press.

Green, S. M. (2011). Cheerio, Laddie! Bidding Farewell to the Glasgow Coma Scale. *Annals of Emergency Medicine, 58*(5), 427–430. doi:10.1016/j.annemergmed.2011.06.009

Gregersen, M. I., & Rawson, R. A. (1943). The disappearance of T-1824 and structurally related dyes from the blood stream. *American Journal of Physiology, 138*(5), 698–707.

Gronwall, D., & Wrightso.P. (1974). Delayed recovery of intellectual function after minor head-injury. *Lancet, 2*(7881), 605–609. Retrieved from <Go to ISI>://WOS:A1974U083900001

Guerreiro, R., Wojtas, A., Bras, J., Carrasquillo, M., Rogaeva, E., Majounie, E., . . . Younkin, S. (2013). TREM2 variants in Alzheimer's disease. *New England Journal of Medicine, 368*(2), 117–127.

Gurdjian, E. S., Lissner, H. R., & Patrick, L. M. (1962). Protection of the head and neck in sports. *Journal of the American Medical Association, 182*, 509–512.

Gurdjian, E. S., & Webster, J. E. (1947). THe mechanism and management of injuries of the head. *Journal of the American Medical Association, 134*(13), 1072–1077. doi:10.1001/jama.1947.02880300014005

Gurdjian, E. S., Webster, J. E., & Lissner, H. R. (1955). Observations on the mechanism of brain concussion, contusion, and laceration. *Surgery, Gynecology & Obstetrics, 101*(6), 680–690. Retrieved from http://europepmc.org/abstract/MED/13274275

Guskiewicz, K. M. (2011). Balance assessment in the management of sport-related concussion. *Clinics in Sports Medicine, 30*(1), 89–102, ix. doi:10.1016/j.csm.2010.09.004

Guskiewicz, K. M., Bruce, S. L., Cantu, R. C., Ferrara, M. S., Kelly, J. P., McCrea, M., . . . McLeod, T. C. (2004). Recommendations on management of sport-related concussion: summary of the National Athletic Trainers' Association position statement. *Neurosurgery, 55*(4), 891–895; discussion 896.

Guskiewicz, K. M., Bruce, S. L., Cantu, R. C., Ferrara, M. S., Kelly, J. P., McCrea, M., . . . Valovich McLeod, T. C. (2004). National Athletic Trainers' Association Position Statement: Management of Sport-Related Concussion. *Journal of Athletic Training, 39*(3), 280–297.

Guskiewicz, K. M., McCrea, M., Marshall, S. W., Cantu, R. C., Randolph, C., Barr, W., . . . Kelly, J. P. (2003). Cumulative effects associated with recurrent concussion in collegiate football players – The NCAA Concussion Study. *JAMA: The Journal of the American Medical Association, 290*(19), 2549–2555. doi:10.1001/jama.290.19.2549

Guskiewicz, K. M., & Mihalik, J. P. (2011). Biomechanics of Sport Concussion: Quest for the Elusive Injury Threshold. *Exercise and Sport Sciences Reviews, 39*(1), 4–11. doi:10.1097/JES.0b013e318201f53e

Guskiewicz, K. M., Mihalik, J. P., Shankar, V., Marshall, S. W., Crowell, D. H., Oliaro, S. M., . . . Hooker, D. N. (2007). Measurement of head impacts in collegiate

football players: Relationship between head impact biomechanics and acute clinical outcome after concussion. *Neurosurgery, 61*(6), 1244–1252. doi:10.1227/01.neu.0000280146.37163.79

Guskiewicz, K. M., Perrin, D. H., & Gansneder, B. M. (1996). Effect of mild head injury on postural stability in athletes. *Journal of Athletic Training, 31*(4), 300–306.

Guskiewicz, K. M., Riemann, B. L., Perrin, D. H., & Nashner, L. M. (1997). Alternative approaches to the assessment of mild head injury in athletes. *Medicine and Science in Sports and Exercise, 29*(7 Suppl), S213–221.

Guskiewicz, K. M., Ross, S. E., & Marshall, S. W. (2001). Postural stability and neuropsychological deficits after concussion in collegiate athletes. *Journal of Athletic Training, 36*(3), 263–273. Retrieved from <Go to ISI>://WOS:000175913800009 http://www.ncbi.nlm.nih.gov/pmc/articles/PMC155417/pdf/attr_36_03_0263.pdf

Guskiewicz, K. M., Weaver, N. L., Padua, D. A., & Garrett, W. E. (2000). Epidemiology of concussion in collegiate and high school football players. *American Journal of Sports Medicine, 28*(5), 643–650. Retrieved from <Go to ISI>://WOS:000089948800004 http://ajs.sagepub.com/content/28/5/643.long

Habgood, M. D., Bye, N., Dziegielewska, K. M., Ek, C. J., Lane, M. A., Potter, A., . . . Saunders, N. R. (2007). Changes in blood-brain barrier permeability to large and small molecules following traumatic brain injury in mice. *European Journal of Neuroscience, 25*(1), 231–238. doi:10.1111/j.1460-9568.2006.05275.x

Hall, E. D. (1985). High-dose glucocorticoid treatment improves neurological recovery in head-injured mice. *Journal of Neurosurgery, 62*(6), 882–887. doi:10.3171/jns.1985.62.6.0882

Hamm, R. J. (2001). Neurobehavioral assessment of outcome following traumatic brain injury in rats: An evaluation of selected measures. *Journal of Neurotrauma, 18*(11), 1207–1216. doi:10.1089/089771501317095241

Hamm, R. J., Dixon, C. E., Gbadebo, D. M., Singha, A. K., Jenkins, L. W., Lyeth, B. G., & Hayes, R. L. (1992). Cognitive deficits following traumatic brain injury produced by controlled cortical impact. *Journal of Neurotrauma, 9*(1), 11–20.

Han, S. D., Bangen, K. J., & Bondi, M. W. (2009). Functional magnetic resonance imaging of compensatory neural recruitment in aging and risk for Alzheimer's disease: review and recommendations. *Dementia and Geriatric Cognitive Disorders, 27*(1), 1–10. doi:10.1159/000182420

Harmon, K. G., Drezner, J. A., Gammons, M., Guskiewicz, K. M., Halstead, M., Herring, S. A., . . . Roberts, W. O. (2013). American Medical Society for Sports Medicine position statement: concussion in sport. *British Journal of Sports Medicine, 47*(1), 15–26. doi:10.1136/bjsports-2012-091941

Hawryluk, G. W., & Manley, G. T. (2015). Classification of traumatic brain injury: past, present, and future. *Handbook of Clinical Neurology, 127*, 15–21. doi:10.1016/b978-0-444-52892-6.00002-7

Hellal, F., Bonnefont-Rousselot, D., Croci, N., Palmier, B., Plotkine, M., & Marchand-Verrecchia, C. (2004). Pattern of cerebral edema and hemorrhage in a mice model of diffuse brain injury. *Neuroscience Letters, 357*(1), 21–24.

Hernandez, F., Wu, L. C., Yip, M. C., Laksari, K., Hoffman, A. R., Lopez, J. R., . . . Camarillo, D. B. (2015). Six Degree-of-Freedom Measurements of Human Mild Traumatic Brain Injury. *Annals of Biomedical Engineering, 43*(8), 1918–1934. doi:10.1007/s10439-014-1212-4

Hicks, R., Giacino, J., Harrison-Felix, C., Manley, G., Valadka, A., & Wilde, E. A. (2013). Progress in developing common data elements for traumatic brain injury research: version two–the end of the beginning. *Journal of Neurotrauma, 30*(22), 1852–1861. doi:10.1089/neu.2013.2938

Hoge, C. W., McGurk, D., Thomas, J. L., Cox, A. L., Engel, C. C., & Castro, C. A. (2008). Mild Traumatic Brain Injury in U.S. Soldiers Returning from Iraq. *New England Journal of Medicine, 358*(5), 453–463. doi:doi:10.1056/NEJMoa072972

Holbourn, A. H. S. (1943). Mechanics of head injuries. *Lancet, 242*(6267), 438–441. doi:http://dx.doi.org/10.1016/S0140-6736(00)87453-X

Holmin, S., Soderlund, J., Biberfeld, P., & Mathiesen, T. (1998). Intracerebral inflammation after human brain contusion. *Neurosurgery, 42*(2), 291–298; discussion 298–299.

Hooper, C., Pinteaux-Jones, F., Fry, V. A., Sevastou, I. G., Baker, D., Heales, S. J., & Pocock, J. M. (2009). Differential effects of albumin on microglia and macrophages; implications for neurodegeneration following blood-brain barrier damage. *Journal of Neurochemistry, 109*(3), 694–705. doi:10.1111/j.1471-4159.2009.05953.x

Hooper, C., Taylor, D. L., & Pocock, J. M. (2005). Pure albumin is a potent trigger of calcium signalling and proliferation in microglia but not macrophages or astrocytes. *Journal of Neurochemistry, 92*(6), 1363–1376. doi:10.1111/j.1471-4159.2005.02982.x

Hyder, A. A., Wunderlich, C. A., Puvanachandra, P., Gururaj, G., & Kobusingye, O. C. (2007). The impact of traumatic brain injuries: a global perspective. *NeuroRehabilitation, 22*(5), 341–353.

Iverson, G. L., Lange, R. T., Waljas, M., Liimatainen, S., Dastidar, P., Hartikainen, K. M., . . . Ohman, J. (2012). Outcome from Complicated versus Uncomplicated Mild Traumatic Brain Injury. *Rehabilitation Research and Practice, 2012*, 415740. doi:10.1155/2012/415740

Jaffer, H., Adjei, I. M., & Labhasetwar, V. (2013). Optical imaging to map blood-brain barrier leakage. *Science Reports, 3*, 3117. doi:10.1038/srep03117

Jantzen, K. J., Anderson, B., Steinberg, F. L., & Kelso, J. A. (2004). A prospective functional MR imaging study of mild traumatic brain injury in college football players. *AJNR. American Journal of Neuroradiology, 25*(5), 738–745.

Johnston, K. M., McCrory, P., Mohtadi, N. G., & Meeuwisse, W. (2001). Evidence-based review of sport-related concussion: Clinical science. *Clinical Journal of Sport Medicine, 11*(3), 150–159. doi:10.1097/00042752-200107000-00005

Jonsson, T., Stefansson, H., Steinberg, S., Jonsdottir, I., Jonsson, P. V., Snaedal, J., . . . Lah, J. J. (2013). Variant of TREM2 associated with the risk of Alzheimer's disease. *New England Journal of Medicine, 368*(2), 107–116.

Kabu, S., Jaffer, H., Petro, M., Dudzinski, D., Stewart, D., Courtney, A., . . . Labhasetwar, V. (2015). Blast-Associated Shock Waves Result in Increased Brain Vascular Leakage and Elevated ROS Levels in a Rat Model of Traumatic Brain Injury. *PLoS One, 10*(5), e0127971. doi:10.1371/journal.pone.0127971

Kane, M. J., Angoa-Perez, M., Briggs, D. I., Viano, D. C., Kreipke, C. W., & Kuhn, D. M. (2012). A mouse model of human repetitive mild traumatic brain injury. *Journal of Neuroscience Methods, 203*(1), 41–49. doi:10.1016/j.jneumeth.2011.09.003

Katz, D. I., Cohen, S. I., & Alexander, M. P. (2015). Chapter 9 – Mild traumatic brain injury. In G. Jordan & M. S. Andres (Eds.), *Handbook of Clinical Neurology.* 127, 131–156.

Kaur, C., & Ling, E. A. (2008). Blood brain barrier in hypoxic-ischemic conditions. *Current Neurovascular Research, 5*(1), 71–81.

Kay, T., Harrington, D., & Adams, R. (1993). American Congress of Rehabilitation Medicine, Head Injury Interdisciplinary Special Interest Group. Definition of mild traumatic brain injury. *Journal of Head Trauma Rehabilitation, 8*(3), 86–87.

Kelly, J. P., & Rosenberg, J. H. (1997). Diagnosis and management of concussion in sports. *Neurology, 48*(3), 575–580. Retrieved from <Go to ISI>://WOS:A1997XC47500005

Knaus, W. A., Draper, E. A., Wagner, D. P., & Zimmerman, J. E. (1985). Apache-II - A severity of disease classificiation-system. *Critical Care Medicine, 13*(10), 818–829. doi:10.1097/00003246-198510000-00009

Koerte, I. K., Ertl-Wagner, B., Reiser, M., Zafonte, R., & Shenton, M. E. (2012). White Matter Integrity in the Brains of Professional Soccer Players Without a Symptomatic Concussion. *JAMA: The Journal of the American Medical Association, 308*(18), 1859–1861. doi:10.1001/jama.2012.13735

Kondo, A., Shahpasand, K., Mannix, R., Qiu, J., Moncaster, J., Chen, C. H., . . . Lu, K. P. (2015). Antibody against early driver of neurodegeneration cis P-tau blocks brain injury and tauopathy. *Nature, 523*(7561), 431–436. doi:10.1038/nature14658

Korn, A., Golan, H., Melamed, I., Pascual-Marqui, R., & Friedman, A. (2005). Focal cortical dysfunction and blood-brain barrier disruption in patients with Postconcussion syndrome. *Journal of Clinical Neurophysiology, 22*(1), 1–9.

Kumar, A., & Loane, D. J. (2012). Neuroinflammation after traumatic brain injury: opportunities for therapeutic intervention. *Brain, Behavior, and Immunity, 26*(8), 1191–1201. doi:10.1016/j.bbi.2012.06.008

Kushner, D. (1998). Mild traumatic brain injury: Toward understanding manifestations and treatment. *Archives of Internal Medicine, 158*(15), 1617–1624. doi:10.1001/archinte.158.15.1617

Langlois, J. A., Rutland-Brown, W., & Wald, M. M. (2006). The epidemiology and impact of traumatic brain injury: a brief overview. *Journal of Head Trauma Rehabilitation, 21*(5), 375–378.

Laurer, H. L., Bareyre, F. M., Lee, V., Trojanowski, J. Q., Longhi, L., Hoover, R., . . . McIntosh, T. K. (2001). Mild head injury increasing the brain's vulnerability to a second concussive impact. *Journal of Neurosurgery, 95*(5), 859–870. doi:10.3171/jns.2001.95.5.0859

Le Freche, H., Brouillette, J., Fernandez-Gomez, F. J., Patin, P., Caillierez, R., Zommer, N., . . . Buee, L. (2012). Tau phosphorylation and sevoflurane anesthesia: an association to postoperative cognitive impairment. *Anesthesiology, 116*(4), 779–787. doi:10.1097/ALN.0b013e31824be8c7

Lee, H., Wintermark, M., Gean, A. D., Ghajar, J., Manley, G. T., & Mukherjee, P. (2008). Focal lesions in acute mild traumatic brain injury and neurocognitive

outcome: CT versus 3T MRI. *Journal of Neurotrauma, 25*(9), 1049–1056. doi:10.1089/neu.2008.0566

Lighthall, J. W. (1988). Controlled Cortical Impact: A New Experimental Brain Injury Model. *Journal of Neurotrauma, 5*(1), 1–15. doi:10.1089/neu.1988.5.1

Lighthall, J. W., Dixon, C. E., & Anderson, T. E. (1989). Experimental models of brain injury. *Journal of Neurotrauma, 6*(2), 83–97.

Lincoln, A. E., Caswell, S. V., Almquist, J. L., Dunn, R. E., Norris, J. B., & Hinton, R. Y. (2011). Trends in concussion incidence in high school sports: a prospective 11-year study. *American Journal of Sports Medicine, 39*(5), 958–963. doi:10.1177/0363546510392326

Lindgren, S., & Rinder, L. (1965). Experimental studies in head injury. I. Some factors influencing results of model experiments. *Biophysik, 2*(5), 320–329.

Lovell, M. R., & Collins, M. W. (1998). Neuropsychological assessment of the college football player. *Journal of Head Trauma Rehabilitation, 13*(2), 9–26. Retrieved from <Go to ISI>://WOS:000072898800004

Lovell, M. R., Pardini, J. E., Welling, J., Collins, M. W., Bakal, J., Lazar, N., . . . Becker, J. T. (2007). Functional brain abnormalities are related to clinical recovery and time to return-to-play in athletes. *Neurosurgery, 61*(2), 352–359; discussion 359–360. doi:10.1227/01.neu.0000279985.94168.7f

Luh, C., Gierth, K., Timaru-Kast, R., Engelhard, K., Werner, C., & Thal, S. C. (2011). Influence of a brief episode of anesthesia during the induction of experimental brain trauma on secondary brain damage and inflammation. *PLoS One, 6*(5), e19948. doi:10.1371/journal.pone.0019948

Maas, A. I. R., Hukkelhoven, C. W. P. M., Marshall, L. F., & Steyerberg, E. W. (2005). Prediction of Outcome in Traumatic Brain Injury with Computed Tomographic Characteristics: A Comparison between the Computed Tomographic Classification and Combinations of Computed Tomographic Predictors. *Neurosurgery, 57*(6), 1173–1182. doi:10.1227/01.neu.0000186013.63046.6b

Maas, A. I. R., Stocchetti, N., & Bullock, R. (2008). Moderate and severe traumatic brain injury in adults. *Lancet Neurology, 7*(8), 728–741. doi:10.1016/s1474-4422(08)70164-9

Manaenko, A., Chen, H., Kammer, J., Zhang, J. H., & Tang, J. P. (2011). Comparison Evans Blue injection routes: Intravenous versus intraperitoneal, for measurement of blood-brain barrier in a mice hemorrhage model. *Journal of Neuroscience Methods, 195*(2), 206–210. doi:10.1016/j.jneumeth.2010.12.013

Marchi, N., Bazarian, J. J., Puvenna, V., Janigro, M., Ghosh, C., Zhong, J., . . . Janigro, D. (2013). Consequences of Repeated Blood-Brain Barrier Disruption in Football Players. *PLoS One, 8*(3). doi:10.1371/journal.pone.0056805

Marmarou, A., Foda, M. A., van den Brink, W., Campbell, J., Kita, H., & Demetriadou, K. (1994). A new model of diffuse brain injury in rats. Part I: Pathophysiology and biomechanics. *Journal of Neurosurgery, 80*(2), 291–300. doi:10.3171/jns.1994.80.2.0291

Marshall, L. F., Becker, D. P., Bowers, S. A., Cayard, C., Eisenberg, H., Gross, C. R., . . . Warren, J. (1983). The national traumatic coma data-bank 1. Design, purpose , goals, and results. *Journal of Neurosurgery, 59*(2), 276–284. doi:10.3171/jns.1983.59.2.0276

Marshall, L. F., Marshall, S. B., Klauber, M. R., Van Berkum Clark, M., Eisenberg, H., Jane, J. A., . . . Foulkes, M. A. (1992). The diagnosis of head injury requires a classification based on computed axial tomography. *Journal of Neurotrauma, 9 Suppl 1*, S287–292.

Mayer, A. R., Bellgowan, P. S. F., & Hanlon, F. M. (2015). Functional magnetic resonance imaging of mild traumatic brain injury. *Neuroscience and Biobehavioral Reviews, 49*, 8–18. doi:10.1016/j.neubiorev.2014.11.016

McAllister, T. W. (2011). Neurobiological consequences of traumatic brain injury. *Dialogues in Clinical Neuroscience, 13*(3), 287–300. Retrieved from http://www.ncbi.nlm.nih.gov/pmc/articles/PMC3182015/

McAllister, T. W., Ford, J. C., Flashman, L. A., Maerlender, A., Greenwald, R. M., Beckwith, J. G., . . . Jain, S. (2014). Effect of head impacts on diffusivity measures in a cohort of collegiate contact sport athletes. *Neurology, 82*(1), 63–69. doi:10.1212/01.wnl.0000438220.16190.42

McAllister, T. W., Saykin, A. J., Flashman, L. A., Sparling, M. B., Johnson, S. C., Guerin, S. J., . . . Yanofsky, N. (1999). Brain activation during working memory 1 month after mild traumatic brain injury: a functional MRI study. *Neurology, 53*(6), 1300–1308.

McAllister, T. W., Sparling, M. B., Flashman, L. A., Guerin, S. J., Mamourian, A. C., & Saykin, A. J. (2001). Differential working memory load effects after mild traumatic brain injury. *Neuroimage, 14*(5), 1004–1012. doi:10.1006/nimg.2001.0899

McCaffrey, M. A., Mihalik, J. P., Crowell, D. H., Shields, E. W., & Guskiewicz, K. M. (2007). Measurement of head impacts in collegiate football players: Clinical

measures of concussion after high- and low-magnitude impacts. *Neurosurgery, 61*(6), 1236–1243. doi:10.1227/01.neu.0000280153.11614.69

McCrea, M., Barr, W. B., Guskiewicz, K., Randolph, C., Marshall, S. W., Cantu, R., . . . Kelly, J. P. (2005). Standard regression-based methods for measuring recovery after sport-related concussion. *Journal of the International Neuropsychological Society, 11*(1), 58–69. doi:10.1017/s1355617705050083

McCrea, M., Guskiewicz, K. M., Marshall, S. W., Barr, W., Randolph, C., Cantu, R. C., . . . Kelly, J. P. (2003). Acute effects and recovery time following concussion in collegiate football players: the NCAA Concussion Study. *JAMA: The Journal of the American Medical Association, 290*(19), 2556–2563. doi:10.1001/jama.290.19.2556

McCrea, M., Kelly, J. P., Randolph, C., Kluge, J., Bartolic, E., Finn, G., & Baxter, B. (1998). Standardized assessment of concussion (SAC): On-site mental status evaluation of the athlete. *Journal of Head Trauma Rehabilitation, 13*(2), 27–35. Retrieved from <Go to ISI>://WOS:000072898800005

McCrory, P. R. (1997). Were you knocked out? A team physician's approach to initial concussion management. *Medicine and Science in Sports and Exercise, 29*(7), S207–S212. Retrieved from <Go to ISI>://WOS:A1997XM28000001

McCrory, P. R., & Berkovic, S. F. (1998). Concussive convulsions – Incidence in sport and treatment recommendations. *Sports Medicine, 25*(2), 131–136. doi:10.2165/00007256-199825020-00005

McCrory, P. R., & Berkovic, S. F. (2000). Video analysis of acute motor and convulsive manifestations in sport-related concussion. *Neurology, 54*(7), 1488–1491. Retrieved from <Go to ISI>://WOS:000086460900019

McCrory, P. R., Bladin, P. F., & Berkovic, S. F. (1997). Retrospective study of concussive convulsions in elite Australian rules and rugby league footballers: Phenomenology, aetiology, and outcome. *BMJ: British Medical Journal, 314*(7075), 171–174. Retrieved from <Go to ISI>://WOS:A1997WD91100021

McCrory, P. R., Johnston, K., Meeuwisse, W., Aubry, M., Cantu, R., Dvorak, J., . . . Schamasch, P. (2005). Summary and agreement statement of the 2nd International Conference on Concussion in Sport, Prague 2004. *British Journal of Sports Medicine, 39*(4), 196–204. doi:10.1136/bjsm.2005.018614

McCrory, P. R., Johnston, K. M., Mohtadi, N. G., & Meeuwisse, W. (2001). Evidence-Based Review of Sport-Related Concussion: Basic Science. *Clinical Journal of Sport Medicine, 11*(3), 160–165. Retrieved from

http://journals.lww.com/cjsportsmed/Fulltext/2001/07000/Evidence_Based_Review_of_Sport_Related_Concussion_.6.aspx

McCrory, P. R., Meeuwisse, W., Aubry, M., Cantu, B., Dvorak, J., Echemendia, R. J., . . . Turner, M. (2013). Consensus statement on concussion in sport: the 4th International Conference on Concussion in Sport held in Zurich, November 2012. *British Journal of Sports Medicine, 47*(5), 250–258. doi:10.1136/bjsports-2013-092313

McCrory, P. R., Meeuwisse, W., Echemendia, R. J., Iverson, G. L., Dvorak, J., & Kutcher, J. S. (2013). What is the lowest threshold to make a diagnosis of concussion? *British Journal of Sports Medicine, 47*(5), 268–271. doi:10.1136/bjsports-2013-092247

McCrory, P. R., Meeuwisse, W., Johnston, K., Dvorak, J., Aubry, M., Molloy, M., & Cantu, R. (2009). Consensus statement on concussion in sport–the 3rd International Conference on concussion in sport, held in Zurich, November 2008. *Journal of Clinical Neuroscience, 16*(6), 755–763. doi:10.1016/j.jocn.2009.02.002

McIntosh, T. K., Noble, L., Andrews, B., & Faden, A. I. (1987). Traumatic brain injury in the rat: characterization of a midline fluid-percussion model. *Central Nervous System Trauma, 4*(2), 119–134. Retrieved from <Go to ISI>://MEDLINE:3690695

McIntosh, T. K., Vink, R., Noble, L., Yamakami, I., Fernyak, S., Soares, H., & Faden, A. L. (1989). Traumatic brain injury in the rat – Characterization of a lateral fluid-percussion model. *Neuroscience, 28*(1), 233–244. doi:10.1016/0306-4522(89)90247-9

McKee, A. C., Alvarez, V., Bieniek, K., Cairns, N., Crary, J., Dams-O'Connor, K., . . . Montine, T. (2015). Preliminary results of the NINDS/NIBIB consensus meeting to evaluate pathological criteria for the diagnosis of CTE (P2. 178). *Neurology, 84*(14 Supplement), P2. 178.

McKee, A. C., Cantu, R. C., Nowinski, C. J., Hedley-Whyte, E. T., Gavett, B. E., Budson, A. E., . . . Stern, R. A. (2009). Chronic traumatic encephalopathy in athletes: Progressive tauopathy after repetitive head injury. *Journal of Neuropathology and Experimental Neurology, 68*(7), 709–735. Retrieved from <Go to ISI>://000267557400001

McKee, A. C., & Daneshvar, D. H. (2015). The Neuropathology of Traumatic Brain Injury. In J. Grafman & A. M. Salazar (Eds.), *Traumatic Brain Injury, Part 1* (pp. 45–67): Elsevier (S&T).

McKee, A. C., Daneshvar, D. H., Alvarez, V. E., & Stein, T. D. (2014). The neuropathology of sport. *Acta Neuropathologica, 127*(1), 29–51. doi:10.1007/s00401-013-1230-6

McKee, A. C., Gavett, B. E., Stern, R. A., Nowinski, C. J., Cantu, R. C., Kowall, N. W., . . . Budson, A. E. (2010). TDP-43 proteinopathy and motor neuron disease in chronic traumatic encephalopathy. *Journal of Neuropathology and Experimental Neurology, 69*(9), 918–929. doi:Doi 10.1097/Nen.0b013e3181ee7d85

McKee, A. C., Stern, R. A., Nowinski, C. J., Stein, T. D., Alvarez, V. E., Daneshvar, D. H., . . . Cantu, R. C. (2013). The spectrum of disease in chronic traumatic encephalopathy. *Brain, 136*(Pt 1), 43–64. doi:10.1093/brain/aws307

McLeod, T. C. V., & Leach, C. (2012). Psychometric Properties of Self-Report Concussion Scales and Checklists. *Journal of Athletic Training, 47*(2), 221–223. Retrieved from <Go to ISI>://WOS:000302386600014

Meaney, D. F., & Smith, D. H. (2011). Biomechanics of concussion. *Clinics in Sports Medicine, 30*(1), 19–31, vii. doi:10.1016/j.csm.2010.08.009

Meaney, D. F., Smith, D. H., Shreiber, D. I., Bain, A. C., Miller, R. T., Ross, D. T., & Gennarelli, T. A. (1995). Biomechanical analysis of experimental diffuse axonal injury. *Journal of Neurotrauma, 12*(4), 689–694. Retrieved from <Go to ISI>://A1995RY92000020

Meehan, W. P., 3rd, d'Hemecourt, P., Collins, C. L., & Comstock, R. D. (2011). Assessment and management of sport-related concussions in United States high schools. *American Journal of Sports Medicine, 39*(11), 2304–2310. doi:10.1177/0363546511423503

Meehan, W. P., 3rd, Zhang, J., Mannix, R., & Whalen, M. J. (2012). Increasing Recovery Time Between Injuries Improves Cognitive Outcome After Repetitive Mild Concussive Brain Injuries in Mice. *Neurosurgery, 71*(4), 885–891. doi:10.1227/NEU.0b013e318265a439

Menon, D. K., Schwab, K., Wright, D. W., Maas, A. I., Demographics, Clinical Assessment Working Group of the, I., . . . Psychological, H. (2010). Position statement: definition of traumatic brain injury. *Archives of Physical Medicine and Rehabilitation, 91*(11), 1637–1640. doi:10.1016/j.apmr.2010.05.017

Middleton, P. M. (2012). Practical use of the Glasgow Coma Scale; a comprehensive narrative review of GCS methodology. *Australasian Emergency Nursing Journal, 15*(3), 170–183. doi:10.1016/j.aenj.2012.06.002

Mihalik, J. P., Bell, D. R., Marshall, S. W., & Guskiewicz, K. M. (2007). Measurement of head impacts in collegiate football players: An investigation of positional and event-type differences. *Neurosurgery, 61*(6), 1229–1235. doi:10.1227/01.neu.0000280147.37163.30

Mihalik, J. P., Greenwald, R. M., Blackburn, J. T., Cantu, R. C., Marshall, S. W., & Guskiewicz, K. M. (2010). Effect of Infraction Type on Head Impact Severity in Youth Ice Hockey. *Medicine and Science in Sports and Exercise, 42*(8), 1431–1438. doi:10.1249/MSS.0b013e3181d2521a

Montenigro, P. H., Baugh, C. M., Daneshvar, D. H., Mez, J., Budson, A. E., Au, R., . . . Stern, R. A. (2014). Clinical subtypes of chronic traumatic encephalopathy: literature review and proposed research diagnostic criteria for traumatic encephalopathy syndrome. *Alzheimer's Research & Therapy, 6*(5), 68. doi:10.1186/s13195-014-0068-z

Moser, R. S., & Schatz, P. (2002). Enduring effects of concussion in youth athletes. *Archives of Clinical Neuropsychology, 17*(1), 91–100.

Mott, F. W. (1916). The effects of high explosives upon the central nervous system. *Lancet, 187*(4824), 331–338, 441–449, 545–553. doi:http://dx.doi.org/10.1016/S0140-6736(00)52963-8

Mouzon, B., Chaytow, H., Crynen, G., Bachmeier, C., Stewart, J., Mullan, M., . . . Crawford, F. (2012). Repetitive mild traumatic brain injury in a mouse model produces learning and memory deficits accompanied by histological changes. *Journal of Neurotrauma, 29*(18), 2761–2773. doi:10.1089/neu.2012.2498

Namjoshi, D. R., Cheng, W. H., McInnes, K. A., Martens, K. M., Carr, M., Wilkinson, A., . . . Wellington, C. L. (2014). Merging pathology with biomechanics using CHIMERA (Closed-Head Impact Model of Engineered Rotational Acceleration): a novel, surgery-free model of traumatic brain injury. *Molecular Neurodegeneration, 9*. doi:10.1186/1750-1326-9-55

Naunheim, R. S., Standeven, J., Richter, C., & Lewis, L. M. (2000). Comparison of impact data in hockey, football, and soccer. *Journal of Trauma-Injury Infection and Critical Care, 48*(5), 938–941. doi:10.1097/00005373-200005000-00020

Nelson, W. E. J., J. A.; Gieck, J. H. (1984). Minor head injury in sports: A new system of classification and management. *Physician and Sports Medicine, 12*, 103–110.

Nilsson, B., Pontén, U., & Voigt, G. (1977). Experimental head injury in the rat: Part 1: Mechanics, pathophysiology, and morphology in an impact acceleration trauma model. *Journal of Neurosurgery, 47*(2), 241–251.

Omalu, B. I., DeKosky, S. T., Hamilton, R. L., Minster, R. L., Kamboh, M. I., Shakir, A. M., & Wecht, C. H. (2006). Chronic traumatic encephalopathy in a national football league player: part II. *Neurosurgery, 59*(5), 1086–1092; discussion 1092–1083. doi:10.1227/01.neu.0000245601.69451.27

Omalu, B. I., DeKosky, S. T., Minster, R. L., Kamboh, M. I., Hamilton, R. L., & Wecht, C. H. (2005). Chronic Traumatic Encephalopathy in a National Football League Player. *Neurosurgery, 57*(1), 128–134. doi:10.1227/01.neu.0000163407.92769.ed

Ommaya, A. K. (1985). Biomechanics of head injury: experimental aspects. In A. K. Ommaya (Ed.), *The biomechanics of trauma* (pp. 245–269): Appleton-Century, Norwalk.

Ommaya, A. K., Faas, F., & Yarnell, P. (1968). Whiplash injury and brain damage: An experimental study. *Journal of the American Medical Association, 204*(4), 285–289

Ommaya, A. K., & Gennarelli, T. A. (1974). Cerebral concussion and traumatic unconsciousness: Correlation of experimental and clinical observations on blunt head-injuries. *Brain, 97*(4), 633–654.

Ommaya, A. K., Hirsch, A., & Martinez, J. L. (1967). Role of whiplash in cerebral concussion. *SAE Technical Paper* 660804, doi:10.4271/660804.

Ono, K., Kikuchi, A., Nakamura, M., Kobayashi, H., & Nakamura, N. (1980). Human head tolerance to sagittal impact reliable estimation deduced from experimental head injury using subhuman primates and human cadaver skulls. *SAE Technical Paper* 801303, 1980, doi:10.4271/801303

Pachter, J. S., de Vries, H. E., & Fabry, Z. (2003). The blood‐brain barrier and its role in immune privilege in the central nervous system. *Journal of Neuropathology & Experimental Neurology, 62*(6), 593–604.

Panter, S. S., Braughler, J. M., & Hall, E. D. (1992). Dextran-coupled deferoxamine improves outcome in a murine model of head injury. *Journal of Neurotrauma, 9*(1), 47–53.

Parkinson, D., West, M., & Pathiraja, T. (1978). Concussion: Comparison of humans and rats. *Neurosurgery, 3*(2), 176–180. Retrieved from <Go to ISI>://WOS:A1978FT42300008

Pellman, E. J., Viano, D. C., Tucker, A. M., & Casson, I. R. (2003). Concussion in professional football: Location and direction of helmet impacts – Part 2. *Neurosurgery, 53*(6), 1328–1340. doi:10.1227/01.neu.0000093499.20604.21

Pellman, E. J., Viano, D. C., Tucker, A. M., Casson, I. R., & Waeckerle, J. F. (2003). Concussion in professional football: reconstruction of game impacts and injuries. *Neurosurgery, 53*(4), 799–812; discussion 812–794.

Peterson, C. L., Ferrara, M. S., Mrazik, M., Piland, S., & Elliott, R. (2003). Evaluation of neuropsychological domain scores and postural stability following cerebral concussion in sports. *Clinical Journal of Sport Medicine, 13*(4), 230–237.

Petraglia, A. L., Plog, B. A., Dayawansa, S., Chen, M., Dashnaw, M. L., Czerniecka, K., . . . Huang, J. H. (2014). The Spectrum of Neurobehavioral Sequelae after Repetitive Mild Traumatic Brain Injury: A Novel Mouse Model of Chronic Traumatic Encephalopathy. *Journal of Neurotrauma, 31*(13), 1211–1224. doi:10.1089/neu.2013.3255

Petraglia, A. L., Plog, B. A., Dayawansa, S., Dashnaw, M. L., Czerniecka, K., Walker, C. T., . . . Nedergaard, M. (2014). The pathophysiology underlying repetitive mild traumatic brain injury in a novel mouse model of chronic traumatic encephalopathy. *Surgical Neurology International, 5*, 184–184. doi:10.4103/2152-7806.147566

Pino, P. A., & Cardona, A. E. (2011). Isolation of brain and spinal cord mononuclear cells using percoll gradients. *Journal of Visualized Experiments: JoVE* (48). doi:10.3791/2348

Planel, E., Richter, K. E., Nolan, C. E., Finley, J. E., Liu, L., Wen, Y., . . . Duff, K. E. (2007). Anesthesia leads to tau hyperphosphorylation through inhibition of phosphatase activity by hypothermia. *Journal of Neuroscience, 27*(12), 3090–3097. doi:10.1523/jneurosci.4854-06.2007

Povlishock, J. T. (1993). Pathobiology of traumatically induced axonal injury in animals and man. *Annals of Emergency Medicine, 22*(6), 980–986.

Powell, E. T., Tokish, J. M., & Hawkins, R. J. (2002). Toradol use in the athletic population. *Current Sports Medicine Reports, 1*(4), 191.

Prins, M. L., & Hovda, D. A. (2003). Developing experimental models to address traumatic brain injury in children. *Journal of Neurotrauma, 20*(2), 123–137. doi:10.1089/08977150360547053

Randolph, C., Millis, S., Barr, W. B., McCrea, M., Guskiewicz, K. M., Hammeke, T. A., & Kelly, J. P. (2009). Concussion Symptom Inventory: An Empirically Derived Scale for Monitoring Resolution of Symptoms Following Sport-Related Concussion. *Archives of Clinical Neuropsychology, 24*(3), 219–229. doi:10.1093/arclin/acp025

Ravin, R., Blank, P. S., Steinkamp, A., Rappaport, S. M., Ravin, N., Bezrukov, L., . . . Zimmerberg, J. (2012). Shear Forces during Blast, Not Abrupt Changes in Pressure Alone, Generate Calcium Activity in Human Brain Cells. *PLoS One, 7*(6), e39421. doi:10.1371/journal.pone.0039421

Remy, S., & Beck, H. (2006). Molecular and cellular mechanisms of pharmacoresistance in epilepsy. *Brain, 129*(Pt 1), 18–35. doi:10.1093/brain/awh682

Riemann, B. L., & Guskiewicz, K. M. (2000). Effects of mild head injury on postural stability as measured through clinical balance testing. *Journal of Athletic Training, 35*(1), 19–25.

Rimel, R. W. (1981). Disability caused by minor head-injury. *Neurosurgery, 9*(3), 221–228. Retrieved from <Go to ISI>://WOS:A1981MG83300001

Rimel, R. W., Giordani, B., Barth, J. T., & Jane, J. A. (1982). Moderate head-inury: Completing the clinical spectrum of brain trauma. *Neurosurgery, 11*(3), 344–351. Retrieved from <Go to ISI>://WOS:A1982PG83600002

Roberts, W. O. (1992). Who plays, who sits: Managing concussions on the sidelines. *Physician and Sportsmedicine, 20*(6), 66–72. Retrieved from <Go to ISI>://WOS:A1992HX59000011

Rohn, T. T. (2013). The triggering receptorexpressed on myeloid cells 2: "TREM-ming" the inflammatory component associated with Alzheimer's disease. *Oxidative Medicine and Cellular Longevity,* 2013: 860959. doi: 10.1155/2013/8609.

Rosenberg, G. A., & Yang, Y. (2007). Vasogenic edema due to tight junction disruption by matrix metalloproteinases in cerebral ischemia. *Neurosurgical Focus, 22*(5), E4.

Ross, D. T., Meaney, D. F., Sabol, M. K., Smith, D. H., & Gennarelli, T. A. (1994). Distribution of forebrain diffuse axonal injury following inertial closed head injuty in miniature swine. *Experimental Neurology, 126*(2), 291–299. doi:10.1006/exnr.1994.1067

Rowson, S., & Duma, S. M. (2011). Development of the STAR evaluation system for football helmets: integrating player head impact exposure and risk of concussion. *Annals of Biomedical Engineering, 39*(8), 2130–2140. doi:10.1007/s10439-011-0322-5

Rowson, S., & Duma, S. M. (2013). Brain injury prediction: assessing the combined probability of concussion using linear and rotational head acceleration. *Annals of Biomedical Engineering, 41*(5), 873–882. doi:10.1007/s10439-012-0731-0

Rubin, A. M., Woolley, S. M., Dailey, V. M., & Goebel, J. A. (1995). Postural stability following mild head or whiplash injuries. *American Journal of Otology, 16*(2), 216–221.

Ruff, R. M., Iverson, G. L., Barth, J. T., Bush, S. S., Broshek, D. K., Policy, N. A. N., & Planning, C. (2009). Recommendations for diagnosing a mild traumatic brain injury: a National Academy of Neuropsychology education paper. *Archives of Clinical Neuropsychology, 24*(1), 3–10. doi:10.1093/arclin/acp006

Saatman, K. E., Duhaime, A. C., Bullock, R., Maas, A. I., Valadka, A., Manley, G. T., . . . Advisory Panel, M. (2008). Classification of traumatic brain injury for targeted therapies. *Journal of Neurotrauma, 25*(7), 719–738. doi:10.1089/neu.2008.0586

Saman, S., Kim, W., Raya, M., Visnick, Y., Miro, S., Saman, S., . . . Hall, G. F. (2012). Exosome-associated tau is secreted in tauopathy models and is selectively phosphorylated in cerebrospinal fluid in early Alzheimer disease. *Journal of Biological Chemistry, 287*(6), 3842–3849. doi:10.1074/jbc.M111.277061

Sawyer, G. A., Anderson, B. C., Raukar, N. P., & Fadale, P. D. (2012). Intramuscular ketorolac injections in the athlete. *Sports Health, 4*(4), 319–327. doi:10.1177/1941738112439686

Serbina, N. V., Jia, T., Hohl, T. M., & Pamer, E. G. (2008). Monocyte-mediated defense against microbial pathogens. *Annual Review of Immunology, 26*, 421–452. doi:10.1146/annurev.immunol.26.021607.090326

Shapira, Y., Setton, D., Artru, A. A., & Shohami, E. (1993). Blood-brain barrier permeability, cerebral edema, and neurologic function after closed head injury in rats. *Anesthesia and Analgesia, 77*(1), 141–148.

Shapira, Y., Shohami, E., Sidi, A., Soffer, D., Freeman, S., & Cotev, S. (1988). Experimental closed head-inury in rats: Mechanical, pathophysiologic, and neurologic properties. *Critical Care Medicine, 16*(3), 258–265. doi:10.1097/00003246-198803000-00010

Shaw, N. A. (2002). The neurophysiology of concussion. *Progress in Neurobiology, 67*(4), 281–344.

Shenton, M. E., Hamoda, H. M., Schneiderman, J. S., Bouix, S., Pasternak, O., Rathi, Y., . . . Zafonte, R. (2012). A review of magnetic resonance imaging and diffusion tensor imaging findings in mild traumatic brain injury. *Brain Imaging and Behavior, 6*(2), 137–192. doi:10.1007/s11682-012-9156-5

Shlosberg, D., Benifla, M., Kaufer, D., & Friedman, A. (2010). Blood-brain barrier breakdown as a therapeutic target in traumatic brain injury. *Nature Reviews. Neurology, 6*(7), 393–403. doi:10.1038/nrneurol.2010.74

Shohami, E., Shapira, Y., & Cotev, S. (1988). Experimental closed head-inury in rats: Prostaglandin production in a noninjured zone. *Neurosurgery, 22*(5), 859–863. Retrieved from <Go to ISI>://WOS:A1988N265900009

Shohami, E., Shapira, Y., Yadid, G., Reisfeld, N., & Yedgar, S. (1989). Brain phospholipase-A2 is activated after experimental closed head-inury in the rat. *Journal of Neurochemistry, 53*(5), 1541–1546. doi:10.1111/j.1471-4159.1989.tb08550.x

Slobounov, S., Cao, C., Sebastianelli, W., Slobounov, E., & Newell, K. (2008). Residual deficits from concussion as revealed by virtual time-to-contact measures of postural stability. *Clinical Neurophysiology, 119*(2), 281–289. doi:10.1016/j.clinph.2007.10.006

Smith, D. H., Chen, X. H., Nonaka, M., Trojanowski, J. Q., Lee, V. M. Y., Saatman, K. E., . . . Meaney, D. F. (1999). Accumulation of amyloid beta and tau and the formation of neurofilament inclusions following diffuse brain injury in the pig. *Journal of Neuropathology and Experimental Neurology, 58*(9), 982–992. doi:10.1097/00005072-199909000-00008

Smith, D. H., Chen, X. H., Pierce, J. E. S., Wolf, J. A., Trojanowski, J. Q., Graham, D. I., & McIntosh, T. K. (1997). Progressive atrophy and neuron death for one year following brain trauma in the rat. *Journal of Neurotrauma, 14*(10), 715–727. Retrieved from <Go to ISI>://A1997YE05700003

Smith, D. H., Chen, X. H., Xu, B. N., McIntosh, T. K., Gennarelli, T. A., & Meaney, D. F. (1997). Characterization of diffuse axonal pathology and selective hippocampal damage following inertial brain trauma in the pig. *Journal of Neuropathology and Experimental Neurology, 56*(7), 822–834. Retrieved from <Go to ISI>://WOS:A1997XJ20200009

Smith, D. H., Nonaka, M., Miller, R., Leoni, M., Chen, X. H., Alsop, D., & Meaney, D. F. (2000). Immediate coma following inertial brain injury dependent on axonal damage in the brainstem. *Journal of Neurosurgery, 93*(2), 315–322. doi:10.3171/jns.2000.93.2.0315

Stahel, P. F., Shohami, E., Younis, F. M., Kariya, K., Otto, V. I., Lenzlinger, P. M., . . . Morganti-Kossmann, M. C. (2000). Experimental closed head injury: Analysis of neurological outcome, blood-brain barrier dysfunction, intracranial neutrophil infiltration, and neuronal cell death in mice deficient in genes for pro-

inflammatory cytokines. *Journal of Cerebral Blood Flow and Metabolism, 20*(2), 369–380. Retrieved from <Go to ISI>://WOS:000085385300019

Starmark, J. E., Stalhammar, D., & Holmgren, E. (1988). The reaction level scale (RLS-85): Manual and guidelines. *Acta Neurochirurgica, 91*(1–2), 12–20. doi:10.1007/bf01400521

Statler, K. D., Alexander, H., Vagni, V., Dixon, C. E., Clark, R. S. B., Jenkins, L., & Kochanek, P. M. (2006). Comparison of seven anesthetic agents on outcome after experimental traumatic brain injury in adult, male rats. *Journal of Neurotrauma, 23*(1), 97–108. doi:10.1089/neu.2006.23.97

Statler, K. D., Alexander, H., Vayni, V., Holubkov, R., Dixon, C. E., Clark, R. S. B., . . . Kochanek, P. M. (2006). Isoflurane exerts neuroprotective actions at or near the time of severe traumatic brain injury. *Brain Research, 1076*, 216–224. doi:10.1016/j.brainres.2005.12.106

Stern, R. A., Daneshvar, D. H., Baugh, C. M., Seichepine, D. R., Montenigro, P. H., Riley, D. O., . . . McKee, A. C. (2013). Clinical presentation of chronic traumatic encephalopathy. *Neurology, 81*(13), 1122–1129. doi:10.1212/WNL.0b013e3182a55f7f

Strich, S. J. (1956). Diffuse degeneration of the cerebral white matter in severe dementia following head injury. *Journal of Neurology, Neurosurgery, and Psychiatry, 19*(3), 163–185. Retrieved from http://www.ncbi.nlm.nih.gov/pmc/articles/PMC497203/

Sullivan, H. G., Martinez, J., Becker, D. P., Miller, J. D., Griffith, R., & Wist, A. O. (1976). Fluid-percussion model of mechanical brain injury in the cat. *Journal of Neurosurgery, 45*(5), 521–534.

Tan, J., Town, T., Paris, D., Mori, T., Suo, Z. M., Crawford, F., . . . Mullan, M. (1999). Microglial activation resulting from CD40-CD40L interaction after beta-amyloid stimulation. *Science, 286*(5448), 2352–2355. Retrieved from <Go to ISI>://WOS:000084318500065

Tanzi, R. E. (2015). TREM2 and risk of Alzheimer's disease: Friend or foe? *New England Journal of Medicine, 372*(26), 2564–2565. doi:10.1056/NEJMcibr1503954

Taubin, G. (1991). Estimation of planar curves, surfaces, and nonplanar space curves defined by implicit equations with applications to edge and range image segmentation. *IEEE Transactions on Pattern Analysis & Machine Intelligence*(11), 1115–1138.

Teasdale, G., & Jennett, B. (1974). Assessment of coma and impaired consciousness: Practical scale. *Lancet, 2*(7872), 81–84. Retrieved from <Go to ISI>://WOS:A1974T535500009

Teasdale, G., Maas, A., Lecky, F., Manley, G., Stocchetti, N., & Murray, G. (2014). The Glasgow Coma Scale at 40 years: standing the test of time. *Lancet Neurology, 13*(8), 844–854. doi:10.1016/s1474-4422(14)70120-6

Thibault, L. E., & Gennarelli, T. A. (1985). Biomechanics and craniocerebral trauma. *Central Nervous System Trauma Status Report, National Institutes of Health*, 379–389.

Tomkins, O., Shelef, I., Kaizerman, I., Eliushin, A., Afawi, Z., Misk, A., . . . Friedman, A. (2008). Blood-brain barrier disruption in post-traumatic epilepsy. *Journal of Neurology, Neurosurgery, and Psychiatry, 79*(7), 774–777. doi:10.1136/jnnp.2007.126425

Tsenter, J., Beni-Adani, L., Assaf, Y., Alexandrovich, A. G., Trembovler, V., & Shohami, E. (2008). Dynamic changes in the recovery after traumatic brain injury in mice: Effect of injury severity on T2-weighted MRI abnormalities, and motor and cognitive functions. *Journal of Neurotrauma, 25*(4), 324–333. doi:10.1089/neu.2007.0452

Uryu, K., Laurer, H., McIntosh, T., Pratico, D., Martinez, D., Leight, S., . . . Trojanowski, J. Q. (2002). Repetitive mild brain trauma accelerates A beta deposition, lipid peroxidation, and cognitive impairment in a transgenic mouse model of Alzheimer amyloidosis. *Journal of Neuroscience, 22*(2), 446–454. Retrieved from <Go to ISI>://WOS:000173204800015 http://www.jneurosci.org/content/22/2/446.full.pdf

VA/DoD. (2009). VA/DoD Clinical Practice Guideline for Management of Concussion/Mild Traumatic Brain Injury. *Journal of Rehabilitation Research and Development, 46*(6), Cp1-68.

Vasterling, J. J., Verfaellie, M., & Sullivan, K. D. (2009). Mild traumatic brain injury and posttraumatic stress disorder in returning veterans: perspectives from cognitive neuroscience. *Clinical Psychology Review, 29*(8), 674–684. doi:10.1016/j.cpr.2009.08.004

Viano, D. C., Casson, I. R., & Pellman, E. J. (2007). Concussion in professional football: biomechanics of the struck player–part 14. *Neurosurgery, 61*(2), 313–327; discussion 327–318. doi:10.1227/01.neu.0000279969.02685.d0

Viano, D. C., Hamberger, A., Bolouri, H., & Saljo, A. (2009). Concussion in professional football: Animal model of brain injury; Part 15. *Neurosurgery, 64*(6), 1162–1173. doi:10.1227/01.neu.0000345863.99099.c7

Viano, D. C., Hamberger, A., Bolouri, H., & Saljo, A. (2012). Evaluation of three animal models for concussion and serious brain injury. *Annals of Biomedical Engineering, 40*(1), 213–226. doi:10.1007/s10439-011-0386-2

Viano, D. C., & Pellman, E. J. (2005). Concussion in professional football: Biomechanics of the striking player; Part 8. *Neurosurgery, 56*(2), 266–280; discussion 266–280.

Wang, Y., Cella, M., Mallinson, K., Ulrich, J. D., Young, K. L., Robinette, M. L., . . . Colonna, M. (2015). TREM2 lipid sensing sustains the microglial response in an Alzheimer's disease model. *Cell, 160*(6), 1061–1071. doi:10.1016/j.cell.2015.01.049

Warner, D. C., Schnepf, G., Barrett, M. S., Dian, D., & Swigonski, N. L. (2002). Prevalence, attitudes, and behaviors related to the use of nonsteroidal anti-inflammatory drugs (NSAIDs) in student athletes. *Journal of Adolescent Health, 30*(3), 150–153.

Wei, X. E., Zhang, Y. Z., Li, Y. H., Li, M. H., & Li, W. B. (2012). Dynamics of rabbit brain edema in focal lesion and perilesion area after traumatic brain injury: a MRI study. *Journal of Neurotrauma, 29*(14), 2413–2420. doi:10.1089/neu.2010.1510

Weissberg, I., Veksler, R., Kamintsky, L., Saar-Ashkenazy, R., Milikovsky, D. Z., Shelef, I., & Friedman, A. (2014). Imaging Blood-Brain Barrier Dysfunction in Football Players. *JAMA Neurology, 71*(11), 1453–1455. Retrieved from <Go to ISI>://WOS:000345145300018 http://archneur.jamanetwork.com/article.aspx?articleid=1920794

Willer, B., & Leddy, J. J. (2006). Management of concussion and post-concussion syndrome. *Current Treatment Options in Neurology, 8*(5), 415–426.

Wong, R. H., Wong, A. K., & Bailes, J. E. (2014). Frequency, magnitude, and distribution of head impacts in Pop Warner football: the cumulative burden. *Clinical Neurology and Neurosurgery, 118*, 1–4. doi:10.1016/j.clineuro.2013.11.036

Xiong, Y., Mahmood, A., & Chopp, M. (2013). Animal models of traumatic brain injury. *Nature Reviews. Neuroscience, 14*(2), 128–142. doi:10.1038/nrn3407

Yu, S., Zhang, X., Sun, Y., Peng, Y., Johnson, J., Mandrell, T., . . . Laizure, C. S. (2006). Pharmacokinetics of buprenorphine after intravenous administration in the mouse.

Journal of the American Association for Laboratory Animal Science, 45(3), 12–16.

Yurdakoc, A., Gunday, I., & Memis, D. (2008). Effects of halothane, isoflurane, and sevoflurane on lipid peroxidation following experimental closed head trauma in rats. *Acta Anaesthesiologica Scandinavica, 52*(5), 658–663. doi:10.1111/j.1399-6576.2008.01635.x

Zhang, J., Yoganandan, N., Pintar, F. A., & Gennarelli, T. A. (2006). Role of translational and rotational accelerations on brain strain in lateral head impact. *Biomedical Sciences Instrumentation, 42*, 501–506.

Zhang, K., Johnson, B., Pennell, D., Ray, W., Sebastianelli, W., & Slobounov, S. (2010). Are functional deficits in concussed individuals consistent with white matter structural alterations: combined FMRI & DTI study. *Experimental Brain Research, 204*(1), 57–70. doi:10.1007/s00221-010-2294-3

Zhang, L., Yang, K. H., & King, A. I. (2001). Biomechanics of neurotrauma. *Neurological Research, 23*(2–3), 144–156. doi:10.1179/016164101101198488

Zhang, L., Yang, K. H., & King, A. I. (2004). A Proposed Injury Threshold for Mild Traumatic Brain Injury. *Journal of Biomechanical Engineering, 126*(2), 226. doi:10.1115/1.1691446

Zhu, G. W., Wang, F., & Liu, W. G. (2009). Classification and prediction of outcome in traumatic brain injury based on computed tomographic imaging. *Journal of International Medical Research, 37*(4), 983–995.

Zlokovic, B. V. (2008). The blood-brain barrier in health and chronic neurodegenerative disorders. *Neuron, 57*(2), 178–201. doi:10.1016/j.neuron.2008.01.003

Zohar, O., Schreiber, S., Getslev, V., Schwartz, J., Mullins, P., & Pick, C. (2003). Closed-head minimal traumatic brain injury produces long-term cognitive deficits in mice. *Neuroscience, 118*(4), 949–955.

Zuercher, M., Ummenhofer, W., Baltussen, A., & Walder, B. (2009). The use of Glasgow Coma Scale in injury assessment: A critical review. *Brain Injury, 23*(5), 371–384. doi:10.1080/02699050902926267

Chapter 7: CURRICULUM VITAE